Astronomically-modulated climate-carbon cycle interactions in the cGENIE Earth System Model

Dissertation

zur Erlangung des Doktorgrades der

Naturwissenschaften

- Dr. rer. nat -

am Fachbereich Geowissenschaften

der Universität Bremen

vorgelegt von

FIONA ROCHHOLZ

Bremen, 2. September, 2019

Rewiever

Prof. Dr. Heiko Pälike

MARUM - Centre for Marine Environmental Sciences, University of Bremen

Leobener Straße 8, 28359 Bremen

hpaelike@marum.de

Dr. Fanny Monteiro

University of Bristol, Geographical Sciences

University Road, Clifton, Bristol, BS8 1SS

F.Monteiro@bristol.ac.uk

Promotionskolloquium am:

5. November, 2019

Versicherung an Eides Statt / *Affirmation in lieu of an oath*

gem. § 5 Abs. 5 der Promotionsordnung vom 18.06.2018 /
according to § 5 (5) of the Doctoral Degree Rules and Regulations of 18 June, 2018

Ich / I, Fiona Rochholz, Seewenjestr. 152, 28237 Bremen
(Vorname / First *Name*, Name / *Name*, Anschrift / *Address*, ggf. Matr.-Nr. / *student ID no., if applicable)*

versichere an Eides Statt durch meine Unterschrift, dass ich die vorliegende Dissertation selbständig und ohne fremde Hilfe angefertigt und alle Stellen, die ich wörtlich dem Sinne nach aus Veröffentlichungen entnommen habe, als solche kenntlich gemacht habe, mich auch keiner anderen als der angegebenen Literatur oder sonstiger Hilfsmittel bedient habe und die zu Prüfungszwecken beigelegte elektronische Version (PDF) der Dissertation mit der abgegebenen gedruckten Version identisch ist. / *With my signature I affirm in lieu of an oath that I prepared the submitted dissertation independently and without illicit assistance from third parties, that I appropriately referenced any text or content from other sources, that I used only literature and resources listed in the dissertation, and that the electronic (PDF) and printed versions of the dissertation are identical.*

Ich versichere an Eides Statt, dass ich die vorgenannten Angaben nach bestem Wissen und Gewissen gemacht habe und dass die Angaben der Wahrheit entsprechen und ich nichts verschwiegen habe*. / I affirm in lieu of an oath that the information provided herein to the best of my knowledge is true and complete.*

Die Strafbarkeit einer falschen eidesstattlichen Versicherung ist mir bekannt, namentlich die Strafandrohung gemäß § 156 StGB bis zu drei Jahren Freiheitsstrafe oder Geldstrafe bei vorsätzlicher Begehung der Tat bzw. gemäß § 161 Abs. 1 StGB bis zu einem Jahr Freiheitsstrafe oder Geldstrafe bei fahrlässiger Begehung. / *I am aware that a false affidavit is a criminal offence which is punishable by law in accordance with § 156 of the German Criminal Code (StGB) with up to three years imprisonment or a fine in case of intention, or in accordance with § 161 (1) of the German Criminal Code with up to one year imprisonment or a fine in case of negligence.*

Bremen, 02.September 2019

Ort / *Place*, Datum / *Date*

Unterschrift / *Signature*

Preface

The research for this dissertation was conducted at MARUM - Center for Marine Environmental Sciences at the University of Bremen, Germany. The work was generously funded from June, 1th 2016 to March, 31th 2019 by the European Research Council Consolidator Grant EARTHSEQUENCING (617462) awarded to Prof. Dr. Heiko Pälike.
Part of the work for this thesis was conducted during a research stay from 17/10/04 to 17/12/17 at University of California, Riverside, CA in collaboration with Sandra Kirtland Turner and Andy Ridgwell.

Acknowledgements

I thank Heiko Pälike for giving me the opportunity to start this PhD and guide me throughout the last years to bring this thesis to a successful end. I am really glad that I could join this project and also present this work on several conferences and workshops. Thank you for all the support and patience around my, in time, chaotic way of keeping track of my work.
Special thanks to Max and David, who were not only the funniest and entertaining colleagues but also the most helpful next-door co-authors I could have wished for. I am grateful for all the time that you both took for scientific discussions and of course coffee-breaks, to get me back on track in times of self-doubt. But above all, thanks for your patience.
Thanks a lot, to every one of the paleoceanography group in Bremen for all the good times in the last three years.
Thanks to Sandra Kirtland Turner and Andy Ridgwell, for supporting me from the moment on I arrived at UCR. All your input to improve the simulations and studies was just right in time to make necessary progress. Also, working together and exchange experiences with people from similar projects helped to further my work. Sandy, your constant belief in the significance of my work kept my motivation going and your inexhaustible amount of ideas made even a dead-end look not that bad.
The biggest hug and many, many kisses go to all my friends, that supported me throughout the whole time, may it have been during phases of ups or downs. Everyone that I have known for ages or met in the last years, I am grateful to have you in my life. I hope that we will never lose the anchor point in our lives that made us connect in the first place, may it have been studies, life, science or sports.
USSP-super cool-people, you have made this summer one of the best in my life and thanks for all the great days and evenings we had at meet-ups and on conferences afterwards.
Thank you, all my friends from Riverside, you have made the time with you so much fun and even welcomed me back a second time to enjoy the never-ending sunshine. Thank you, Pam, for your support and help around failed simulations and the many hours of discussing science via skype.
Rieke and Laura, thank you for being most patient house-mates and supporting friends I could have wished for in the last months.
Last, I want to thank my family that supported me all these years in so many different ways. Without your continuous encouragement throughout endless years of studying, I wouldn't have been able to finish this thesis.

Abstract

Quasi-periodic fluctuations of the Earth's astronomical parameters define the amount and distribution of solar radiation received by the Earth and dominate the pacing of Earth's natural climate variation on long timescales. Recently, anthropogenic climate change has been interfering with environmental conditions and climate on Earth as humans have known it for generations. CO_2 added to the atmosphere by human activity, mainly by burning fossil fuels and deforestation, causes global warming. The Earth's climate system is a complex combination of feedbacks responding to environmental and climatic variability. Under continuing warming, some of these feedbacks may change in direction and magnitude.

Carbon cycle processes redistribute CO_2 from the atmosphere into the ocean. This mitigates the warming effect of atmospheric CO_2 but warming of the ocean and uptake of CO_2 induce new environmental conditions, e.g. acidification of the ocean, dissolution of carbonate sediments. As warming continues, the ocean's capability to absorb CO_2 decreases and the attenuating effect on global warming will cease. Despite the efforts to understand the response of the global carbon cycle to continued warming, not all of the amplifying and mitigating feedbacks within the complex system of the marine carbon cycle are yet sufficiently understood. For instance, the exact path of anthropogenic CO_2 in the ocean and the full consequences for the global climate still need to be investigated.

In this study I investigate the mechanisms which allow the carbon cycle to respond to atmospheric CO_2, and define the global climate response to the resulting climate state. I apply the cGENIE Earth System Model of Intermediate Complexity to simulate the interactions of the carbon budget and global climate on different timescales. cGENIE comprises a 3-D dynamical ocean circulation model, a 2-D energy-moisture balance model of the atmosphere and a thermodynamic sea ice model. While it incorporates a complex module for the carbon cycle with production, export and remineralization of organic and inorganic carbon as marine sediments, it is computationally efficient enough to simulate the Earth System over timescales of several thousand to hundred-thousand years. Specifically, the model is applied on astronomical timescales in order to test the climate response to carbon cycle perturbations in past and future and climate-carbon cycle

interactions under greenhouse climate conditions.
The third chapter of this thesis 'Climate state modifies the climatic response to astronomical variation' is designed to test the global response to astronomically forced climatic variations. This study consists of a set of long simulations representing variable climate states using four different CO_2 concentrations for the duration of one million years for a time slice set during the Eocene (34.5-35.5 million years before present) which includes Eocene paleogeography conditions. CO_2 values are chosen to capture the possible range of Eocene CO_2 variations, subsequently representing 1x pre-industrial CO_2 value (278 ppm), 3x (834 ppm), 6x (1668 ppm) and 12x (3668 ppm). These Eocene simulations exhibit a climate-state dependent response to astronomical variability and amplify the climatic response to 100-kyr eccentricity cycles in a warm climate state relative to the dominant 41-kyr obliquity cycles in climate under cold state. Even without ice-sheets as potential amplifier, the obliquity response is notably stronger under cold climate. We hypothesize that the higher radiative forcing effect of atmospheric CO_2 under warm climate conditions strengthens the variation on eccentricity cycles.
In the fourth chapter 'Rethinking drivers of carbonate saturation state in high-CO_2 worlds', the same simulations are applied to investigate the magnitude and direction of the carbon cycle response to climatic perturbation. Simulations indicate that the climate state, i.e. the atmospheric CO_2 concentration, controls which feedbacks of the marine carbonate system dominate the response to astronomically-induced climate variability. Carbonate chemistry changes under warming climate and the relation between carbonate ion concentration and temperature as primary drivers on the carbonate saturation changes with increasing CO_2.
In the fifth chapter 'Anthropogenic CO_2 effect on astronomically forced climate', I test the effect of the astronomical constellation on modifying an anthropogenic-like (A1B) CO_2 emission scenario by implementing it under various astronomical configurations. Results show that the magnitude of the anthropogenic CO_2 forcing overrules the climatic effect of the astronomical constellation at the time of the forcing. Although the climate system can return to a new quasi-equilibrium state warmer than 'pre-industrial' state, the long-term consequence of the CO_2 perturbation includes significantly modified ocean chemistry and environmentally critical conditions for calcifying organism.
The main results of this thesis suggest that global warming significantly affects climate-carbon interactions on many different timescales. The stabilizing and attenuating effect of the marine carbon cycle on atmospheric CO_2 is likely to be shifted under the climatic changes induced by human activities.

Zusammenfassung

Zyklische Fluktuationen der Erdorbitalparameter über die Zeit bestimmen die Intensität und die Verteilung der Sonneneinstrahlung auf der Erdoberfläche. Sie prägen die natürlichen Klimaveränderungen der Erde auf langen Zeitskalen, den so genannten 'astronomischen Zeitskalen'. Der menschengemachte Klimawandel verändert den Zustand der Umwelt und das natürliche Klima, welches die Menschheit seit Generationen erlebt. Durch die Verbrennung von fossilen Rohstoffen und Abholzung von Wäldern erhöht die menschliche Aktivität den Atmosphärengehalt von CO_2 und somit die globalen Temperaturen. Das Erdsystem ist eine Verbindung von einer Reihe von komplizierten Mechanismen, die auf Umwelt- und Klimabedingungen reagieren. Einige dieser Mechanismen werden unter globaler Erwärmung ihre Wirkungsweiße verändern. Momentan wird der Klimawandel durch Prozesse des Kohlenstoffkreislaufs, die für Speicherung von anthropogenem CO_2 im Ozean sorgen, abgeschwächt. Jedoch nimmt dieses Speicherungspotential des Ozeans mit fortschreitender globaler Erwärmung ab. Trotz aller Studien über die Reaktion des Kohlenstoffkreislaufs auf Erwärmung, sind nicht alle internen Interaktionen vollständig verstanden und Fragen über die genaue Zukunft von anthropogenem CO_2 im Ozean bleiben offen.

In dieser Studie nutzen wir das cGENIE Erdsystemmodel intermediärer Komplexität, um Interaktionen zwischen dem marinen Kohlenstoffkreislauf und dem globalen Klima auf unterschiedlichen Zeitskalen und unter Treibhausklima zu simulieren. cGENIE beinhaltet ein 3D- dynamisches Model für Ozeanzirkulation, ein 2D Atmosphärenmodel mit Energie- und Feuchtigkeitsaustausch und ein 2D thermodynamisches Meereis-Model. Das Modul des komplexen Kohlenstoffkreislaufes mit Bildung, Ablagerung und Remineralisierung von organischen und anorganischen Karbonatsedimenten kann aktiviert werden. Trotz der hohen Komplexität der marinen biogeochemischen Vorgänge ist cGENIE technisch effektiv genug, um Simulationen mit einer Lauflänge von mehreren tausenden bis hin zu hundert-tausenden Jahren zu erstellen. Wir untersuchen Rückkopplungsmechanismen des Kohlenstoffkreislaufs, die Einfluss auf das atmosphärische CO_2 nehmen und dadurch das globale Klima verändern können. Im Besonderen ist das Model angewendet worden, um änderungen im Kohlenstoffkreislauf und deren

Auswirkungen auf das Klima auf langen astronomischen Zeitskalen zu testen.
Kapitel drei dieser Arbeit umfasst eine Reihe von Simulationen mit verschiedenen Klimazuständen, die erstellt wurden, um die Abhängigkeit von klimatischen Veränderungen aufgrund von astronomischen Fluktuationen mit dem vorherrschenden Zustand zu testen. Diese Simulationen spiegeln das Klima unter vier verschiedenen atmosphärischen CO_2 Zuständen wider, die auf die Paläogeographie des Eozäns (34.5-35.5 Millionen Jahre vor heute) angewendet wurden. Mit der Wahl von vier verschiedenen CO_2 Werten (278 ppm, 834 ppm, 1668 ppm, 3668 ppm) wurde die mögliche Spannbreit von CO_2 Variabilitä des Eozäns abgedeckt. Unsere Ergebnisse zeigen, dass Klimavariabilität in den Simulationen mit niedrigen CO_2 Werten auch ohne die verstärkende Wirkung durch Eisschilde von 41-tausend Jahr langen Zyklen geprägt ist. Simulationen mit hohen atmosphärischem CO_2 zeigen hingegen 100-tausend Jahre lange Zyklen in den klimatischen Parametern, was wir mit einer Verstärkung des Strahlungsantrieb von CO_2 unter höheren globalen Atmosphärenkonzentrationen erklären.
In Kapitel vier wird mit den gleichen Simulationen getestet, ob der Klimazustand die Magnitude und Richtung der Reaktion des Kohlenstoffkreislaufs bestimmt. Die Experimente zeigen, dass die Atmosphärenkonzentration von CO_2 bestimmt, welcher Rückkopplungsmechanismus vorrangig aktiv ist. Die Karbonatchemie im Ozean und damit auch das Verhältnis zwischen Karbonationenkonzentration und Temperatur als primärere Treiber der Karbonatsättigung verändern sich unter wärmerem Klima.
In Kapitel fünf wende ich cGENIE an, um Klimaveränderung aufgrund einer anthropogenähnliche Emission (ein A1B Szenario des IPCC -Reports) zu simulieren. Unsere Simulationen zeigen, dass die Magnitude anthropogen-ähnliche Emission so stark ist, dass die Konstellation der astronomischen Parameter keinen Einfluss auf die Klimareaktion haben. Während der Emissionen reagieren alle getesteten Klimaparameter stark auf den atmosphärischen CO_2 Anstieg, erholen sich jedoch mit dem Ende der Emissionen wieder. Insgesamt stabilisiert sich das Klima auf einen wärmeren Zustand als zu Beginn der Emissionen. Weiterhin kann sich die Chemie im Ozean auf lange Sicht nicht vollständig erholen, sodass sich die Ozeanchemie stark verändert und kritische Umweltbedingungen für kalzitbildende Organismen entstehen.
Die Hauptergebnisse dieser Arbeit zeigen, dass globale Erwärmung die Klima- Kohlenstoff Interaktionen unabhängig von den Zeitskalen stark beeinflusst. Der stabilisierende und abschwächende Effekt des marinen Karbonatzyklus auf atmosphärisches CO_2 wird sich unter dem anthropogenen Klimawandel stark verändern.

Table of Contents

List of Figures

Motivation

Variability in the amount of solar radiation impinging on Earth is the dominant pacing of all Earth processes and the underlying driving force for many biological and chemical processes on various timescales. The incoming solar radiation is defined by the Earth's astronomical parameters which describe the path around the sun and the Earth's relative position to the sun during the seasons. Natural climate changes in Earth's history are dominated by quasi-periodic shifts in Earth's astronomical parameters.

Modern anthropogenic interference with the natural carbon system generates climatic conditions, unknown for the recent Earth's climate history. Burning fossil carbon resources throws the natural system out of its balance while carbon from geologic reservoirs is reorganized into short-time atmospheric reservoirs. The global ocean and the marine carbon cycle play a fundamental role in controlling atmospheric CO_2 concentrations. Processes in the carbonate system regulating the uptake of global atmospheric CO_2 have long been described. Still, the fate of anthropogenic CO_2 and the natural climate response to anthropogenic interference requires further research to determine conceivable future trends.

Past climate reconstructions indicate a climate state-dependent response of the carbon cycle to astronomically forced climate variability. While the current climate warming is progressing rapidly, the carbon cycle's response to further anthropogenic perturbation is difficult to be estimated at present and many unsolved questions exist.

Earth System Models are useful tools to test the climate response to carbon cycle perturbations in the past and future. Nowadays, Earth System Models comprising most relevant Earth system modules including a complex representation of the carbon cycle can be run over long astronomical time scales on desktop computers.

Mechanisms connecting climate feedbacks to modify atmospheric CO_2 and the global climate response to external forcing on astronomical timescales can be tested with these kinds of models.

In this thesis, an Earth System Model of Intermediate Complexity is used to test feedbacks within the marine carbonate system and to address the following research objectives:

Hypothesis 1: The climatic system response to astronomical variation is climate state dependent.

High-resolution proxy records reveal alternations in the response of the climate system to changes in astronomical forcing. Over the course of the Cenozoic Earth's climate response to astronomical forcing changed from $\delta^{18}O$- benthic signal dominated by eccentricity-modulated precession (66-13 Ma) to an obliquity-driven signal after the mid-Miocene climatic transition (13-0.8 Ma) into the 100-kyr world of the late Pleistocene (0.8-0 Ma) (Chalk et al., 2017; De Vleeschouwer et al., 2017; Zachos, Pagani, et al., 2001).

The most apparent difference between these periods are often the size and extend of the cryosphere which has led to the assumption that the climate state, whether Earth is in a 'greenhouse' or a 'icehouse' climate, drives the variation in response to astronomical forcing.

This thesis aims to explore this state-dependency behavior of the climate system in response to astronomical variation in an Earth System Model of Intermediate Complexity. Ocean circulation, cryosphere and the carbon cycle are potential agents to initiate the response-shift to astronomical forcing. Their role will be examined and evaluated to solve an important gap in understanding Earth's past climate evolution.

Hypothesis 2: The control of the carbonate saturation state changes under greenhouse conditions.

Considerable amounts of anthropogenic CO_2 are absorbed by the global ocean, attenuating the effect of rising CO_2 on global warming. However, the continuing uptake of CO_2 fundamentally affects the carbonate chemistry in the ocean water and leads to acidification of the ocean. This has significant implications for the stability of marine carbonates and has already caused a decline in the coral-reef forming capacity (Kleypas et al., 1999). Temperature and carbonate ion concentration control carbonate saturation state of the ocean, i.e. the precipitation and dissolution of marine carbonate sediments. Continuous warming of atmosphere and ocean and progressing ocean acidification will certainly affect the relation of climate-carbon feedbacks. By examining state behavior of the marine carbonate system under rising CO_2 applying the cGENIE Earth

System Model of Intermediate Complexity, this thesis aims to further the understanding of changes within the carbonate chemistry under progressing warming.

Hypothesis 3: The magnitude of the anthropogenic CO_2 forcing overrules the climatic effect of astronomical variation.

Dramatic carbon cycle perturbations in the history of Earth's climate have been linked to insolation maxima modulated by orbital variability, indicating a close correlation between strong warming events and the underlying orbital configuration (e.g. De Vleeschouwer et al., 2017; Hays et al., 1976). The Holocene, is an extraordinary long and stable interglacial period caused by low eccentricity and high Northern Hemisphere summer insolation. Anthropogenic climate change has contributed to the astronomically 'favorable' warm climate and already is thought to prolong the warm period further into the future (Ganopolski, Winkelmann, et al., 2016). This thesis investigates the extent to which the astronomical composition affects the climatic response to anthropogenic CO_2- emissions. Here we address the question how different astronomical configurations contribute to global warming under anthropogenic CO_2 forcing. A better picture of the dependencies is essential to estimate long-lasting effects of the current anthropogenic emissions on the future climate system.

Thesis Outline and Author Contributions

This dissertation is divided into six chapters, four chapters of research performed within the dissertation are prefaced by a short introduction and summed up in a concluding chapter. Introductory chapter **§1** outlines important concepts about astronomical forcing and the connection to global climate, presents a brief overview of the marine carbon cycle and a description of the Earth System model ('cGENIE') used for this study. Technical and practical support for all studies was provided by Heiko Pälike.

Chapter **§2** comprises a sensitivity study to test the response of the Earth's climate system in cGENIE to astronomical forcing under different boundary conditions. Here, a low-resolution version of cGENIE is applied for an ocean-atmosphere-only setup to compare the climatic response to astronomical changes with results of a setup including the complex carbon cycle module. To test the amplifying effect of raising the atmospheric CO_2, simulation sets are performed under 'cold' pre-industrial and 'warm' climate conditions.

Chapters **§3**, **§4** and **§5** have been written as manuscripts for international scientific journals and will be submitted after a final round of review by all co-authors. Contributions to the research by all authors will be indicated in the following paragraphs.

In chapter **§3,** we apply a complex setup from the Eocene with time-varying astronomical variation. During the Eocene, Earth has experienced greenhouse climate conditions, similar to what studies estimate to be a future-like scenario under anthropogenic warming. A set of simulations with one-million-year duration under different atmospheric CO_2 conditions in the range from 278 ppm to 3336 ppm allows us to describe a varying response to the underlying orbital forcing. Changes in the response of the carbon cycle feedback mechanisms are responsible to shift the astronomical signal dependent on the precedent climate state. To our knowledge, this is the first study to perform several one-million-year simulations in a carbon cycle model and

describe a complex climate response to astronomical forcing. This study was designed by Fiona Rochholz, Sandra Kirtland Turner and Heiko Pälike. FR performed all experiments and modified a published cGENIE-setup to perform the simulations. Spin-ups were run by FR; one spin-up was run by Pam Vervoort. Input was provided all co-authors and model simulations were reviewed by SKT, PV and HP. PV and SKT provided additional simulations to test for all scientific theories presented in the study. Results for these simulations are not used within the publication and therefore not presented.

In chapter **§4** we explore the consequences of CO_2 variability on the marine carbonate system under a warming world. We employ cGENIE to simulate changes in carbonate saturation and its drivers under a sequence of different climate states, controlled by the concentration of atmospheric CO_2 (1x, 3x, 6x, 12xCO_2). This study is based on simulations for chapter **§3** and the same contributions concerning the model simulations apply as in the previous chapter. The study itself was designed by FR, David De Vleeschouwer, Maximilian Vahlenkamp, SKT and HP. FR, DDV and MV contributed equally to the scientific content and the manuscript with input from all co-authors.

Chapter **§5** implements an anthropogenic-like (IPCC scenario A1B) CO_2 forcing under different orbital configuration and simulates the climatic response to the combined effect. It addresses the question to what extend the response of the climate system to the anthropogenic emissions will be modified by the underlying orbital forcing. This study was designed by FR and DDV. FR performed all model simulations with scientific input from DDV. Model simulations were reviewed by SKT and HP and the manuscript was written by FR and DDV with input from all co-authors.

1 Introduction

1.1 Astronomical cycles and their control on Earth's climate

Quasi-periodic cycles of the Earth's astronomical parameters modulate the shape of the Earth's orbital path around the sun as well as the distribution of insolation over seasons and latitudes (Berger, 1978, 1989).

Precession, obliquity and eccentricity are the three key orbital parameters and define the insolation received at a certain position on Earth over the course of a year and vary periodically over long timescales, known as the Milankovitch cycles (Berger, 1978; Imbrie and Imbrie, 1980; Laskar, Robutel, et al., 2004; Milankovitch, 1941). Variation of orbital parameters over the last 5 million years as well as the change of position relative to the sun is illustrated in Fig. 1.1.

Earth's orbital eccentricity (e) describes the shape of the Earth's orbit around the sun, varying between an elliptic path and a perfect circle. Eccentricity is the only astronomical parameter that controls the absolute amount of insolation received on Earth over the year and varies primarily in cycles of 95, 124 and 405 thousand years (kyr) (Frakes et al., 1992; Imbrie and Imbrie, 1980). However, the direct impact of eccentricity variations on insolation is small, the effect on total annual insolation is about 0.2% change in insolation. Seasonal variation caused by eccentricity change is larger than the annual effect and is expressed by the temperature difference between aphelion and perihelion (as in Laskar, Fienga, et al., 2011, eq.[1]). Exemplified for a black-body, the temperature difference between aphelion and perihelion ($\delta T_{P/A}$) can be calculated by $\delta T_{P/A} = e * \text{Total outgoing long-wave radiation}$. The outgoing long-wave radiation of a black-body is 300 K (26.65°C). A change of 0.02 in eccentricity would translate to a $\delta T_{P/A}$ of 0.0537 °C ((ibid.)[eq. 1]).

Precession (ω) is the 'longitude of perihelion', the measure of the angle between the vernal

equinox and the perihelion (Berger, 1988) and varies on cycles between 19 and 23 kyr (Berger, 1978). By defining the time when Earth passes perihelion (nearest point to the sun) or aphelion (furthest point to the sun), precession determines the strength of the season, but hardly affects the total annual insolation. Eccentricity acts as a modulator of the amplitude of precession and the combined effect of precession and eccentricity (P=e* sin(ω)) is called 'climatic precession'. The variation of eccentricity strongly influences the effect of precession; under a circular orbit, the effect of precession is nullified, while it is the strongest under an elliptical orbit. With a circular orbit, Sun-Earth distance at perihelion and aphelion are approximately equivalent, minimizing differences in insolation across seasons in opposite hemispheres. With a more elliptical orbit, the Earth-sun distance at perihelion is minimized, leading to an enhanced seasonal contrast, that is especially pronounced in the high latitudes (Imbrie and Imbrie, 1980).

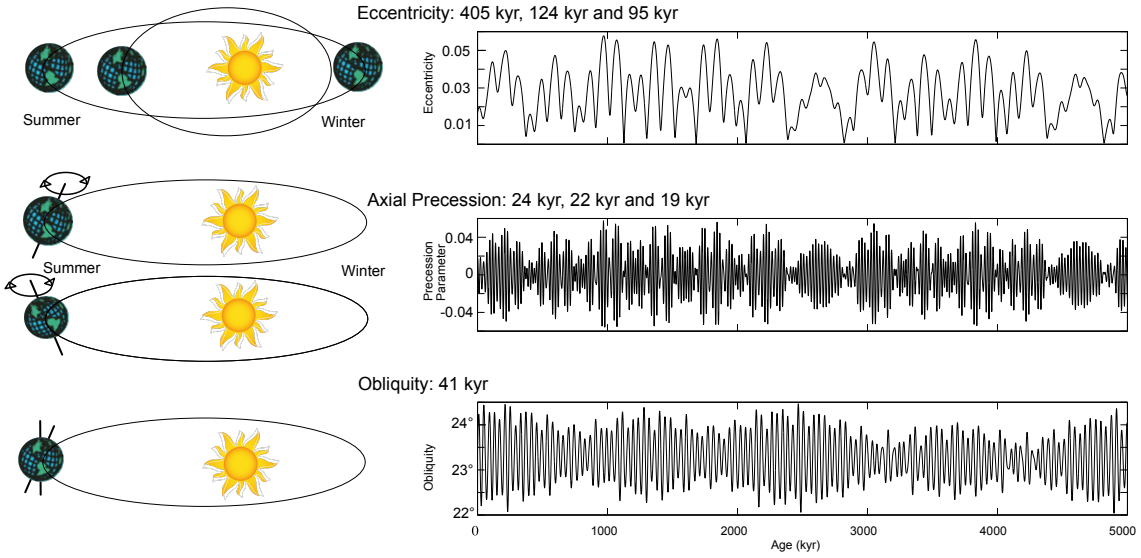

Figure 1.1: Astronomical parameters and time scales of eccentricity, precession parameter and obliquity for the last 5 Myr (adapted from Zachos, Pagani, et al., 2001). Values for astronomical parameters are from La04 (Laskar, Robutel, et al., 2004).

The Earth's axial tilt, obliquity (ε), determines the latitudinal distribution of incoming solar radiation and varies between 21.2° and 25° on mainly 41-kyr cycles. A high obliquity angle will amplify the seasonal contrast in a given hemisphere, while a lower obliquity angle will dampen the seasonal contrast, most apparent in the high latitudes (Imbrie, Berger, et al., 1993). Obliquity defines seasonality depending on the tilt towards or away from the sun in combination with

the precession angle (Berger, 1978; Mantsis et al., 2011). In general, high eccentricity and high obliquity have been linked to globally warmer climates in Earth history (e.g. Ganopolski and Roche, 2009).

1.2 Astronomical cycles in the geologic record

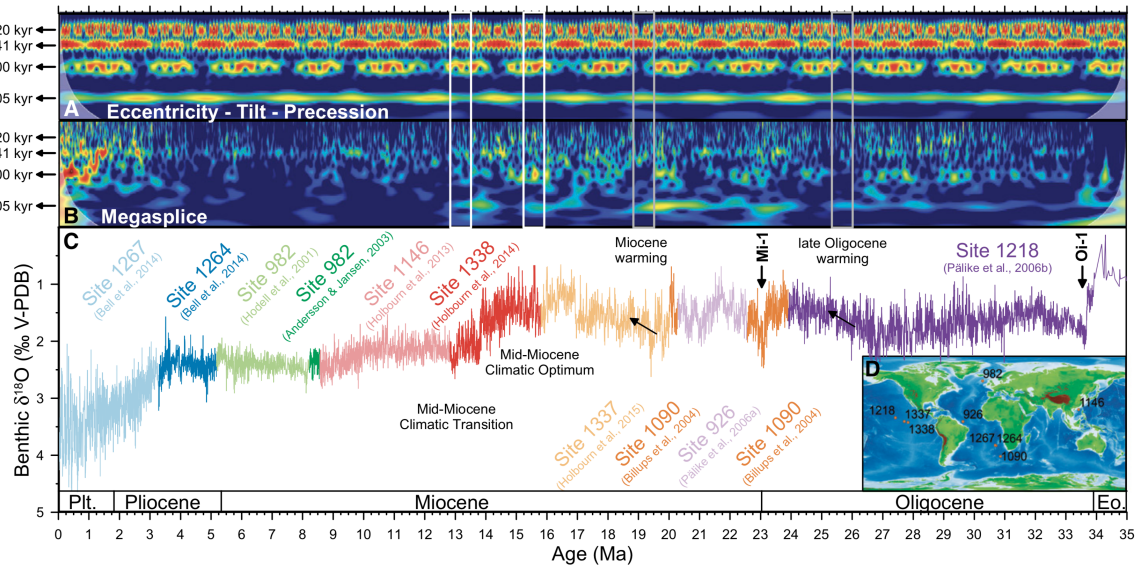

Figure 1.2: 35 kyr long benthic $\delta^{18}O$ splice ('megasplice') (De Vleeschouwer et al., 2017) to illustrate climate variability throughout Earth's history.

The impact of quasi-periodic variations in Earth's astronomical parameters on climate is well established throughout the climate history of the Earth (Cramer et al., 2003; Lisiecki et al., 2005).

High-resolution climate reconstructions of the Cenozoic era (66 millions years before present (Ma) until today) document shifts in the dominant astronomical pacing (e.g. De Vleeschouwer et al., 2017; Kirtland Turner, 2014; Pälike et al., 2006; Zachos, Pagani, et al., 2001) (Fig. 1.2). During warm periods of Paleogene and early Neogene (66-13 Ma ago) climate records largely vary on astronomical cycles of eccentricity (~405 kyr and ~100 kyr). With the onset of the Neogene icehouse (13-0.8 Ma ago) variations corresponding to changes in Earth's obliquity (~41 kyr) dominate the climatic spectrum during substantial portions of this climatic periods (De Vleeschouwer et al., 2017; Zachos, Pagani, et al., 2001). After the mid-Pleistocene transition, 0.8 Ma ago, declining greenhouse gas concentrations allow for ice sheets to grow large and stable

enough to sustain temperature changes on obliquity timescales (Chalk et al., 2017). The climate is fluctuating in 100-kyr cycles, known as glacial and interglacial variation (Petit et al., 1999). These climatic variations are pictured in the typical saw-tooth pattern of $\delta^{18}O$ records, recovered from ice-cores, as well as sedimentary records (Imbrie, Boyle, et al., 1992; Petit et al., 1999). The distinct correspondence of orbital variation and changes in proxy records has led to the interpretation that orbital changes are the reason for glacial-interglacial variability during the Pleistocene (Hays et al., 1976).

Considering the overall effect of eccentricity changes (0.7 W/m^2 at top of the atmosphere), combined with feedbacks of the albedo and the effect of the planetary radiation budget, δT°C resulting from a maximum eccentricity change is around 0.5°C in the global average temperature (Crowley et al., 1991). Looking closer at the effect of the variation of the orbital parameters on the energy budget, it is obvious, that this cycling can potentially pace glacial-interglacial variations but is not strong enough to drive these cycles without any accompanied processes (Genthon et al., 1987; Sigman et al., 2000).

Different environmental boundary conditions might contribute to determining the Earth's response to astronomical forcing. These include atmospheric CO_2 variations within the carbon cycle, tectonic shifts in land-ocean distribution and the size of the cryosphere. By intensifying incoming solar radiation, atmospheric CO_2 as a greenhouse gas can act as a driver for global temperatures (Genthon et al., 1987; Petit et al., 1999; Sigman et al., 2000). Around 13-20% (Southern Hemisphere) to max. 64% (Northern Hemisphere) of climatic forcing is contributed by insolation while CO_2 contribution is around 50 - 84% (Genthon et al., 1987). Studies have long shown that the carbon cycle's potential to modify the carbon content of the atmosphere and ocean is the most important control on the temperature response to external forcing. Not only can this include the direct control on CO_2 by storage or release in or from deep-sea carbonate, a change in ocean chemistry can fundamentally affect the oceans capability of storing CO_2 (Goodwin et al., 2009).

1.3 The global carbon cycle

The global carbon cycle describes the exchange of atmospheric CO_2 between and the storage of carbon in various carbonate reservoirs. Fluxes among atmospheric and continental (soils, vegetation, freshwater) reservoirs are rapid, acting on timescales of a few years. Exchange of carbon between surface ocean waters and surface sediments act on timescales of decades to millennia. Quick turnover and brief storage times of carbon characterize this fast domain of the carbon cycle (Fig. 1.3).

The slow carbon cycle domain describes the storage of large amounts of carbon in the geologic reservoir comprising rocks and sediments on timescales of 10^3 to 10^6 years. The atmospheric carbon reservoir comprises around 600-700 PgC and biosphere and soils on land about 2.100 PgC. In the surface and deep ocean, carbon is mostly available as dissolved inorganic carbon (~ 38.000 PgC) and dissolved organic carbon (~700 PgC) which makes the global ocean the largest carbonate reservoir (Ciais et al., 2014; Mackensen et al., 2019) (Fig. 1.3).

Both slow and fast domain exchange carbon through balance of CO_2 from volcanic emissions and metamorphic rock alteration by weathering and deposition as marine carbonate sediments in the deep ocean (Berner, 1999; Berner and Caldeira, 1997; Ridgwell and Zeebe, 2005; Sundquist, 1986).

Although the flux between the fast and slow carbon cycle is small (below 0.3 PgC/yr), weathering of terrestrial silicate rocks and deposition as sediments in the ocean is one of the major sinks of carbon and the most effective long-term stabilizer of atmospheric CO_2. The formation of marine carbonates by accumulation of calcareous shells of marine microorganisms describes the export from surface ocean to deep ocean reservoirs where carbon is stored for a long time (Ciais et al., 2014). The weathering process, drawing down CO_2 by the reaction with $CaCO_3$ is connected to the oceanic carbonate accumulation by providing reactants for the formation of carbonate sediments. Warm climatic conditions enhance weathering and CO_2 drawdown. In form of carbonate sediments on the sea floor, CO_2 is removed from the system for hundred to millions of years. Dissolution of carbonate rocks or decarbonization by subduction into the upper mantle can return carbonate back into the cycle (Berner and Caldeira, 1997; Ridgwell and Zeebe, 2005; Walker, Hays, et al., 1981).

Anthropogenic activity has perturbed the near steady state of the fast carbon cycle domain by extracting significant amounts of fossil carbon from slow geologic reservoirs, inserting it into

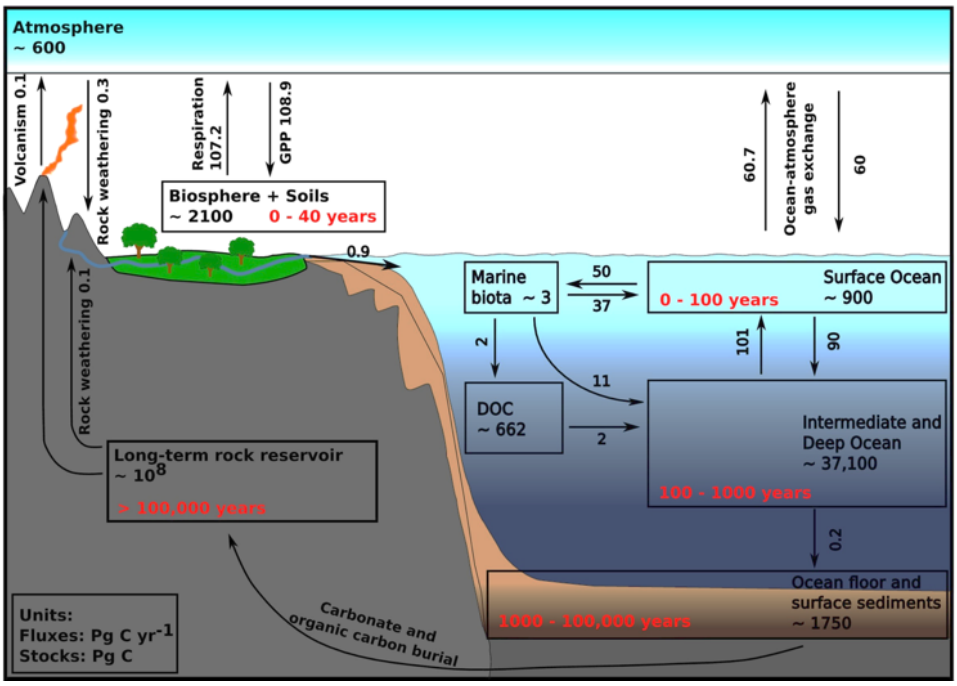

Figure 1.3: The global carbon cycle in a schematic including carbon stocks in PgC and annual carbon fluxes in PgCyr^{-1} (Hülse, Arndt, Wilson, et al., 2017). Time-scales at which each of the carbon reservoirs acts on changing the atmospheric CO_2 concentration are indicated by numbers in years. Carbon reservoirs of oceanic sediments and rocks control atmospheric carbon concentrations on timescales of 1.000 to 100.000 years. After CO_2 has been absorbed by the surface ocean, the flux of carbon between the surface and the intermediate ocean is the most effective one.

the atmosphere. In addition, extensive land change (deforestation) has significantly altered the capability of the land vegetation to store carbon by plant photosynthesis (Ciais et al., 2014).

Most of the anthropogenic carbon entering the atmosphere will be absorbed by the ocean via gas exchange at the atmosphere-ocean interface, driven by the differences in partial CO_2 (pCO_2) pressure between air and water (Archer, Kheshgi, et al., 1998; Ridgwell and Zeebe, 2005). Increasing concentrations of CO_2 in the water significantly changes the ocean chemistry, altering the capability of the ocean to absorb additional carbonate and interfere in global warming. Differences in the storage times of carbonate in the various reservoirs implies that feedbacks within these individual reservoirs vary in response-times to climatic changes as well as in the direction of the efficiency (negative or positive feedbacks).

While the weathering component acts over millions of years and counteracts climatic warming, the formation of carbonate sediments in the marine realm can contribute to rising atmospheric CO_2 concentrations on time-scales below 100.000 years (Berner, 1999; Berner and Caldeira,

1997; Ridgwell and Zeebe, 2005). This has implications for the sequence of responses due to the anthropogenic CO_2 perturbation and the effect on temperature. It will also affect the response of the climate system to temperature changes forced by astronomical variations, similarly acting on different time scales.

The chemical reactions of the removal of atmospheric CO_2 and the deposition of sediment in the ocean can be described by a series of chemical equations (Berner, 1991; Berner and Caldeira, 1997; Caldeira, Akai, et al., 2005; Ridgwell and Zeebe, 2005; Sundquist, 1993; Walker and Kasting, 1992; Zeebe and Wolf-Gladrow, 2001).
Initially, the ocean takes up atmospheric CO_2 ($CO_{2(aq)}$):

$$H_2O + CO_{2(aq)} = H^+ + HCO_3^- \tag{1.1}$$

Once CO_2 is dissolved in the ocean it dissociates into different carbonate species, that make up the total concentration of dissolved inorganic carbon (DIC) in the ocean water:
$\text{DIC} : CO_{2(aq)} + HCO_3^- + H_2CO_3 + CO_3^{2-}$
The concentration of DIC defines the solubility of CO_2 and control together with the temperature and the pH value the capability of the ocean water to take up CO_2 and remove it from the atmosphere. The concentration of carbonate ions $[CO_3^{2-}]$ rapidly decreases with seawater acidification, limiting carbonate buffer capacity of the ocean.
Dissolved CO_2 will react with calcium carbonate of the sea floor and cause dissolution of existing sediments, consuming CO_2. A consequence is a restored balance between carbonate species in the ocean and a recovery of the pH value. The effect of carbonate formation on atm. CO_2 is controlled by the capability of the ocean to take up atm. CO_2, the carbonate saturation (Ωcarb). A reduction of CO_2 in the ocean thermodynamically favors formation of $CaCO_3$ over dissolution, to equilibrate for missing dissolved CO_2.

$$\Omega = \frac{[Ca^{2+}][CO_3^{2-}]}{K_{sp}} \tag{1.2}$$

K_{sp} is the solubility product for the specific $CaCO_3$ mineral and is a function of temperature, salinity, and pressure (depth) (Millero, 1995; Mucci, 1983).

$$K_{sp} = [Ca^{2+}][CO_3^{2-}] \tag{1.3}$$

K_{sp} is temperature and salinity dependant by:

$$\begin{aligned} logK^*_{sp}(cal) = &-171.9065 - 0.077993 * T \\ &+ 2839.319/T + 71.595 * \log T \\ &+ (-0.77712 + 0.0028426 * T + 278.34/T)S^{\frac{1}{2}} \\ &- 0.7711 * S + 0.004149 * S^{\frac{1}{2}} \end{aligned} \tag{1.4}$$

Another important measure in the carbonate system is the alkalinity, an indicator of charges, the sum of cations and anions in the water. In terms of carbonate, alkalinity can be defined as: $CA = [HCO_3^-] + 2[CO_3^{2-}]$, as part of the total alkalinity (TA):

$$\begin{aligned} TA = &[HCO_3^-] + 2[CO_3^{2-}] + [B(OH)_4^-] + [OH^-] \\ &- [H^+] + [HPO_4^{2-}] + 2[PO_4^{3-}]] + [H_3SiO_4^-] \\ &+ [NH_3] + [HS^-] - [HSO_4^-] - [HF^-] - [H_3PO_4] \end{aligned} \tag{1.5}$$

Biological and chemical synthesis of calcium carbonate ($CaCO_3$) in the ocean can be described by the following equation:

$$2HCO_3^- + Ca^{2+} -> CaCO_3 + H_2O + CO_2 \tag{1.6}$$

Silicate minerals as remains from the weathering process of continental rocks are transported into the ocean provide dissolved Ca^{2+} for further chemical reactions:

$$3H_2O + 2CO_2 + CaAl_2Si_2O_8 = Al_2Si_2O_5(OH)_4 + Ca^{2+} + 2HCO_3^- \tag{1.7}$$

The complete process of weathering, transport, dissolution and deposition has in the end consumed atm. CO_2 and deposited in chemically linked solid forms in the deep ocean. This reservoir an only be reinserted into the system over long geologic time scales by uplift or tectonic activity.

$$CO_2 + 2H_2O + CaAl_2Si_2O_8 + Al_2Si_2O_5(OH)_4 + CaCO_3 \tag{1.8}$$

Despite all efforts to entangle the path of anthropogenic CO_2, there are large uncertainties about the fate of anthropogenic CO_2. One example is the assessment of the direction and magnitude of biologic fixation of carbonate in the surface waters and export to deeper waters and the effect on changing the ocean chemistry (Sarmiento et al., 2006).
Applying carbon cycle models on past and future climatic events is the key to tackle unsolved questions about the carbon cycle response to short- and long-term perturbations.

1.4 Earth System Modelling

Numerical simulations of Earth System processes in Earth System Models of Intermediate Complexity (EMICs) are the key to test carbon cycle feedbacks on long astronomical timescales. They build the bridge between computationally expensive General Circulation Models and simplified box-models. Although the resolution is restricted and some processes are parametrized, they allow for complex simulations of up to several million-year simulations in large ensembles and still represent (paleo)climate dynamics in detail (Claussen et al., 2002). Early carbon cycle models of Walker, Hays, et al., 1981 (WHAK), Berner, Lasaga, et al., 1983 (BLAG) and Volk, 1987 were the first studies to test the role of carbonate and silicate weathering on the evolution of climate applying models of different complexities (Brady, 1991). Since these first box models, the development of three-dimensional models representing ocean, land and atmosphere in a more complex manner has significantly revised the accuracy of models to reproduce past climate variations (Review in Hülse, Arndt, Wilson, et al., 2017). The complete history of applying different kind of models on climate reconstructions is long and beyond the scope of this thesis chapter (refer to Brady, 1991; Claussen et al., 2002; Eby et al., 2013; Flato et al., 2013; Hülse, Arndt, Wilson, et al., 2017). However, constant development and advances in Earth System modelling has created a variety of EMICs with detailed representation of the carbon cycle. Especially the inclusion of temperature dependency of the weathering feedbacks and carbonate formation in models has largely improved the temperature reconstructions using Earth System Models (Brady, 1991).

1.4.1 cGENIE Earth System Model

The 'Grid ENabled Integrated Earth' System Model of Intermediate Complexity (GENIE) is a modularised framework for Earth System Modelling. Similar to other Earth System Models of Intermediate Complexity (EMICs), many processes in GENIE are parametrized, rather than formulated in physical equations compared to computationally expensive General Circulation Models (GCMs). This allows simulations in GENIE to approximate the dynamics of many complex processes that occur in the ocean, atmosphere and sediments while still being able to run in large ensembles or for a long simulation time (several thousand up to a few millions of years). The base of the model comprises a 3-D dynamical ocean circulation model, the 'Goldstein'-Ocean, a 2-D energy-moisture balance model of the atmosphere, and a thermodynamic sea ice model

(Edwards et al., 2005). The version used for this thesis ('carbon-GENIE', or 'cGENIE' - current branch: cgenie.muffin, (support by Ridgwell, 2019)), refers to a model extension developed to facilitate computationally efficient runs of up to multi-million year simulations with a complex representation of biogeochemistry, marine carbon cycling (Ridgwell, Hargreaves, et al., 2007), weathering of continental rocks (Colbourn, Ridgwell, and Lenton, 2013) and sedimentation of organic (Hülse, Arndt, Daines, et al., 2018) and inorganic carbonate (Ridgwell and Hargreaves, 2007) in the deep ocean.

To implement astronomical forcing, incoming solar radiation is formulated by the translation of

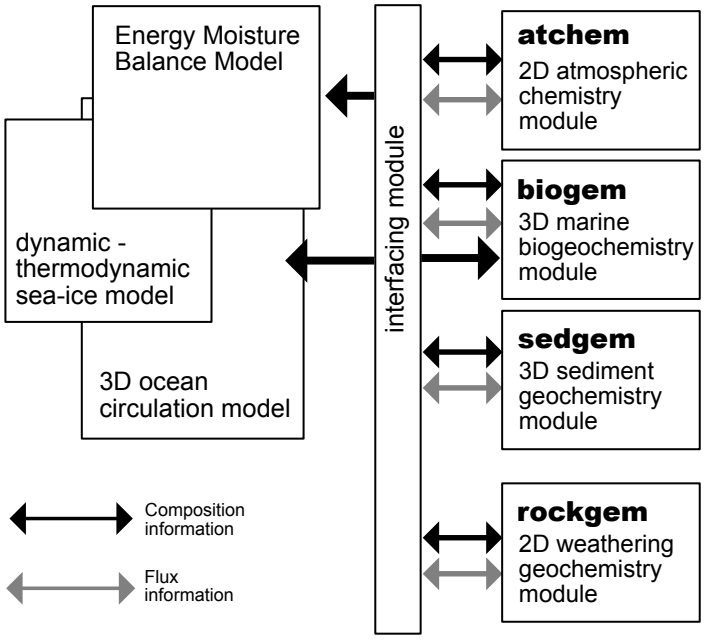

Figure 1.4: Schematic illustration of cGENIE modules. Adapted from Colbourn, Ridgwell, and Lenton, 2013

orbital parameters for eccentricity, obliquity, and precession into time and latitude-dependent insolation as per Berger, 1976.

All available modules can be linked together for the required level of complexity. The user can perform low-complexity test in a 'box-model' by solely linking the atmosphere and a (shallow) 2D-ocean or simulate a highly complex Earth System with processes in the atmosphere and ocean as well as a full ocean circulation.

- Energy Moisture Balance module (eb) (Weaver et al., 2001)
- 3D GOLDSTEIN Ocean module (go) (Edwards et al., 2005) (including a sea-ice module)

- 2D Atmospheric chemistry module (ac) (Ridgwell, Hargreaves, et al., 2007)
- Marine biogeochemical module (bg) (ibid.)
- Sedimentary Geochemical module (sg) (Ridgwell and Hargreaves, 2007)
- Rock geochemical module (eg) (Colbourn, Ridgwell, and Lenton, 2013)
- Organic Matter ENabled SEDiment model (OMEN-SED) (Hülse, Arndt, Daines, et al., 2018)
  (not implemented in simulations of this thesis)

The wide-spread application of cGENIE as well as other GENIE-versions for Eocene climate reconstruction and data-comparison studies has proven the capability of the model to reproduce past climatic conditions (e.g Keery et al., 2018; Kirtland Turner, 2018; Panchuk et al., 2008; Ridgwell and Schmidt, 2010). A review of GENIE's modules in comparison to other EMIC's can be found in Eby et al., 2013; Flato et al., 2013. In combination with the high computational efficiency, cGENIE's complex representation of marine biogeochemistry make this model a good choice for this study.

1.4.2 Implementation of carbon cycle experiments in cGENIE

Simulations in cGENIE require two 'spin-up' configuration files that initiate the values for the climate system, which set the baseline for the desired state of the climate. Once all necessary boundary conditions are set and the ocean circulation is in equilibrium, experiments can be performed.

The 'base configuration' comprises information for the continental setup, i.e. boundary and topography conditions for the ocean and the atmosphere, grid information for the sediment (sedgem) and rock-weathering (rokgem) module as well as a list of simulated ocean, sediment and atmosphere tracers and their default or adjusted initial values. In the addition, some 'physical climate configuration' parameters are defined, such as ocean diffusivity, ocean salinity, and others.

Carbon cycling in the oceans is represented through the production, export, and remineralization of both organic and inorganic forms of carbon and ocean circulation. To use a system with a full carbon cycle and a weathering flux, several steps have to be performed.

Firstly, the system is set up as a 'closed system', meaning that the total amount of sedimentary calcium carbonate ($CaCO_3$) preservation is calculated based on the initial values for ocean

alkalinity and prescribed levels of CO_2, while the carbonate weathering rate is automatically balanced with the $CaCO_3$ burial rate. The ocean, atmosphere and biogeochemistry respond to fixed atmospheric CO_2, which all control the flux of buried carbonate at the end of this equilibrated spin-up stage.

For the next step, the model can be set up to be 'open' with respect to the inorganic carbon cycle via inclusion of temperature-dependent terrestrial rock weathering and burial of carbonate in deep sea sediments (Colbourn, Ridgwell, and Lenton, 2013; Kirtland Turner and Ridgwell, 2013; Ridgwell and Hargreaves, 2007; Ridgwell, Hargreaves, et al., 2007). This implies that the weathering fluxes in this step are manually (instead of automatically) set equal to the burial flux of carbonates from the previous experiment, but distributed between silicate and carbonate weathering. In simulations for this thesis, we use a 50:50 ratio for silicate and carbonate weathering fluxes. Additionally, the weathering rates are not fixed, but rather set to vary as a function of surface land temperature whereby higher temperatures lead to more intense weathering. Carbonate weathering is balanced by (volcanic) CO_2 out-gassing (set equal) and silicate weathering has to be corrected for a surplus or deficit in weathered Ca^{2+} that is caused by seasonal and inter-hemispheric temperature differences. The temperature dependency of the weathering feedback is corrected for by setting the reference to the surface land temperature retrieved from the previous run. Weathering is eroding carbonate and silicate rocks on the continents and run-off into the ocean is based on watersheds, that are defined for the continental configuration (Edwards et al., 2005). We note, that cGENIE has an option to implement run-off dependency of the weathering module, but due to the low impact of this parameter on climate and CO_2 (Colbourn, Ridgwell, and Lenton, 2013), we have chosen not to include this into our experiments.

The 'user configuration' sets a number of parameters that define the experiment itself (e.g. biologic production, organic and inorganic export, remineralization and sedimentation conditions, greenhouse gas concentrations fixed or changing throughout the experiment), followed by technical instructions for the amount of data saved or how many debug-information will be given to the user. In addition to standard experiments, we require to add orbital parameters that we can either fix at certain values (if not default) or implement them as time-varying orbit option.

For simulation performed for this thesis using orbital variability as a forcing for long-term climate, we enabled the CO_2-climate feedback to reconstruct how effects on the carbon cycle affect global climate.

Climate sensitivity to astronomical variations in cGENIE

2

Abstract

A close connection between the carbon cycle and climate has long been established, often via changes in atmospheric CO_2 and ocean carbon sequestration. Carbon cycle feedbacks which impact atmospheric CO_2 concentrations in response to changes in the amount or distribution of insolation can modify the response of the climate state to astronomical forcing.

The cGENIE Earth System Model of Intermediate Complexity is a useful tool to assess the Earth's response to astronomical forcing under diverging environmental boundary conditions. cGENIE provides a complex formulation of the carbon cycle and marine biogeochemistry and can be used with a low grid-resolution allowing for million-year long simulations over astronomical timescales. Here, we conduct sensitivity experiments to quantify the effect of astronomical forcing on climate as a function of different baseline atmospheric CO_2 levels (834 ppm - ice-free ('warm state'), 278 ppm ('cold state')), for a simplified single continent setup in cGENIE. In order to better understand how carbon cycle feedbacks induced by astronomical variations impact climate, we conduct tests including a representation of the carbonate and silicate weathering feedback mechanisms which are important controls on long-term climate. These experiments quantify how weathering intensity and marine bioproductivity as part of the carbon cycle can alter the surface air temperature distribution relative to incoming insolation.

2.1 Scientific Background

Earth's radiative balance on long timescales ($10^4 - 10^5$ years) is driven both by modifications in distribution of incoming solar radiation as a function of astronomical forcing and the outgoing long-wave radiation linked to changes in atmospheric greenhouse gas concentration. Internal feedbacks can modify the response of the climate system to astronomical forcing. Indeed, increasingly high-resolution reconstructions of deep-time climate, often very different from the climate of the Neogene, have revealed a variable imprint of astronomical variability (Pälike et al., 2006; Vahlenkamp et al., 2018). Firstly, the dominant orbital period in global benthic oxygen isotope records has shifted across the Cenozoic Era (last 65 My) (e.g. De Vleeschouwer et al., 2017). Secondly, the amplitude of changes in the global carbon cycle have differed in the past. During relatively warm periods of the Eocene (Zachos, Pagani, et al., 2001), carbon isotope of the deep-ocean carbon reservoir fluctuate on orbital timescales with a lower amplitude than during relatively cold periods such as Oligocene, the Pliocene and the Pleistocene (De Vleeschouwer et al., 2017). The weathering feedback provides a plausible mechanism (Zachos, Pagani, et al., 2001) that could amplify or dampen the temperature response to astronomical forcing depending on the prevailing climate state.

The impact of quasi-periodic variations in Earth's orbital parameters on climate is well established. Precession, obliquity and eccentricity are the three key orbital parameters that control both the amount and the seasonal and latitudinal distribution of insolation. They define the insolation received at a certain position on earth over the course of a year and vary periodically over long time scales, known as the Milankovitch cycles (Berger, 1978; Imbrie and Imbrie, 1980; Laskar, Robutel, et al., 2004; Milankovitch, 1941).

Eccentricity quantifies the shape of the Earth's orbit around the sun and is the only astronomical parameter that controls the absolute amount of insolation received by Earth over the year.

The seasonal effect by eccentricity variation is also more important than the annual effect on temperature. The total effect of eccentricity on the temperature distribution over the year can be calculated by the temperature difference between aphelion and perihelion (as in Laskar, Fienga, et al., 2011 (eq.[1])). Temperature difference between aphelion and perihelion ($\delta T_{P/A}$) can be calculated by $\delta T_{P/A} = e *$ Total outgoing long-wave radiation . Assuming a black body outgoing long-wave radiation of 300 K (26.65°C). A change of 0.02 in eccentricity would translate to temperature change between aphelion and perihelion ($\delta T_{P/A}$) of 0.0537 °C (ibid.,[1]), which indicates

that the direct impact of eccentricity on global annual temperature is small.
Precession is the measure of the angle between the vernal equinox and the perihelion (Berger, 1988) and impacts the strength of the seasons by defining when summer/winter occur in either hemisphere. The variation of eccentricity strongly influences the effect of precession, as during a circular orbit the effect of precession is nullified, while it is the strongest during an elliptical orbit. With a circular orbit, Sun-Earth distance at perihelion and aphelion are approximately equivalent, minimizing differences in insolation across seasons in opposite hemispheres. With a more elliptical orbit, the Earth -sun distance at perihelion is minimized, leading to an enhanced seasonal contrast, that is especially pronounced in the high latitudes (Imbrie and Imbrie, 1980).
The Earth's axial tilt, obliquity, determines the latitudinal distribution of incoming solar radiation. A high obliquity angle will amplify the seasonal contrast in a given hemisphere, while a lower obliquity angle will dampen the seasonal contrast. This effect is most effective in the high latitudes. In general, high eccentricity and high obliquity have been linked to globally warmer climates in Earth history (e.g. Ganopolski and Roche, 2009). The combination of all three orbital parameters in extreme values and the resulting insolation distribution on each hemisphere defines a 'cold' or 'warm' orbit (Bounceur et al., 2015; Ganopolski and Roche, 2009) and helps to simulate climatic effects under extreme orbital contrasts.
One possible mechanism that can amplify the effect of insolation changes from astronomical variation on the climate response (Ruddiman, 2003; Ruddiman and Raymo, 2003; Shackleton et al., 2000; Zachos, Pagani, et al., 2001) is the weathering feedback of carbonate and silicate rocks as part of the carbon cycle. The main control on this process is the long-term, geochemical carbon cycle that removes atmospheric CO_2 by the weathering of continental silicate rocks.
Weathering is presumed to respond to global temperature and is the balance between geological carbon sequestration by silicate weathering and volcanic outgassing. By controlling the relative distribution of carbon between the atmosphere and oceans via changes in ocean alkalinity it is part of the long-term carbon cycle (Berner, 1991, 1994, 1999; Berner and Caldeira, 1997; Berner, Lasaga, et al., 1983).

Separating the effect of climate state, weathering and astronomical forcing on the climatic response has it's difficulties in a model including time-varying astronomical forcing to control climate variability and feedbacks responding to these variations, such as the temperature and CO_2-dependant feedbacks in ocean and atmosphere. To grasp the magnitude of these effects on

altering the climatic response to the insolation forcing, it is worthwhile to test these effects on climate in simplified model simulations, separating for individual impact.
Sensitivity simulations of this chapter are set up to describe the range of temperature variation that are caused by maximal changes in obliquity and eccentricity. We compare this temperature variation to the impact of carbon cycle feedbacks and weathering on the baseline climate. This is tested by comparing a set of equilibrium runs with a simple 'climate-only' setup and a more complex setup with an implemented carbon cycle and weathering module. As the background climate is an important factor in controlling the climatic response to astronomical variation by determining the strength of feedback mechanisms. We quantify both the climate response to astronomical forcing as well as the 'carbon cycle effect' between cold versus warm background climate states in cGENIE. This will help to determine the expected magnitude in temperature variability forced by all considered boundary conditions.

2.2 Model setup and design

We set up cGENIE with a relatively low-resolution 18x18 grid (equal area in longitude and the sine of latitude) with 8 ocean levels that increase in thickness with depth and employ a continental scheme encompassing one pole-to-pole continent, four grid cells wide, and one ocean basin, 3575.6 m deep at the lowest level.
We conduct 'climate-only' simulations that include an abiotic ocean and no weathering or sedimentation, which creates a 'box-model'-like setup of cGENIE with reduced physics. We then repeated our experiments utilizing a more complex setup with a full marine carbon cycle, terrestrial rock weathering and carbonate sedimentation. Experimental setup and how to implement a temperature dependent weathering is described in §1.4.2. A link to model setups and output can be found in §A.To test the impact of a weathering feedback on the response to astronomical forcing, we further simulate two baseline climate states. We simulate icehouse and greenhouse climate by predefining different initial atmospheric CO_2 start- conditions (icehouse climate - 278 ppm and greenhouse - 834 ppm). For each baseline (as in Tab. 2.1), we spin-up the model with all orbital parameters set at a minimum value and the carbon cycle closed in a first step and open in a second step (both run for 200.000 years).

2.2.1 Astronomical variation and effect on climate

The orbital sensitivity experiments are steady-state simulations in which we test various combinations of fixed eccentricity, precession and obliquity (Tab. 2.1). We define either low or high values for eccentricity and obliquity, representative of cold and warm orbital states (Berger, 1978; Ganopolski and Roche, 2009) that lead to different insolation forcing. The choice of the precession angle is important to define which hemisphere reaches perihelion in winter or summer and does not change throughout our experiments. For a 'low' obliquity forcing experiment, we combine a precession angle of 90° (Northern hemisphere winter at perihelion, i.e. modern value), eccentricity value of 0.06 (maximum ellipse) and the obliquity angle of 22.1° (minimum tilt). For a 'high' obliquity forcing experiment, other parameters remain unchanged but the obliquity angle changes to 24.4° (maximum tilt).

2.2.2 Seasonality, orbital and climate state effect

Surface air temperature (SAT, °C) as latitudinal averages from North to South and the seasonality of SAT (ΔSAT) identifies how the orbital configuration influences seasonal temperature change per latitude. We calculate seasonality of surface air temperature (SAT) as:

$$\Delta\text{Seasonality}_{SAT}(\Delta SAT) = T_{Summer} - T_{Winter} \tag{2.1}$$

where we define T_{Summer} and T_{Winter} as the monthly average temperature of the hottest and coldest months, respectively for each hemisphere.

Following Short et al., 1991, who tested the impact of astronomical forcing on climate using a simplified 2-D EBM, we calculate the effect of orbital configuration using the difference in temperature between configurations with high (high insolation) and low (low insolation) astronomical forcing.

For example, the obliquity effect (ΔO_{Eff}) on seasonality is given by the difference between seasonality on surface air temperature at maximum and minimum obliquity.

$$\text{Obl. Effect}_{\text{Surf. Air T}}(\Delta O_{Eff}) = \text{T}_{\text{Season.(hO)}} - \text{T}_{\text{Season.(lO)}} \tag{2.2}$$

Differences in ΔSAT between the cold and warm climate state of our experiment ensemble indicate the effect of the climate state on the temperature response to orbital variations.

$$\text{Climate Effect}_{\text{l. Ecc}} = \Delta\text{SAT}_{\text{834 ppm, l. Ecc.}} - \Delta\text{SAT}_{\text{278 ppm, l. Ecc}} \tag{2.3}$$

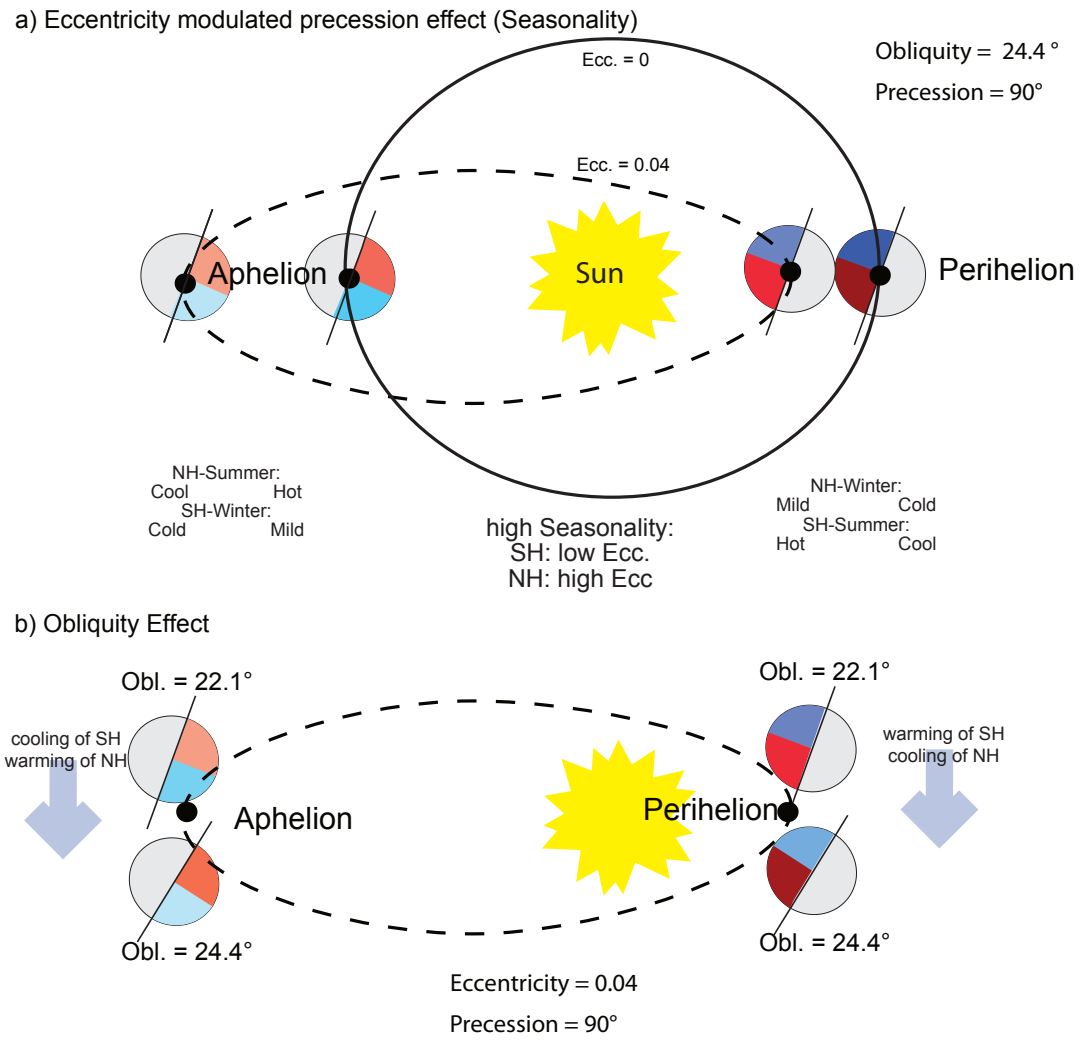

Figure 2.1: We illustrate the differences in temperature on both hemispheres individually, that should arise from only changing the orbital configuration. Dark colours (dark red, dark blue) represent warmest temperature in the respective season (blue - Winter, red - Summer), while lightest colours represent the coolest season. Eccentricity variation is presented as seasonality and closely connected to the choice of precession angle. As changing solely precession will have no influence on the yearly insolation, we have reduced the results to the eccentricity modulated precession effect, that is conveyed in seasonality variation (a). Changing the obliquity angle mostly affects the intensity of the temperatures on the hemispheres.

2.2.3 Data extraction and illustration

Data extraction from multidimensional model output (NetCDF) is performed using scripting language 'Python' (Python Software Foundation., 2019, Version 2.7.1., GCC Version 4.2.1.). Illustration is done with Python as well as vector-graph programm 'Affinity designer' (Version 1.6.1), and 'Panoply' (NASA Goddard Institute for Space Studies, 2019, Version 4.5.1.).

Table 2.1: Orbital Values and starting atm. CO_2 (ppm) values of the experiments used in this study.

Experiment	Precession	Eccentricity	Obliquity	CO_2
Ecc hE	90°	0.06	24.4	287 & 834 ppm
Ecc lE	90°	0.004	24.4	287 & 834 ppm
Obl. hO	90°	0.06	24.4	287 & 834 ppm
Obl. lO	90°	0.06	22.1	287 & 834 ppm

2.3 Sensitivity experiments

Global seasonal temperature distribution is controlled by changes in the astronomical configuration. Spatial maps of air temperature convey an equator-to-pole gradient amplified over the continent relative to the ocean. We find an emphasize on the Southern hemisphere summer relative to the Northern hemisphere summer over both land and ocean (Fig. 2.2). Raising atmospheric CO_2 level from 278 ppm to 834 ppm causes global air temperature to warm around 4.6°C and 4.7°C for high eccentricity and low eccentricity and obliquity, respectively (Tab. 2.2).

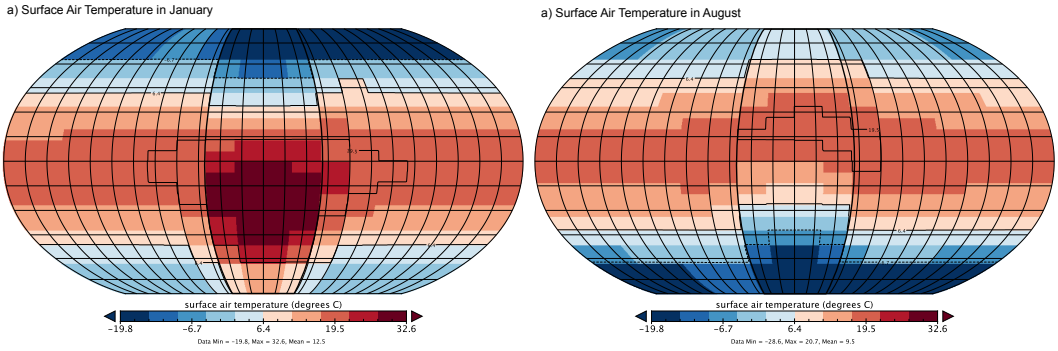

Figure 2.2: Spatial maps of surface air temperature distribution during NH-summer and winter for one experiment (high eccentricity). The continent position is indicated in the middle of the globe.

2.3.1 Seasonality of surface air temperature

ΔSAT increases exponentially with latitude in the 'cold state' and linearly in the 'warm state' experiments (Fig. 2.3). In the mid latitudes, differences in SAT are mainly forced by the orbital effect causing a temperature difference of about 0.5°C on both hemispheres. In higher latitudes above 50° North and South, low values of the climatic and orbital effect indicate higher seasonal-

Table 2.2: Classification of experiments by globally averaged surface air temperature for all experiments as yearly average

Experiment	CO_2	Yearly Av. Surf. Air T.	CO_2	Yearly Av. Surf. Air T.
Ecc hE	278	11.76	834	16.38
Ecc lE	278	10.79	834	15.54
Obl. hO	278	11.76	834	16.38
Obl. lO	278	12.05	834	16.82

ity in cold climate state experiments. We attributed this to the albedo and temperature effect of sea-ice in high latitudes under cold climate state to control seasonal variation. Under a circular orbit, sea-ice never fully retreats on the southern hemisphere, correlating to slightly higher seasonality even under warm climate.

Seasonality for the hemisphere reaching perihelion during summer is amplified under a elliptic orbit (high eccentricity) compared to a circular orbit (low eccentricity). For the hemisphere reaching perihelion during winter, the circular orbit forces higher seasonality.

In our experiments, the summer-perihelion hemisphere is the Southern hemisphere (SH), while the perihelion-winter hemisphere is the Northern (NH) one (i.e. modern value). We argue, that this is purely a choice of our precession angle of 90°C and is mirrored in an experiment with a precession angle of 270°.

This causes the yearly and globally averaged SAT temperatures mirroring a low effect of eccentricity (Tab. 2.2) and bewildering higher SAT under low obliquity, but this is a pure response to the 'switched' eccentricity effect per hemisphere.

2.3.2 Seasonality of surface ocean temperature

Seasonality in surface ocean temperature (ΔSST °C) increases with latitude, but is additionally controlled by ocean circulation. On both hemispheres, maximum seasonality occurs at high ocean velocity areas around 45-50°N and S (Fig. 2.5). Our single continent configuration results in a single prominent wind-driven gyre on each hemisphere. The boundaries of these gyres correspond to the location of maximum seasonality at 45°(Fig. 2.5).

As described in ΔSAT, the timing of winter and summer-perihelion controls the relative impact of high or low eccentricity. The effect of astronomical changes on ΔSST is stronger than on ΔSAT, though we find eccentricity variation having a greater effect on SAT than obliquity variations.

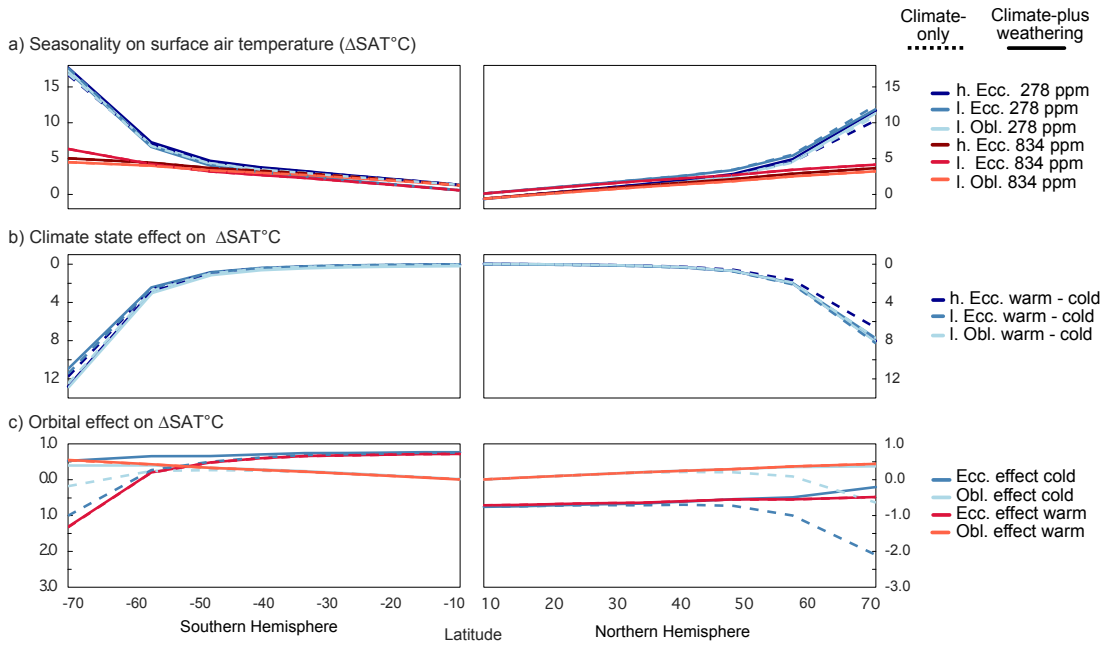

Figure 2.3: Seasonality of surface air temperature (°C) as a N-S profile. Seasonality is calculated as difference in temperature between summer and winter for each hemisphere individually.

2.3.3 Sea-ice cover effect on astronomically forced temperature

The increase of seasonality in both SAT and SST at high latitudes suggests the importance of sea-ice cover in amplifying the response to astronomical forcing. To isolate the effect of sea-ice, we run a further set of experiments prohibiting sea-ice formation even when thermodynamically favourable. Without sea ice, the temperature effect on mean ΔSAT is strongly reduced and shows hardly any differences. This demonstrates that the increase of seasonality in SAT and SST above 50° North and South is mostly forced by the albedo of sea-ice. Differences in temperature that arise between an inversed 90° and a 270° experiment can be retraced to the formation of sea-ice, that has a slight preference to form in the southern hemisphere. Disabling sea-ice formation in an additional experiment rules out these differences completely. These observations fit well to an expected pattern of seasonality differences between the NH and SH, if we consider the incoming solar radiation from the sun being only modulated by eccentricity and obliquity, as displayed in Fig. 2.1. Our results quantify the effect of sea-ice cover on the climatic response to obliquity forcing. This facilitates the observation in several proxy record studies that show

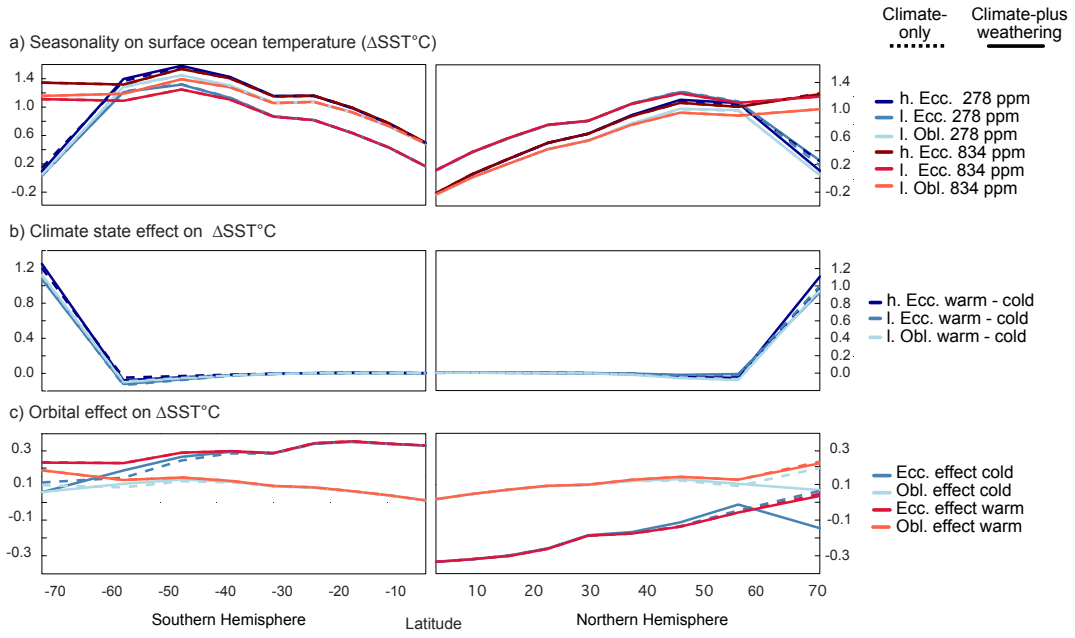

Figure 2.4: a) Seasonality of surface ocean temperature (°C) as a N-S profile. Seasonality is calculated as difference in temperature between summer and winter for each hemisphere individually, calculated as in Eq. 2.1. b) Effect of climate state, by calculating the difference between warm and cold climate state experiment for each orbital configuration (high and low Eccentricity/Obliquity). c) Effect of orbital change for each climate state, calculated as in Eq. 2.2.

an amplification of the climatic response under the presence of ice sheets (De Vleeschouwer et al., 2017; Lourens et al., 2005). Our results demonstrate the importance of the cryosphere to amplifying astronomical forcing, though in our model these must be under-estimated effects since we include only sea-ice and no land-based ice.

2.3.4 Differences in temperature response to astronomical variation on land and ocean

Diverging heat capacities of land and sea cause a different climatic response to astronomically forced insolation (Short et al., 1991; Tuenter et al., 2003). In our model, this results not only in an increase of seasonality over land relative to the ocean but also in a different response to orbital variation.

We find a higher effect of eccentricity effect over land than over ocean, during both summer and winter. We attribute most of the NH oceanic response in high latitudes to the sea-ice effect, as it is diminished with warming climate. Warmer temperatures over the SH continent are forced by

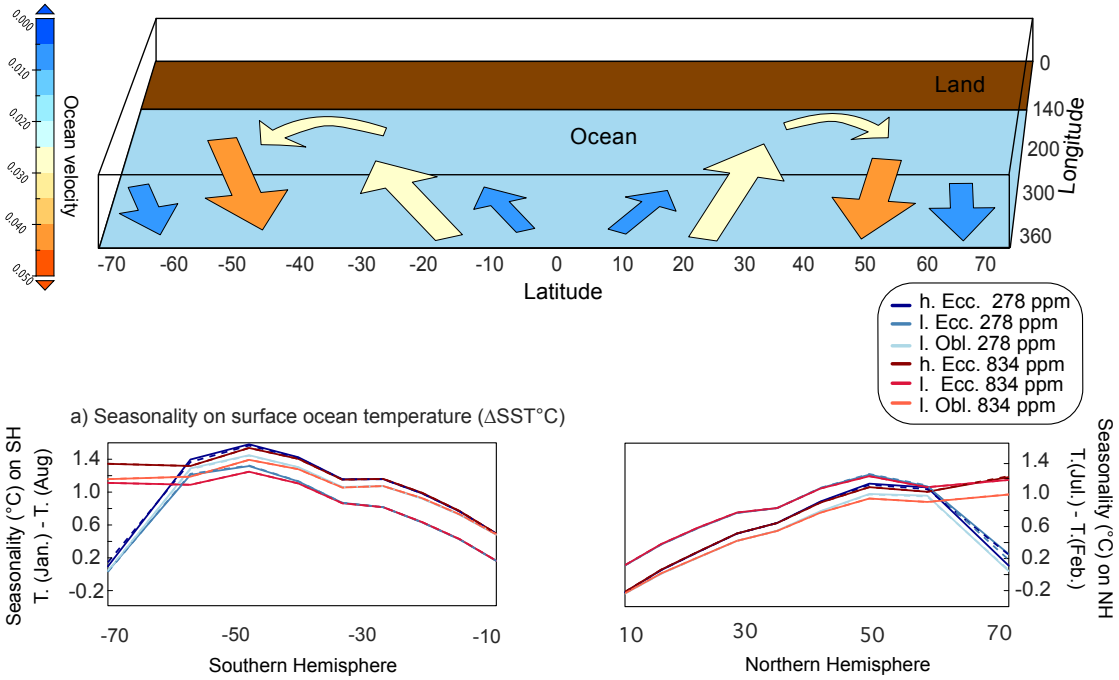

Figure 2.5: Seasonality forced by eccentricity modulated precession on surface ocean temperature, presented in latitudinal N-S profiles. We differentiate from seasonality on the southern hemisphere (Jan. - Aug.) and on the northern (July - Feb.) and compare the results to the velocity of ocean circulation (upper panel).

the timing of the perihelion during summer on this hemisphere, which has greater effect under a elliptic orbit rather than a circular one. Under warming climate, higher temperatures over both ocean and land are forced by an elliptic orbit, rather than a circular one, which indicates a decreasing importance of seasonality under high radiative CO_2 forcing.

The effect of obliquity is weaker than the effect of eccentricity over both ocean and continent and only weakly changes under warmer climate.

High obliquity forces a greater effect on summertime temperature over the continent and low obliquity forces a greater effect on wintertime temperature over the continent. A stronger response in high latitude ocean cells is caused by the sea-ice albedo effect, as seasonal differences in sea-ice concentration are enhanced during high obliquity.

Modelling studies have previously investigated the influence of continental mass on the amplification of the climate response to astronomical forcing. Short et al., 1991 test the effect of the land-sea distribution on the seasonal air temperature response to astronomical forcing

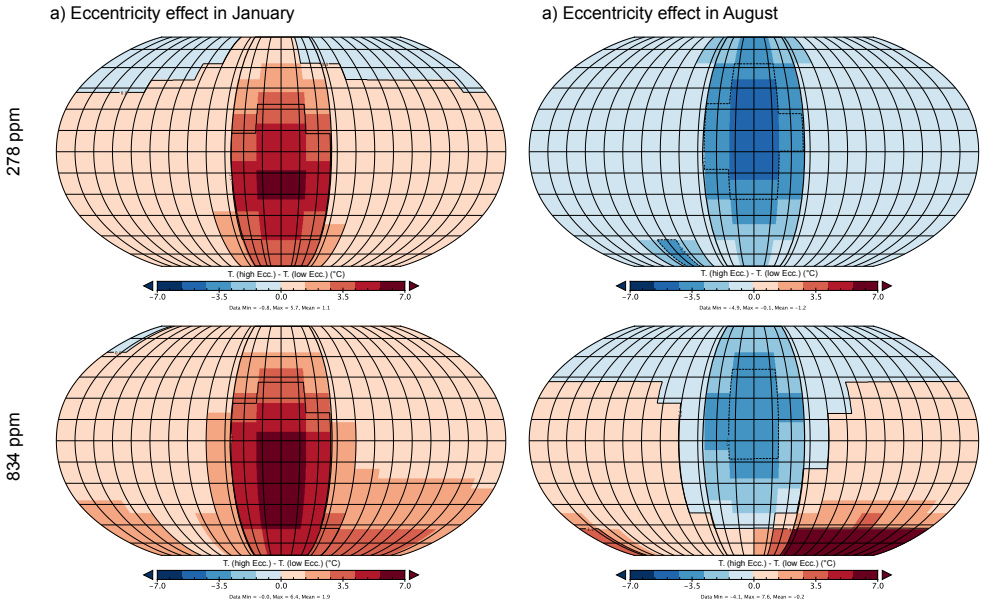

Figure 2.6: Spatial maps of eccentricity effect on SAT.

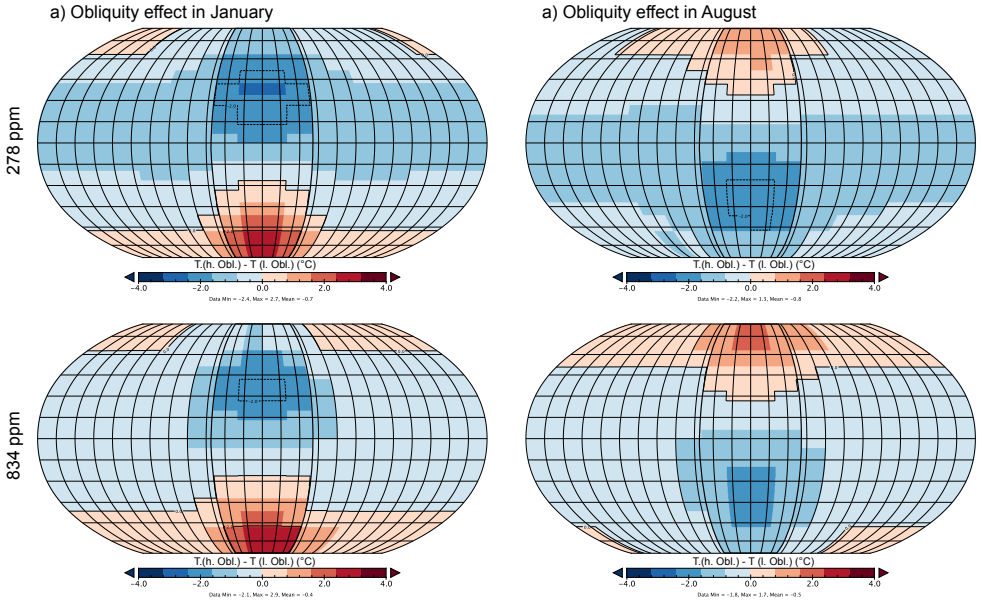

Figure 2.7: Spatial maps of obliquity effect on SAT.

using an Earth Balance Model (EBM) coupled to a 1-layer ocean (North et al., 1983). This model was built to represent heat storage, transport, loss and gain by absorption of in-and outgoing radiation at every modelled step. Though the model is only capable of modelling the seasonal

cycle without any additional feedbacks of biogeochemistry or processes such as ice-formation, they observe a direct connection between astronomical forcing and seasonal temperature response at mid latitude continental areas. They show that large continental masses such as the Eurasian continent notably amplify the effect of obliquity on surface temperature. In our results we find that high obliquity or eccentricity increases the summer temperatures over the mid to high latitude continent relative to the ocean, while low obliquity or eccentricity increases the winter surface air temperature over the continent relative to the ocean. Their results show a superposition of ocean circulation on the temperature response in oceanic regions. In contrast to the strong orbital effect over continents, the orbital effect over the ocean is modified by a redistribution of temperature anomalies due to ocean circulation. Short et al., 1991 found an obliquity effect over the continents from about 4°C (high latitudes) to 1°C (mid latitudes). An increase of the orbital effect over the continent corresponds well to our findings. However, with the simulation of a multi- layer-ocean and consequently a more realistic 3D ocean circulation (in contrast with the single layer ocean used by ibid., coupled to a sea ice model, we are able to simulate more climate-relevant processes during winter months. This reduces our modelled obliquity effect over ocean areas compared to ibid. in mid latitudes while it strongly increases the effect in the high latitude, sea-ice covered areas.

2.4 Summary of results and implication for further simulations

Seasonality in the mid latitudes is to the largest part controlled by the choice of the astronomical configuration. A minor effect on the seasonality is inferred by ocean overturning at areas of bounding east-west circulation in the ocean that can compensate short termed temperature variations. High latitude sea-ice effect on temperature overprints on astronomical effect during cold climate, but is strongly reduced in both the warm climate state (too warm to form sea-ice) and an experiment with disabled sea-ice formation. Seasonal contrast is largest during eccentricity minima on the winter-perihelion hemisphere, while eccentricity maxima cause an increase in seasonality on the summer-perihelion hemisphere, which pictures the importance of the choice of orbital parameter on the seasonal temperature distribution.

Implementing a full weathering feedback into our steady-state experiments hardly influences seasonal temperature variation. We expect feedbacks within the carbon-cycle to act as a response to short-term changes in temperature or CO_2, as they would come from dynamical orbital

variation, which are not provided in steady-state simulations.

We summarize from this observation, that a carbon cycle implementation only weakly contributes to a change in the baseline climate. We argue, that carbon cycle feedbacks will become more apparent in modifying the climate response once variable climate dynamics act on the system, which we haven't included in simulations in this study.

While a climate state change hardly influences the seasonality across all grid cells, the land- SAT response to astronomical variation is affected by a temperature increase. On both hemispheres, the response to astronomical changes increases with CO_2, though the direction of response change is regionally variable. For further analysis, we infer to consider this latitude dependency on the climatic response.

Climate state modifies the climatic response to astronomical variation

3

Fiona Rochholz[1, a], Sandra Kirtland Turner[2], Pam Vervoort[2], Maximilian Vahlenkamp[1], Andy Ridgwell[2], Heiko Pälike[1]

[a] frochholz@marum.de

[1] MARUM Center for Marine Environmental Sciences, University of Bremen, Germany

[2] Department of Earth Sciences, University of California, Riverside, California

Abstract

Over the course of the Cenozoic, Earth's climate response to astronomical forcing changed from $\delta^{18}O$ - benthic signal dominated by eccentricity-modulated precession (66-13 Ma) to an obliquity-driven signal after the mid-Miocene climatic transition (13-0.8 Ma) into the 100-kyr world of the late Pleistocene (0.8-0 Ma). Climate-state dependent environmental boundary conditions such as variations in the extent and stability of polar of ice sheets and sea ice, the carbon cycle and the large-scale ocean circulation have been shown to shape the response of Earth climate to astronomical forcing. Simulations in the cGENIE Earth System Model for a one-million-year time slice of the late Eocene demonstrate that background climate state modifies the climate response to orbital forcing, by influencing both the amplitude of temperature variability as well as the relative sensitivity of the climate system to different astronomical parameters.

Even in absence of a cryosphere, we find that the obliquity signal decreases with a warming of the climate state implying that processes other than ice volume dynamics are responsible for the shift in the orbital signal.

3.1 Introduction

Earth's astronomical cycles of eccentricity (~405 kyr and ~100 kyr), while variations corresponding to changes in Earth obliquity (~41 kyr) dominate the climatic spectrum during substantial portions of the Neogene icehouse (13-0.8 Ma) (De Vleeschouwer et al., 2017; Zachos, Pagani, et al., 2001). However, 0.8 Ma ago, during the mid-Pleistocene transition, declining greenhouse gas concentrations crossed a threshold allowing ice sheets to grow large and stable enough to sustain temperature changes on obliquity timescales (Chalk et al., 2017) resonating on a ~100-kyr timescale once again.

The absence of substantial changes in astronomical forcing and the weakness of eccentricity in the direct insolation indicate that internal climate feedback mechanisms cause these alternations. The prevailing theory is that the emergence of ice sheets in the high latitudes, most sensitive to changes in obliquity, led to the amplification of the climatic response to obliquity during the Cenozoic cooling (e.g. Ruddiman and McIntyre, 1981; Zachos, Pagani, et al., 2001). An additional role of tectonic changes in seaways (Haug et al., 1998; Zachos, Pagani, et al., 2001) or various components of the climate system including sea ice (Detlef et al., 2018; Gildor et al., 2001; Tziperman et al., 2003) the carbon cycle (Berner, 1999; Berner and Caldeira, 1997; Ridgwell and Zeebe, 2005) as well as atmospheric (Crowley et al., 1991) and oceanic circulation (Lunt, Valdes, et al., 2010). The latter study showed how orbital changes have the potential to trigger reorganizations of ocean circulation dependent on the background climate. Specifically, Southern Hemisphere overturning is more sensitive to changes in eccentricity-modulated precession and obliquity under increased greenhouse gas concentrations ((ibid.). Similarly, North Atlantic overturning intensity has been shown to be sensitive to obliquity forcing under Eocene boundary conditions (Vahlenkamp et al., 2018). These studies highlight the potentially critical role of the ocean circulation as the determinant of the climatic response to orbital forcing under varying boundary conditions.

At the end of the Eocene, between 40 to 36 Ma (Zachos, Pagani, et al., 2001), an intense climate change, including a change in pCO_2, marked the transition from the Eocene greenhouse to the Oligocene icehouse known as the Eocene-Oligocene Transition (EOT). While the early Eocene was a global greenhouse with up to 1400 ppm CO_2 (Anagnostou et al., 2016; Pearson, Foster, et al., 2009) in the atmosphere, the EOT is marked by declining temperature and decreasing CO_2 concentrations.

Analytical uncertainty and incomplete records restrict the reconstruction of the absolute atmospheric CO_2 change throughout the full interval. Reconstructions suggest concentrations of about 2x to 6x pre-industrial values and a pCO_2 drop from around 1100 ppm to 700 ppm in the Eocene throughout the EOT (Anagnostou et al., 2016; Pearson, Foster, et al., 2009; Pearson and Palmer, 1999, 2000).

Here we use the cGENIE Earth System Model of Intermediate Complexity to investigate the amplifiers and propagators of the orbital signal in the climate system. The time epoch of the late Eocene with variable atmospheric CO_2 concentrations can serve as a reference for both icehouse and greenhouse climate, while investigating the orbital forcing. We will present results from a modelling study that indicate how the climate state, defined by atmospheric CO_2 will imprint into the climatic reaction to orbital forcing. We run a 1-Ma long period with a time varying orbital solution at four different CO_2 concentrations and choose 278 ppm (1x CO_2), 834 ppm (3x CO_2), 1668 ppm (6x CO_2) and 3336 ppm (12x CO_2), to capture the possible range of Eocene CO_2 variations. We ran all subsequent experiments using the La04 solution for a time slice during the Eocene (34.5-35.5 Ma).

We find a background climate state dependency to drive the appearance of strong eccentricity or obliquity in ocean and surface air temperature, independent of changes in cryosphere or land-ocean distribution. We suggest, that the transition from an obliquity driven climate variability under cold climate to an eccentricity dominated world under hot climate is to a large extend driven by the increase of radiative forcing on eccentricity timescales.

3.2 Methodology

We apply cGENIE, an Earth System Model of Intermediate Complexity to test the sensitivity of the climate system to orbital variations as a function of the background climate state. cGENIE is an Earth System Model that comprises a 3-D dynamical ocean circulation model, the 'Goldstein'-Ocean, a 2-D energy-moisture balance model of the atmosphere, and a thermodynamic sea ice model (Edwards et al., 2005). Carbon cycling in the oceans is represented through the production, export, and remineralization of both organic and inorganic forms of carbon. The model is 'open' with respect to the inorganic carbon cycle via inclusion of terrestrial rock weathering and burial of carbonate in deep sea sediments (Ridgwell and Hargreaves, 2007; Ridgwell, Hargreaves, et al., 2007). Organic carbon burial or export is not included into our simulations. For our study we use a resolution of 36x36 grid-cells (equal area in longitude and the sine of latitude) with 16 ocean levels that increase in thickness with depth. We use an Eocene configuration with adjusted continental configuration, albedo, and ocean chemistry (Ridgwell and Schmidt, 2010).

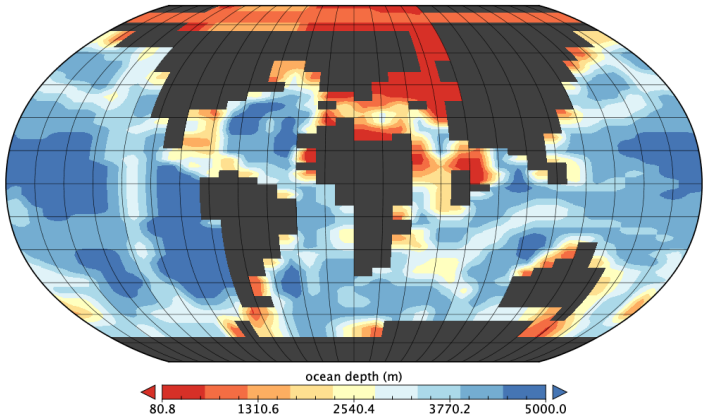

Figure 3.1: Land-Sea mask used in our experiments with a resolution of 36x36 grid cells and an ocean depth of 16 layers (Ridgwell and Schmidt, 2010)

The model is spun-up for 20.000 years as an open system with respect to inorganic carbon, with weathering and sedimentation balanced using a temperature-dependent weathering parameterization (Colbourn, Ridgwell, and M. Lenton, 2015; Turner et al., 2016). During model spin-up, orbital parameters are set to modern values from La04 (Laskar, Robutel, et al., 2004). We ran four sets of spin-ups, to varying steady state levels of atmospheric CO_2. We choose 278 ppm (1x CO_2), 834 ppm (3x CO_2), 1668 ppm (6x CO_2) and 3336 ppm (12x CO_2), to capture the possible range of Eocene CO_2 variations. We ran all subsequent experiments using the La04 solution for

Table 3.1: Experiment names including atm. CO_2 and Surf. Air T. (°C) at the beginning of the experiments. In the model, we define the climate state by varying the starting atmospheric CO_2 level (atm. CO_2), so the naming convention for the experiments is '1xCO_2' for the experiment with atm. CO_2 of 278 ppm. '3x, 6x, 12x CO_2' is representative for 3x, 6x, 12x 278 ppm as a starting atm. CO_2 level.

Experiment	CO_2	Surf. Air T. at beginning of the experiment
1x CO_2	277.9 ppm	18.12
3x CO_2	833.9 ppm	22.92
6x CO_2	1675.3 ppm	26.22
12x CO_2	3311.0 ppm	29.61

a time slice during the Eocene (34.5-35.5 Ma). Model setups can be accessed at https://github.com/FionRo/ThesisAttachmentPublic/tree/master/Chap03:4.

We extract the time-series of surface air temperature (SAT °C) as globally and yearly averaged. Ocean temperature (OCNT °C) is presented as global averages and as global averages separated in surface and deep ocean. Additionally, we present the ocean overturning strength (Sv).
For spectral analysis of our results we use the 'R' package 'astrochron'. Pie plots of frequencies in figures 3.2 and 3.3 are obtained by spectral analysis of temperature on diagnostic frequencies for each orbital parameter. We constrain the frequency range for precession between cycles of 25 and 19 kyr. For obliquity, we use frequencies between 28 and 55 kyr and for (short) eccentricity, all frequencies between 92 and 142 kyr are added up. The share of each orbital parameter is calculated as percentage from all combined orbital frequencies.

3.3 State dependant response of temperature to astronomical forcing

Temperature in the surface ocean (SST, Fig. 3.2) and atmosphere (SAT, Fig. 3.6) exhibits a climate state dependent response to orbital forcing. In both these temperature time series, the relative power of eccentricity is amplified during periods of high CO_2 while obliquity and precession are diminished (Fig. 3.2). In contrast to this observation, temperature indicates a strong response to obliquity when atmospheric CO_2 is low. With higher CO_2, the obliquity signal weakens at the expense of eccentricity. The relative increase of eccentricity power with temperature rise is similarly recorded in ocean as in the overlying air temperature (Fig. 3.6). Eccentricity power significantly increases with CO_2 at all ocean depths, relative to obliquity power.

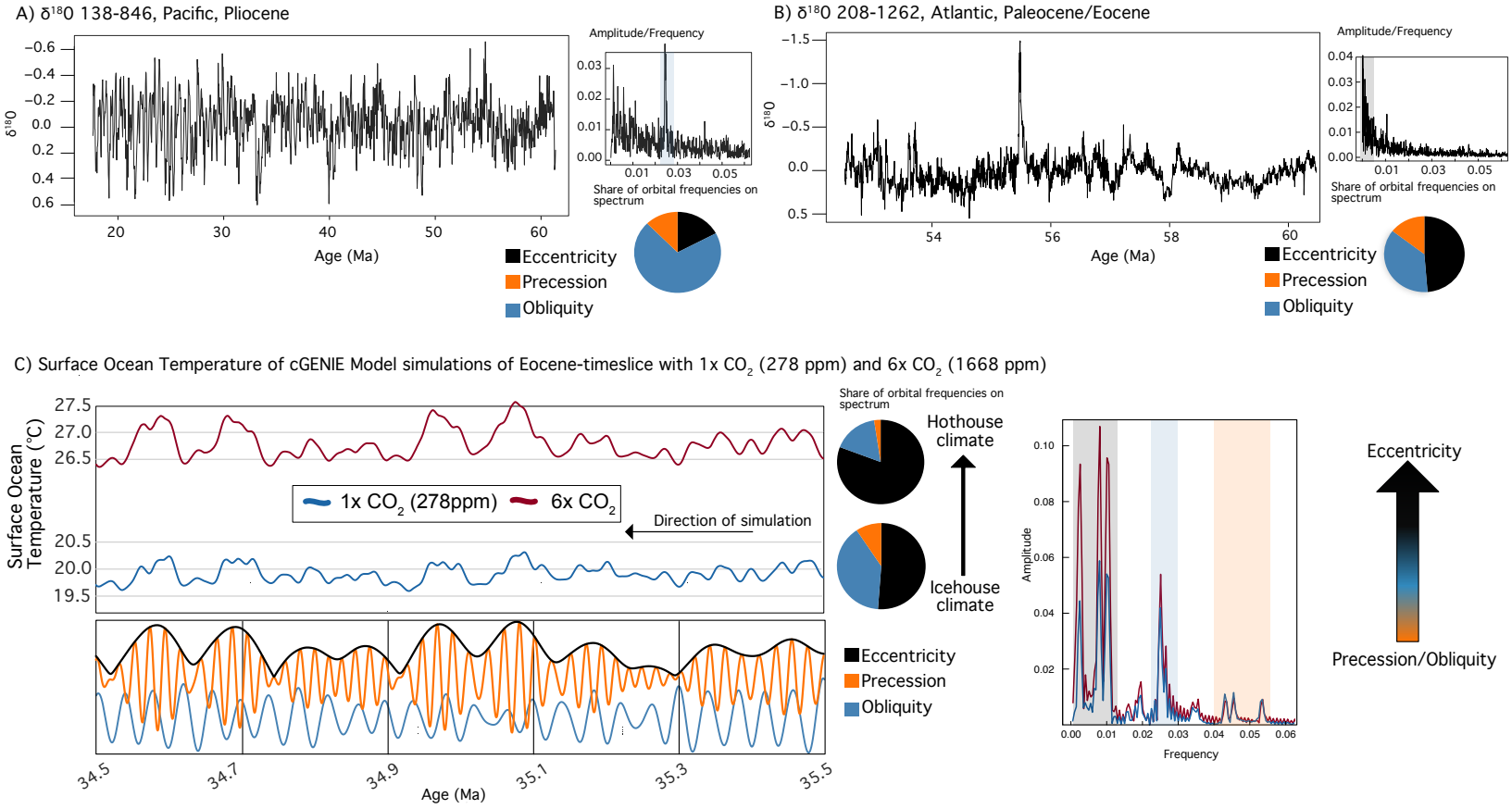

Figure 3.2: Surface ocean temperature (lower panel) for experiments 1x and 6x CO_2 . The pie plots indicate the ratio of each orbital parameter in the frequency spectrum. We additionally indicate the increase of temperature together with the shift from an obliquity-dominated world to a eccentricity-dominated world.

3.4 Independence of response shift to ice sheets, sea ice or gateway changes

In previous studies, a shift in the dominant orbital period and amplification of the amplitude under warmer climate has mainly been attributed to high latitude sheets amplifying the climatic response to obliquity (Ruddiman and McIntyre, 1981; Zachos, Pagani, et al., 2001) or changes in the seaways (e.g. Vahlenkamp et al., 2018).

While cGENIE is not coupled to an ice-sheet model and the continental configuration is fixed throughout the experiments, only the effect of sea-ice formation and albedo in the high latitudes could substitute the effect of the continental cryosphere.

To test for the effect of sea-ice on the amplitude response of the climate to the astronomical forcing, we run a 1x CO_2 with sea-ice formation disabled (Fig. 3.7). Both SH-overturning and SAT response is equivalent to 1x CO_2 with sea-ice enabled. We exclude sea-ice albedo as potential feedback mechanism to trigger the shift from a cold-obliquity to a warm-eccentricity dominated world.

3.5 Ocean circulation is not responsible for the shift in response

Modelling studies applying complex Earth System models on the Eocene climate found a high impact of the climate state on the ocean circulation as a response to orbital variability (Lunt, Dunkley Jones, et al., 2012). Simulations of warming climate suggest a reorganization of ocean overturning under high CO_2 (e.g. Lunt, Valdes, et al., 2010; Winguth et al., 2010) and an increase of the eccentricity driven Southern Hemisphere ocean circulation under high CO_2 (Lunt, Ridgwell, et al., 2011).

In our model, deep-water formation occurs in the Southern Hemisphere with no significant contribution of Northern Hemisphere sinking in our cGENIE Eocene configuration (Kirtland Turner and Ridgwell, 2013).

Ocean overturning strength increases with atm. CO_2 and spectral analysis of the SH-driven ocean circulation reveals a dominance of eccentricity-modulated precession in both cold and

warm CO_2 worlds (Fig. 3.3). However, when background climate is cold, the obliquity signal has a stronger relative power compared to a warm background climate. Energy transport between frequencies is most likely to occur from low to high frequencies, slower processes acting as a low-pass filter. While the prevalent frequency signal in ocean circulation is higher than in the overlying air temperature, it is more likely, that the spectral pattern in ocean circulation is a response to the temperature forcing, rather than a driver.

3.6 Leads and lags of climate and carbon cycle parameters

The carbon cycle response under cold climate is strongly controlled by the weathering intensity, recorded in alkalinity as a measure of available Ca^{2+} for the formation of carbonate sediments ($CaCO_3$). A temperature increase under eccentricity maxima forces the weathering response and triggers a subsequently lagged atm. CO_2 drawdown. Dissolved inorganic carbon concentration in the ocean (DIC) follows CO_2 and deposition of carbonates is favourable under high alkalinity values. The sequence of carbonate system response is supported by a LOSCAR - carbon cycle study investigating the origin of the 400-kyr eccentricity cycle in $\delta^{13}C$ records of the Paleocene - Eocene (Zeebe, Westerhold, et al., 2017). The LOSCAR weathering flux is forced by CO_2 which results in an alkalinity lag over CO_2. In cGENIE, the temperature forces weathering flux which causes a lead over CO_2 in the simulations. We find strong weathering rates in the cold simulations stabilizing the carbonate system by providing necessary Ca^{2+} for the deposition of carbonate sediments. The negative feedback of weathering on CO_2 overrules the CO_2 release during $CaCO_3$ deposition. Under warm climate, a low pH value in the ocean water forces dissolution of $CaCO_3$. High DIC and low $CaCO_3$ values indicate that most of the CO_2 is stored in dissolved form in the ocean, rather than being deposited as solid carbonate at the ocean floor. Ocean and atmosphere exchange CO_2 on shorter timescales, reducing the residence time of carbonate in the ocean. This acceleration of carbon cycle feedbacks are reflected in the response to shorter frequencies in DIC relative to the colder climate simulation (Fig. 3.4) and in a reduced lag of atm. CO_2 relative to temperature and alkalinity (Fig. 3.4, lower panel). Low weathering rates under high CO_2 are ineffective to force CO_2 drawdown, $CaCO_3$ formation controls the release of CO_2 into the atmosphere. Amplitude of SST and CO_2 on eccentricity timescales increases with warming climate (Fig. 3.8), indicating a greater effect of CO_2 on eccentricity timescales on temperature variability.

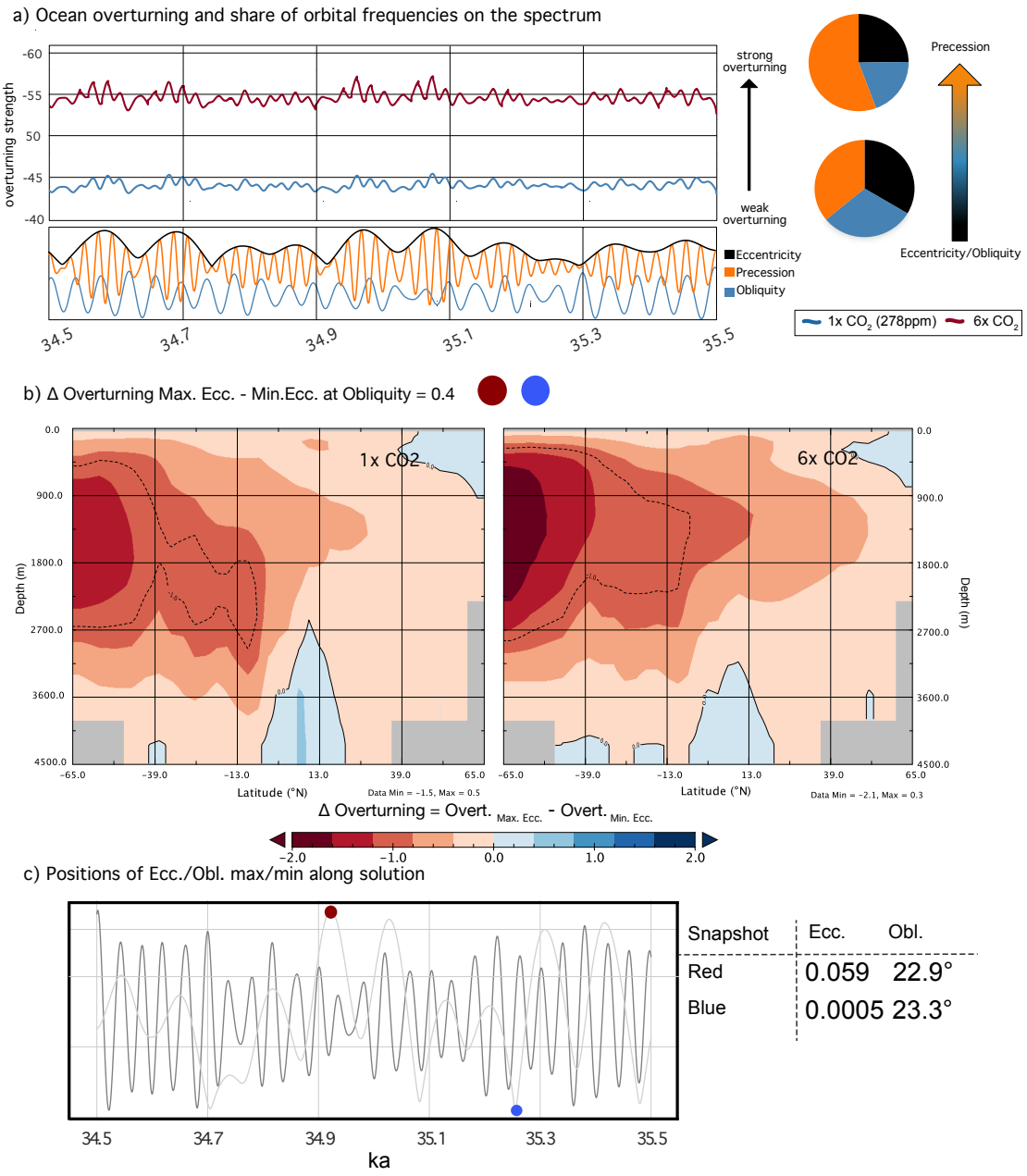

Figure 3.3: Global overturning (streamfunction) as time series of two indicative experiments (1x and 6x CO_2) (a). With increasing CO_2, the absolute intensity of overturning increases, in this setup driven by Southern hemisphere deep water formation. Ocean overturning as depth profiles for two positions along the time series with eccentricity and obliquity at maxima and minima values indicate the change of overturning strength with rising CO_2 (b). Positions are indicated in panel c to demonstrate the orbital solution at this point.

We test the reason for an increased response of the CO_2 signal on temperature by estimating the share of insolation and CO_2 on the total radiative forcing. A hypothetical 'surface ocean temperature' time series is calculated by summing up insolation forcing (65°N) and CO_2 (Fig. 3.5). While the SST time series at low CO_2 resembles a relation of 3x CO_2 plus 1x insolation forcing, the 12x CO_2- SST response can be reproduced by a hypothetical time series with 10x CO_2 plus 1x insolation forcing. A shift in the temperature signal towards an eccentricity response in the warm climate is to a large share driven by the amplification of CO_2 forcing on the total radiative forcing.

3.7 Conclusions

We find a strong response to obliquity changes under cold climate and an increase of the response to eccentricity variation under warm climate. Neither sea-ice albedo nor ocean circulation variation can be ascribed to cause the shift in astronomical response. The control of the carbonate system in the ocean shifts to assign a higher importance of atmospheric CO_2 on driving carbon cycle and subsequent climate variations on astronomical timescales. In the cold climate state, precession and obliquity signal of the insolation prevails in forcing temperature and subsequently weathering intensity. In warm climate, insolation loses in importance for the total radiative forcing and CO_2 varying on eccentricity time scales takes a greater importance in driving climatic variability. The increased eccentricity component under high CO_2 conditions can be exemplified by multiplying the insolation at 65°N with the CO_2 time series. For our 1x CO_2 simulation we find that weighing the CO_2 with a factor of 3 and adding it up with the insolation resembles global SST for this simulation. For the 12x CO_2 simulation we obtain a good fit with summing up insolation and 10xCO_2 time series.

Model limitation:

A reduced input of alkalinity from weathering under warm climate is a model internal issue caused by the technical enabling of temperature-dependant weathering. We intend to solve this issue in a further model simulation. For now, we related this to enhanced land vegetation growth reducing the flux of Ca^{2+} from the continent into the ocean.

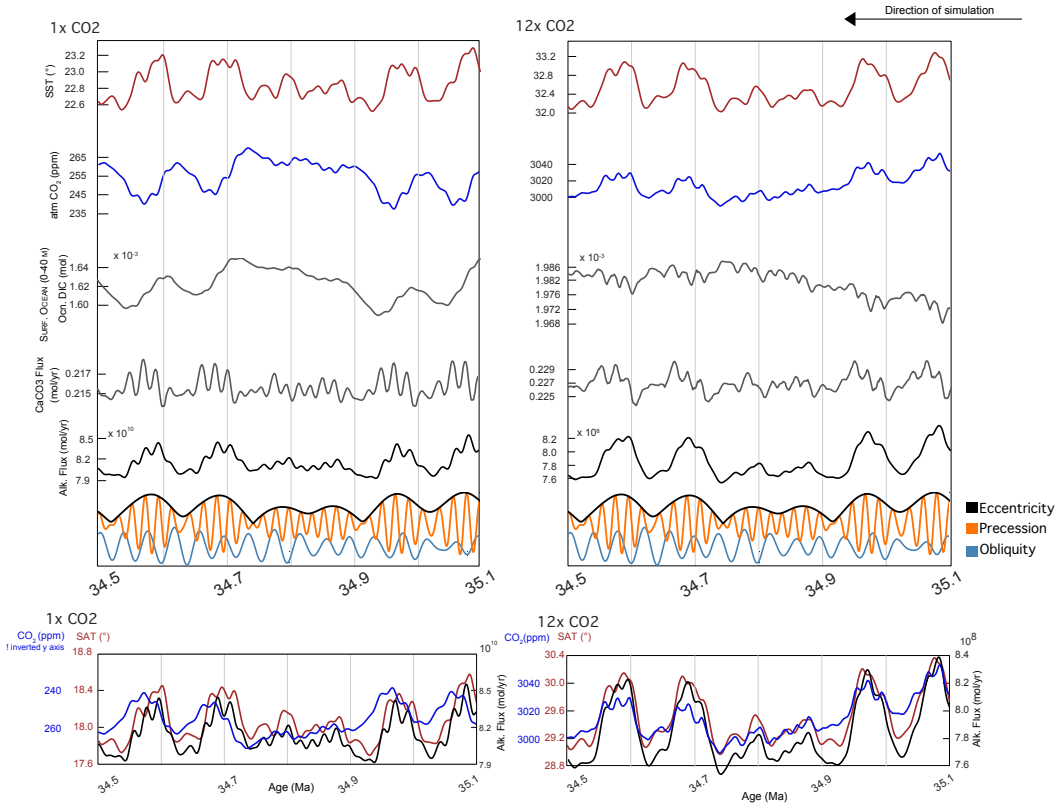

Figure 3.4: The carbon cycle response under warm and cold climate (we present results from extreme simulations of this study in a time slice of distinct eccentricity variability between 35.1 and 34.5. Ma) exhibits a difference in the response to the astronomical forcing. Weathering in cGENIE is a direct response to the temperature driven by insolation, while CO_2 is largely controlled by the negative effect of weathering drawing down the atm. CO_2 response. Carbonate sediment formation plays a reduced role in rising atm. CO_2 concentrations. Under warm climate, high dissolved inorganic carbon (DIC) indicates a dominance of the dissolved carbonate species in the ocean relative to the amount of deposited $CaCO_3$ (not shown). Due to weaker negative weathering effect on CO_2, CO_2 release of carbonate formation controls the atm. CO_2 concentration.

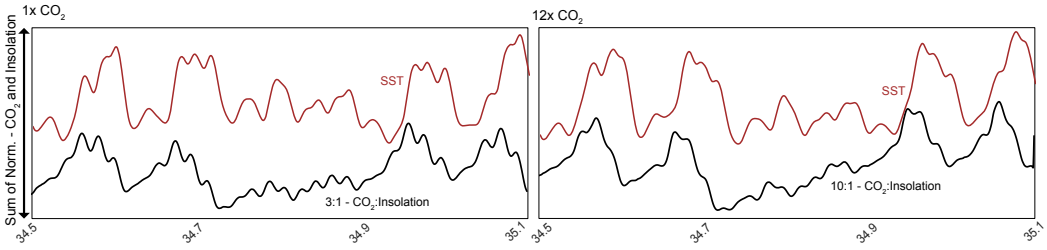

Figure 3.5: The sum of normalized CO_2 time series for 12x and 1x CO_2 and insolation at 65 °N can be calculated by weighting the two time series differently. We calculated the sum in a ratio of 3:1 and 10:1 (3*CO_2 + Insolation, 10*CO_2 + Insolation) for both simulations to indicate the increasing effect of CO_2 on surface air and ocean temperature.

Supplementary Figures

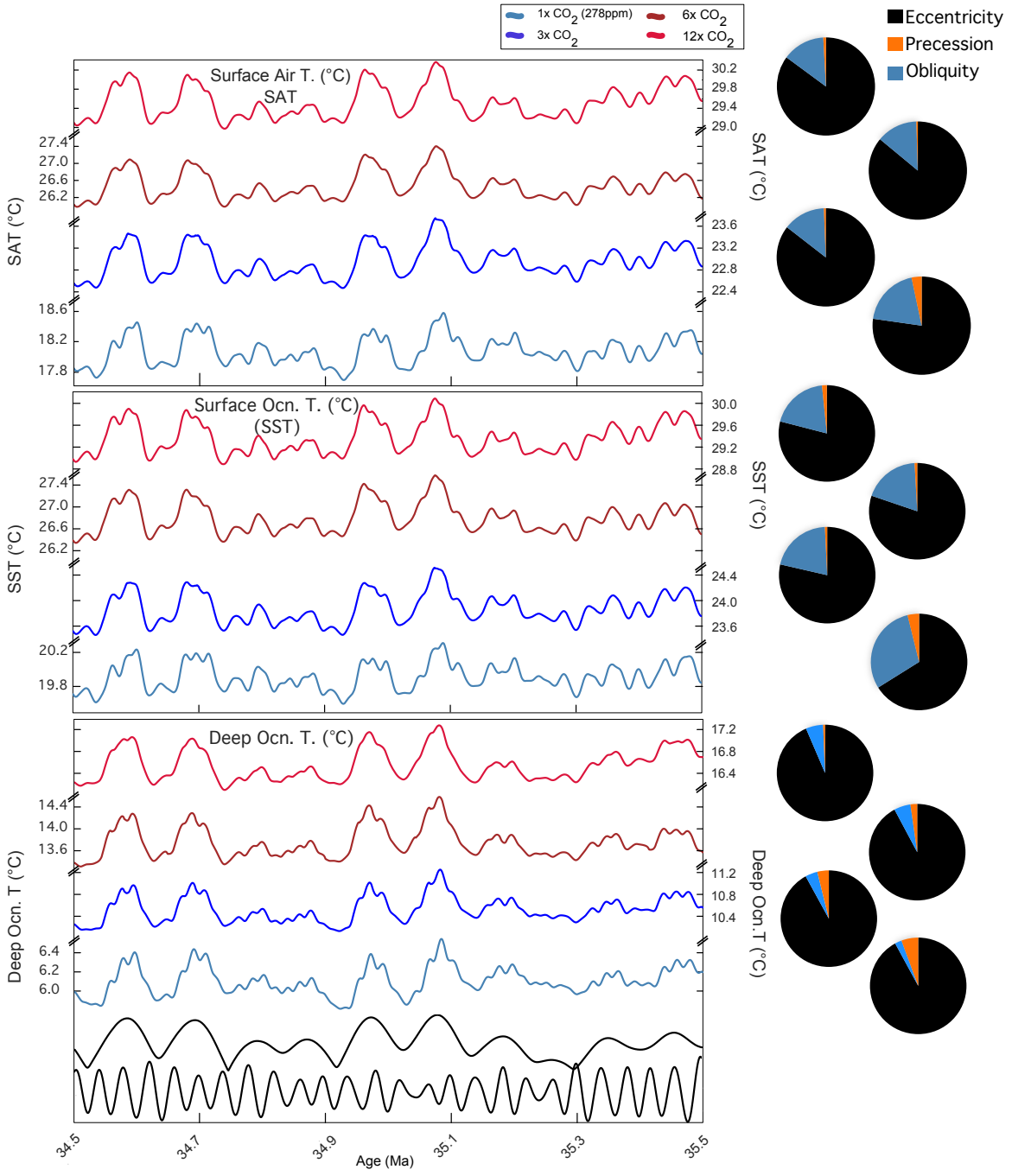

Figure 3.6: Global SAT, SST and deep ocn. T. (°C) for all simulations of this study. The share of each astronomical parameter is indicated in the pie-plots next to each time-series, the method to calculate the forcing share is described in the method section of this chapter (§3.2).

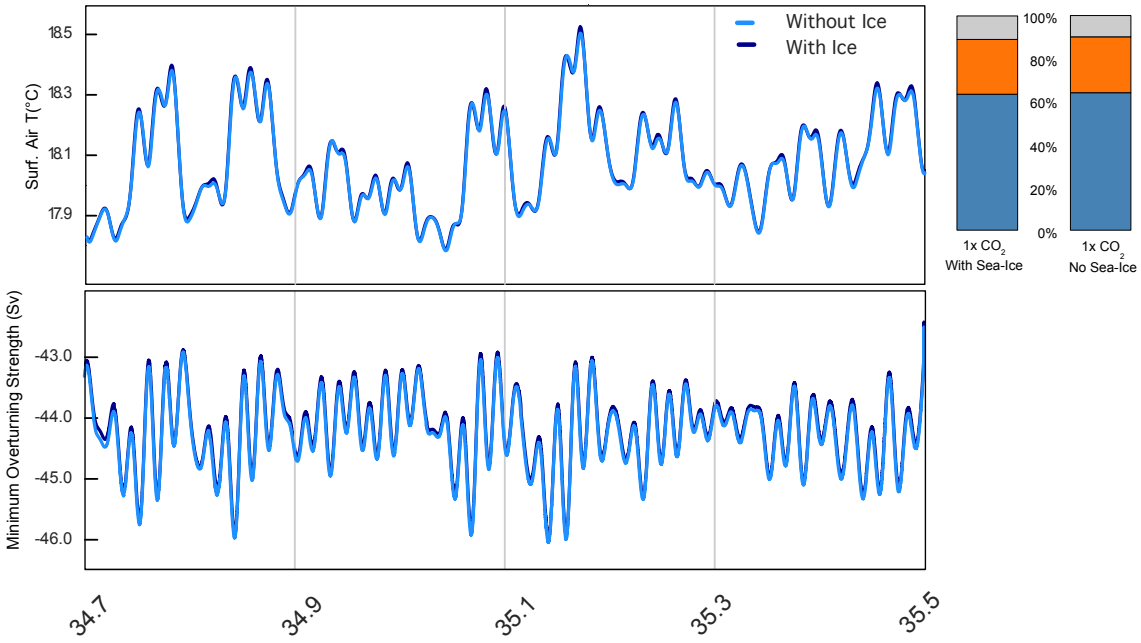

Figure 3.7: Surface Air Temperature (°C) and minimum (southern hemisphere) overturning strength for two test-runs. One with sea-ice formation enabled (dark blue) and one with sea-ice formation disabled (light blue). To display the effect of sea-ice on the temperature response to astronomical forcing, we calculate the share of each parameter on SAT in the same methods as described earlier (§3.2). We find a minimized effect of sea-ice formation on the response to astronomical forcing.

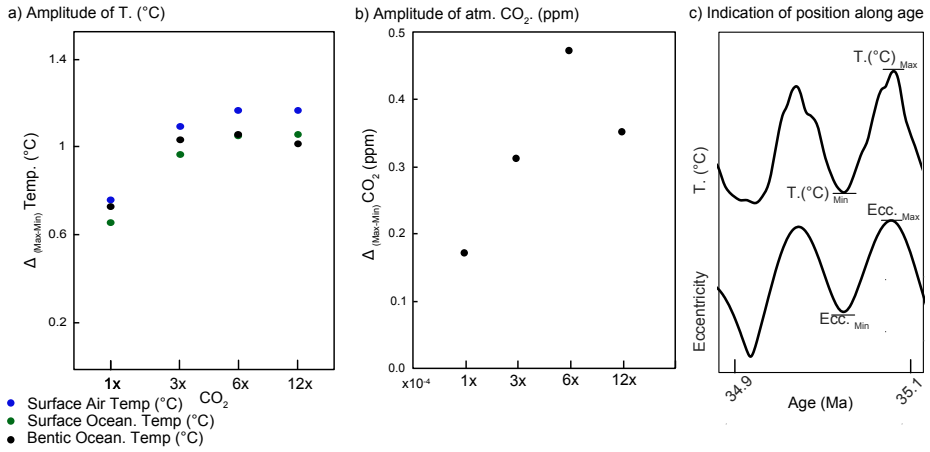

Figure 3.8: We calculate $\Delta_{Max-Min}$ T. (°C) of surface air, ocean and deep ocean temperature as well as atm. CO_2 over one significant eccentricity cycle between 35.1 and 35.0 ka to illustrate the increase in amplitude as a response to eccentricity increase.

Rethinking drivers of carbonate saturation state in high-CO_2 worlds

4

Fiona Rochholz[1*], David De Vleeschouwer[1*], Maximilian Vahlenkamp[1*], Sandra Kirtland Turner[2], Pam Vervoort[2], Heiko Pälike[1]

Corresponding authors: frochholz@marum.de, ddevleeschouwer@marum.de, mvahlenkamp@marum.de

[*] First three authors contributed equally to this work.

[1] MARUM Center for Marine Environmental Sciences, University of Bremen, Germany

[2] Department of Earth Sciences, University of California, Riverside, California

Abstract

Current anthropogenic carbon dioxide (CO_2) emissions lead to ocean acidification and induce fundamental changes in seawater chemistry (Sabine et al., 2004). Today, ocean carbonate ion concentration exerts the primary control on the carbonate saturation state of seawater (Ωcarb) and thus on the precipitation and dissolution of carbonate ($CaCO_3$) sediments. Water temperature is a secondary influence on carbonate stability, with greater solubility at lower temperature. The effects of man-made greenhouse gas emissions on ocean acidification and decreasing Ωcarb can be clearly observed, for example in the decline in coral-reef forming capacity (Kleypas et al., 1999). However, the power-relation between the primary (carbonate ion concentration) and secondary (temperature) driver will inevitably shift with increasing pCO_2. Here, we use simulations in an Earth System Model of Intermediate Complexity to quantify the relative influence of carbonate ion concentration and temperature on Ωcarb in different climate states. In our simulations with one- and threefold pre-industrial (PI) CO_2 concentrations, $CaCO_3$ content of sediments and pCO_2 are anti-correlated on orbital time-scales (i.e. carbonate content is low when CO_2 is relatively high). This observation can be explained with current climate-carbon feedback mechanisms. In our high-CO_2 simulations (6 and 12 x PI CO_2), however, we find that $CaCO_3$ and pCO_2 are in-phase on orbital time-scales (i.e. carbonate content is high when CO_2 is relatively high). This counterintuitive result arises from the increasingly dominant impact of temperature on Ωcarb with increasing pCO_2, eventually overriding the effect of ocean acidification. Hence, our results show that carbonate precipitation in high-CO_2 climate states follows fundamentally different mechanistic sequences compared to today. Nevertheless, ocean acidification will continue to dominate the current anthropogenic perturbation. The increasingly-strong positive effect of temperature on Ωcarb in a warm high-CO_2 world will be insufficient to counteract this outcome.

The production of primarily by pelagic calcifying organism and burial of $CaCO_3$ in marine sediments is responsible for the transfer of large masses of C from the fast-cycling surface reservoirs (ocean, atmosphere, biosphere), into the geological repository. The ability of planktonic and benthic organisms such as coccolithophores, foraminifera, pteropods, and invertebrates such as mollusks and corals to produce their $CaCO_3$-shells is sensitive to the saturation state of carbonate in seawater Ωcarb (Doney et al., 2009). For $CaCO_3$ to precipitate, seawater must be super-saturated with respect to carbonate minerals (Ωcarb >1) (Doney et al., 2009; Feely, Sabine, et al., 2004). Ωcarb of seawater is defined as

$$\Omega = \frac{[Ca^{2+}][CO_3^{2-}]}{K_{sp}} \tag{4.1}$$

The carbonate ion content of seawater $[CO_3^{2-}]$ exerts the primary control on Ωcarb, and this concentration rapidly decreases with the rise of atmospheric (and seawater) CO_2, which also leads a decrease in ocean pH (eq. 4.1). The $CaCO_3$ solubility product K_{sp} is a function of temperature, salinity, and pressure (Millero, 1995; Mucci, 1983). Saturation state decreases with ocean depth, where pH and temperature are low and pressure is high. The saturation horizon occurs where waters are exactly at saturation; below this depth, the ocean is undersaturated (Ωcarb <1) and carbonate starts to dissolve. At present, the calcite saturation horizon lies between ~3000-4500m (Archer, 1996; Naviaux et al., 2019) and is marked in sediments by the lysocline (i.e. the depth where dissolution of carbonate sediments is evident). The carbonate compensation depth (CCD) resides several hundred meters deeper and marks the depth at which the downward flux of carbonate rain delivered from calcifying organisms is balanced by dissolution, i.e. no carbonate is preserved in sediments below the CCD.

On millennial timescales the burial or dissolution of carbonate sediments in the deep ocean linked to deepening or shoaling of the saturation horizon plays an important role in regulating Earth's climate by buffering the oceanic carbon cycle and the climate system against perturbations (Archer, Kheshgi, et al., 1998; Broecker, 2003). Burial or dissolution of $CaCO_3$ counteract the initial change in atmospheric CO_2: burial and dissolution affect the alkalinity of the ocean and thus respectively decrease and increase the uptake capacity of the ocean with respect to CO_2 (Broecker and Peng, 1987).

Today, the global ocean is a net absorber of anthropogenic CO_2. This process partially mitigates the rise in atmospheric CO_2, but the uptake of CO_2 leads to ocean acidification (i.e. the decrease in the ocean saturation state, Ωcarb). Since the industrial era, the negative effect of CO_2 addition on Ωcarb has overwhelmed the tendency of rising ocean temperatures to decrease carbonate solubility (Feely, Doney, et al., 2009). In other words, the ocean's Ωcarb significantly declined over the past decades, with dramatic consequences for carbonate-building marine organisms and environments. However, an explicit evaluation of environmental controls on Ωcarb in high-CO_2 worlds is currently lacking. This is however important, as climate-carbon feedback processes in a greenhouse world are likely to operate differently compared to today.

Here, we employ the cGENIE Earth System Model of Intermediate Complexity to simulate changes in Ωcarb and its drivers under a sequence of different climate states, simulated by varying the concentration of atmospheric CO_2 (1x, 3x, 6x, 12xCO_2). We use a model configuration with Eocene paleogeography and time-varying orbital parameters. This set-up was designed to track the response of System Earth to variations in insolation due to changing orbital geometry, but without including the influence of ice-sheets.

The sequence of Earth System model experiments yields different climate states corresponding with increasing atmospheric CO_2. Average sea surface temperatures (SST, 60°S - 60°N) increase from 23.5°C (1xPI) to 33.2°C (12xPI). A similar escalation of deep-ocean temperatures indicates that the warming applies to the entire water column. The sequential increase in CO_2 also induces ocean acidification, illustrated by a gradual decrease in carbonate deposition between the different experiments (Fig. 4.1).

In this study, we focus on the detailed behavior of the climate-carbon system within experiments, and different dynamics between experiments. All variability within experiments is the direct or indirect result of insolation forcing, as all simulations ran with time-varying astronomical forcing. Hence, we employ these simulations to asses diverging Earth System response to insolation variability induced by astronomical forcing under different climate states. We observe a fundamental change in climate-carbon feedbacks when looking at the phase-relationship between pCO_2 and sedimentary $CaCO_3$ content between the 1xCO_2 and 12xCO_2 experiments (Fig. 4.2). Atmospheric pCO_2 and sedimentary wt% $CaCO_3$ are anti-phased with no significant phase-lag in the 1xCO_2 experiment. In the 12xCO_2 experiment, on the other hand, these variables are

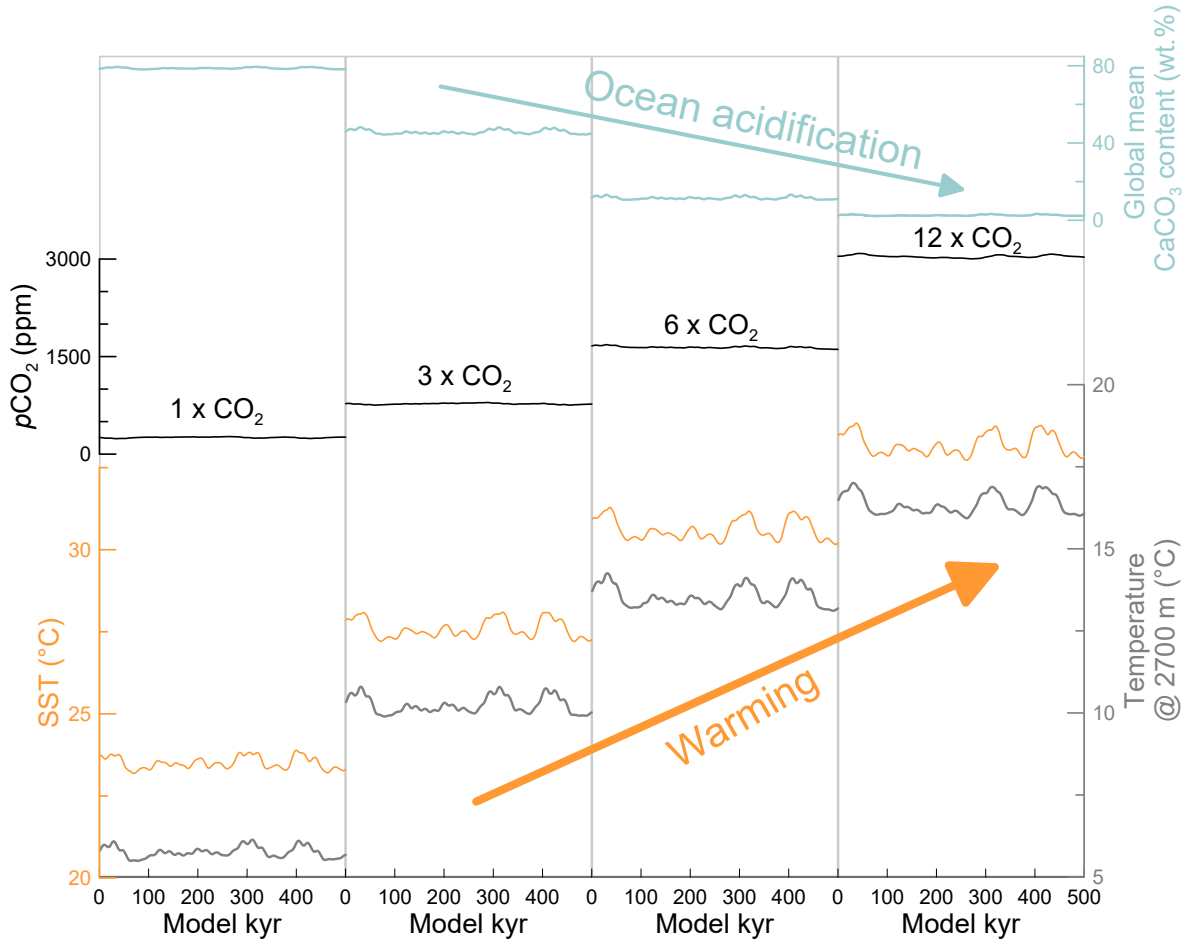

Figure 4.1: Simulated time-series, modelled with time-varying astronomical forcing and 1x, 2x, 6x and 12x pre-industrial atmospheric CO_2 concentration. Sea-surface (SST) and deep-water (2700 m water depth) temperatures increase with increasing pCO_2 levels. Yet, ocean acidification in high-CO_2 worlds hampers calcification, causing the global mean carbonate content in ocean sediments to decrease.

in-phase with a ~15 kyr phase-lag of pCO_2 with respect to $CaCO_3$.

The fundamental mechanism that generates the anti-correlated phase relationship between pCO_2 and $CaCO_3$ series is CO_2 invasion. Variations in atmospheric CO_2 concentration in the 1xCO_2 experiment largely reflect climate-driven changes in silicate weathering. This variability is propagated from the atmosphere into surface seawater, leading to an increase in acidity. Along with the decline in seawater pH, Ωcarb also decreases, restricting the zone of carbonate stability. We illustrate this mechanism in Fig. 4.3a, where rectangles delineate the simulated pCO_2-SST solution spaces for all four experiments. The solution space for the 1xCO_2 simulation, with SSTs between 23.2 and 23.9°C and pCO_2 between 238 and 270 ppm, corresponds to a surface Ωcarb

value of 5 for the combination of the above temperature and CO_2 minima. The combination of both maxima yields a lower Ωcarb value of 4.73. The Ωcarb gradient lines run quasi-vertically through the solution space of the 1xCO_2 simulation. That means that seawater temperature, depicted on the y-axis, plays a negligible role in determining Ωcarb in the 1xCO_2 climate state. The vast majority of saturation state variability is thus driven by pCO_2. In other words, the mechanism that determines the internal $CaCO_3$ variability in the 1xCO_2 experiment is identical to the mechanism that explains the progressive decline of $CaCO_3$ between the experiments. In the deep ocean, the observed patterns and discussed mechanisms are identical (Fig. 4.3b). Supersaturation (Ωcarb >1) extends to 2700 m water depth.

$$2HCO_3^- + Ca^{2+} -> CaCO_3 + H_2O + CO_2 \tag{4.2}$$

The in-phase and phase-lagged relationship between the pCO_2 and $CaCO_3$ series of the 12xCO_2 experiment marks fundamentally different climate-carbon dynamics compared to the 1xCO_2 experiment. The rectangles that depict the solution spaces of the 12xCO_2 experiment in Figs. 4.3a-b provide a first clue to the story: In contrast to the 1xCO_2 experiment, we observe higher Ωcarb values for the combination of relative maxima in pCO_2 and temperature (1.04 and 0.31, for surface and deep-ocean resp.), compared to the combination of minima (1.02 and 0.30). With flatter Ωcarb gradient lines as CO_2 increases in Fig. 4.3, the role of temperature variability within an experiment becomes more important in determining Ωcarb and this causes carbonate to precipitate somewhat easier during relatively warm/high-CO_2 spells within the 12xCO_2 experiment. Moreover, the lysocline occurs at greater depth during these warm/high-CO_2 spells, which entails a larger surface area of ocean floor where carbonates can be deposited. The observed variability in $CaCO_3$ does not exhibit co-variation with surface-water alkalinity, confirming that the $CaCO_3$ alternations are purely the result of seawater temperature change. It should be noted though that supersaturation (Ωcarb >1) only occurs in the upper ~300 m of the water column, hence the extremely low overall $CaCO_3$ sedimentary content in this model-run (Fig. 4.1). Despite the low numbers, temperature-driven experiment-internal $CaCO_3$ variations suffice to exert a control on atmospheric CO_2. Indeed, calcification may be a sink for carbon, but dissolved CO_2 is also produced in the process (eq. 4.2). The result is that calcification propels CO_2 from the ocean into the atmosphere. The portion of released CO_2 increases with increasing

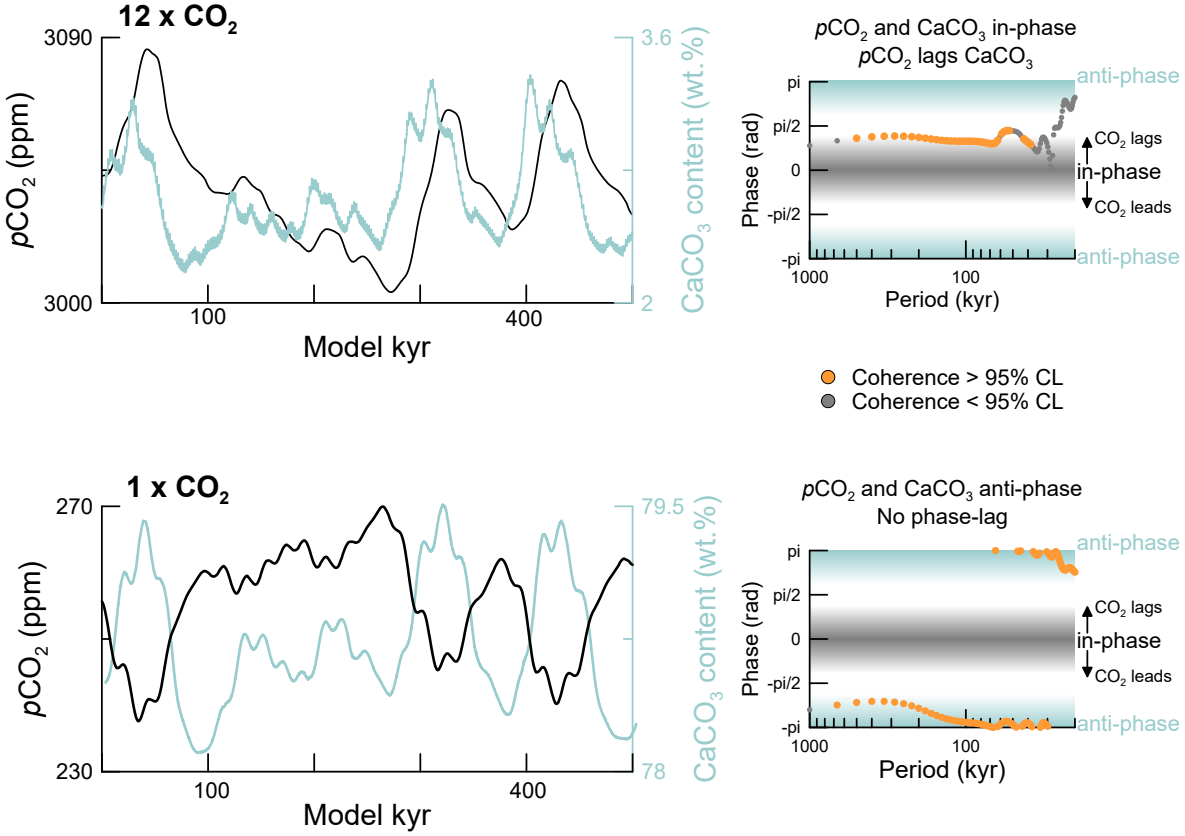

Figure 4.2: pCO_2 and $CaCO_3$ variability switches its phase-relationship from the pre-industrial (1 x CO_2) to the extreme greenhouse (12 x CO_2) simulation. In the pre-industrial simulation, pCO_2 and $CaCO_3$ are anti-correlated because an increase in pCO_2 decreases the saturation of the ocean with $CaCO_3$ (Ωcarb). Under extremely high-CO_2 conditions, however, temperature influences Ωcarb more dominantly and overpowers the CO_2 effect on Ωcarb. As CO_2 is produced during calcification, pCO_2 and $CaCO_3$ are in-phase.

pCO_2 (Frankignoulle et al., 1994), which makes this process particularly powerful in the 12xCO_2 experiment.

The Paleocene-Eocene Thermal Maximum (PETM, ~56 Ma) is a pronounced global-warming and carbon-release event, with far-reaching consequences for ocean chemistry. We use temperature and pCO_2 reconstructions from refs (Gutjahr et al., 2017; Zachos, Dickens, et al., 2008) to assess this geological event in the light of our conceptual representation of changing climate-carbon dynamics (Fig. 4.3). This data-model comparison confirms that the abrupt increase in pCO_2 caused the dissolution of carbonates that can be observed in marine sediment cores from all around the world through ocean acidification (Penman et al., 2014). The positive effect of temperature on Ωcarb was insufficient to counteract this outcome.

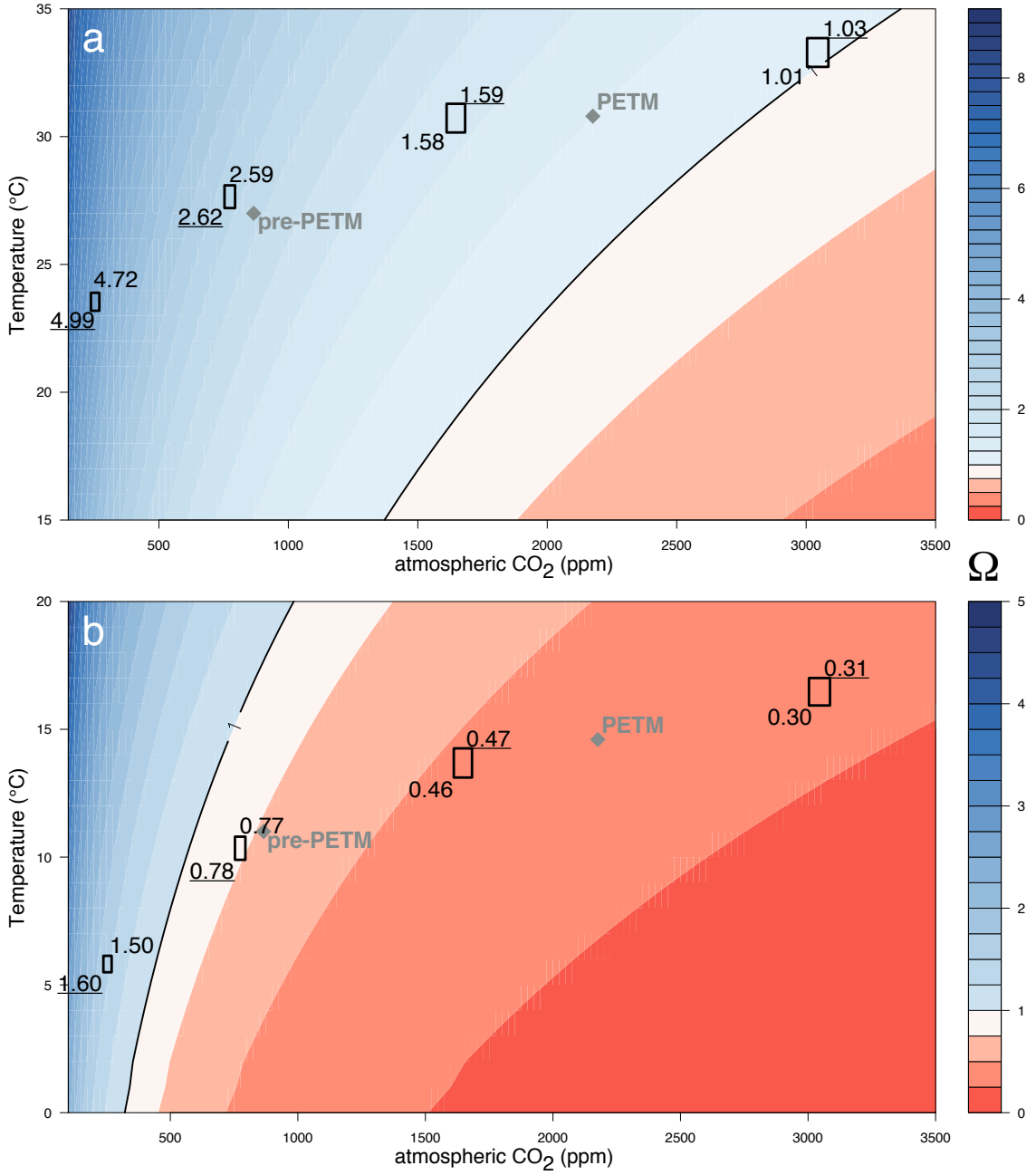

Figure 4.3: Calcite saturation state (Ωcarb) as a function of pCO_2 and temperature. Carbonate chemistry calculated using seacarb17 at Eocene salinity of 33.9 PSU and total alkalinity of 1950μmol/kg seawater (A) at 40 m and (B) at 2700 m water-depth. Rectangles indicate the orbitally-forced temperature and pCO_2 ranges of the four simulations. The Ωcarb values for the top and bottom values are calculated to illustrate the switch from a pH-dominated system to a temperature-dominated system, with increasing pCO_2.

Carbonate sedimentation constitutes an important link in climate - carbon feedback mechanisms. This modelling study shows that the dynamics of this system significantly change with increasing pCO_2. We document a switch in carbonate sedimentation dynamics in response to astronomically-induced insolation changes, from a system dominated by the silicate weathering negative feedback mechanisms (1xCO_2 simulation) to a system dictated by the marine calcification positive feedback mechanism (12xCO_2 simulation). One could anticipate an analogue shift for the Anthropocene as soon as CO_2 concentrations exceed the 3xPI level. However, such conclusion does not consider the importance of timescales, as we illustrated with the PETM case-study. The climate-carbon system perturbation during the PETM, as well as today, occurs at least one order-of-magnitude faster than the shortest astronomical cycle. Just as during the PETM, the anthropogenic perturbation is dominated by a rapid shift to high-CO_2 values, a rapid acidification of the oceans and a consequent rapid decrease in carbonate content in marine sediments. It will take several millennia before the current carbon cycle imbalance is processed. Only after that time, Earth will have attained a new steady state with respect to the anthropogenic perturbation. The pCO_2 concentration of this new climate state will determine which climate-carbon feedback mechanism will dominate: the silicate weathering negative feedback, or the calcification positive feedback mechanism. Our simulations suggest that the threshold between both possibilities lies somewhere between 3x and 6x pCO_2.

Acknowledgements. This research was made possible through ERC Consolidator Grant "EARTHSEQUENCING" awarded to HP. DDV is currently funded through the Cluster of Excellence "The Ocean Floor - Earth's Uncharted Interface".

Author contributions. All authors designed the research. FR ran the cGENIE Earth System Model simulations. FR, DDV and MV wrote the manuscript with input from all co-authors.

Competing interests. The authors declare no competing interests.

Methods

Earth System and carbon cycle model. The cGENIE Earth System Model of Intermediate Complexity (Ridgwell, Hargreaves, et al., 2007) is composed of a three-dimensional dynamic ocean circulation model with a two-dimensional dynamic sea-ice and a non-dynamical atmosphere component (Edwards et al., 2005) and the incorporation of the carbon cycle including preservation and burial of biogenic carbonates in accumulating marine sediments of the open ocean (Ridgwell and Hargreaves, 2007) and terrestrial weathering (Colbourn, Ridgwell, and M. Lenton, 2015). We use cGENIE in an early Eocene (PETM) configuration with adjusted continental configuration, albedo, and ocean chemistry (Ridgwell and Schmidt, 2010) and a resolution of 36x36 grid-cells (equal area in longitude and the sine of latitude) with 16 ocean levels that increase in thickness with depth. We ran experiments with 278 ppm (1xPI CO_2), 834 ppm (3xPI CO_2), 1668 ppm (6xPI CO_2) and 3336 ppm (12xPI CO_2), to capture the possible range of Eocene CO_2 variations. Initially, the model was configured as a 'closed' system, i.e., with no gain of solutes to the ocean from weathering or losses through burial of $CaCO_3$ under fixed modern astronomical configuration. Subsequently, each experiment was run as an open system with respect to inorganic carbon, with weathering and sedimentation balanced using a temperature-dependent weathering parameterization (Colbourn, Ridgwell, and M. Lenton, 2015; Kirtland Turner and Ridgwell, 2016)for at least 1 Myr using time-varying astronomical parameters. We employed the solutions of eccentricity, obliquity and precession in La200424 between 34.5 and 35.5 Ma to force the open-system experiments. It should be noted that in this phase, carbon cycle dynamics are explicitly modeled, hence atmospheric pCO_2 concentration responds to environmental changes and consequent carbon-cycle imbalances. In this study, we present and analyze the final 500 kyr of each simulation. This approach allows all simulations to reach steady state with the implied boundary conditions. All model experiments can be accessed at: https://github.com/FionRo/ThesisAttachmentPublic/tree/master/Chap03:4.

Solubility of calcite.

$$K_{sp} = [Ca^{2+}][CO_3^{2-}] \tag{4.3}$$

K_{sp} is temperature and salinity dependant by

$$\begin{aligned} logK^{*}_{sp}(cal) = & -171.9065 - 0.077993 * T \\ & + 2839.319/T + 71.595 * \log T \\ & + (-0.77712 + 0.0028426 * T + 278.34/T)S^{\frac{1}{2}} \\ & - 0.7711 * S + 0.004149 * S^{\frac{1}{2}} \end{aligned} \tag{4.4}$$

R-package seacarb. In order to quantify the influence of CO_2- and temperature-induced changes on carbonate saturation, we use the R package 'seacarb 3.2.12' (*Package 'seacarb'* 2019) that calculates various parameters of the carbonate system in seawater (Orr et al., 2015).

Phase analysis. Frequency-dependent phase relationships between atmospheric CO_2 and $CaCO_3$ were calculated through Blackman-Tukey cross-spectral analysis, as implemented in the AnalySeries software (Paillard et al., 1996). Linear trends were removed, the data were pre-whitened and normalized, and 95% confidence levels were computed on coherence.

Anthropogenic CO_2 effect on astronomically forced climate

5

Fiona Rochholz[1, a], David De Vleeschouwer[1], Sandra Kirtland Turner[2], Heiko Pälike[1]

[a] frochholz@marum.de

[1] MARUM Center for Marine Environmental Sciences, University of Bremen, Germany

[2] Department of Earth Sciences, University of California, Riverside, California

Abstract

The consequences of the ongoing human-made carbon emissions are by now witnessed all over the world. Yet, the fate of anthropogenic carbon in the atmosphere and ocean system on multi-thousand years remains unclear. It is now clear that anthropogenic greenhouse gas emissions are prolonging the current interglacial, aided by an extraordinary long period of low eccentricity. The ongoing perturbation of the global carbon cycle will have effects on time-scales of thousands to tens of thousands of years. On these time-scales, astronomically-forced variations in insolation come into the picture.

In this study, we address the question whether the timing of human emissions will have an effect on their influence on natural climate interactions. In other words, we assess the interaction between astronomical and anthropogenic forcing on 10^5 year time-scales. We design an experimental setup with the Earth System Model Intermediate Complexity cGENIE, in which an anthropogenic-like perturbation is implemented under different astronomical forcing configurations. The computational efficiency of cGENIE allows each of these simulations to run for 500 thousand years and the effects of natural Milankovitch insolation forcing are considered in our simulations. This allows for a quantitative comparison of the effects of orbital and man-made forcing on multi-thousand-year time-scales. We compare the results of the different simulations to the modern scenario, which obviously runs under a modern orbital configuration.

We identify eccentricity as the only astronomical parameter to cause a climatic deviation between the simulations, yet its effects are neglectable in comparison to the size amplitude of the climate change in response to the anthropogenic perturbation. We can thus conclude that astronomical forcing is completely overwhelmed by anthropogenic forcing.

5.1 Introduction

Palaeoclimatologists study past climates with the objective of providing insight into climate variability in Earth's history, in response to natural climate forcing. A good understanding of past climate response to natural forcing is invaluable to make informed predictions of the future climate response to anthropogenic forcing through the emission of greenhouse gasses.

The first argument for the valuable character of paleoclimatology is based on the concept 'the past is the key to the present is the key to the future'. Planet Earth experienced drastic perturbations of the carbon cycle and/or climate system in its 4.5-billion-year history. Some of these perturbations have had major consequences for life on Earth ('mass exctinction') following carbon release events and drastic warming ('hypothermals') such as the Paleocene-Eocene Thermal Maximum (PETM, 55.5 Ma) (e.g. Zachos, Röhl, et al., 2005) or the Eocene Thermal Maximum 2 (ELMO-Event) (Lourens et al., 2005). Maxima in insolation modulated by orbital variability and their effect on climate (carbon) system internal reactions have been correlated to trigger these warming events (Galeotti et al., 2010; Lourens et al., 2005). Insights in the cause-and-effect chains between astronomical forcing and carbon system reactions across these aberrations help to understand the thresholds that characterize Earth's future climate system.

Despite the fact that the current anthropogenic emissions might well cause these thresholds to shift beyond known values (Blackford et al., 2007; Joos et al., 2008; Lüthi et al., 2008; Zeebe, Ridgwell, et al., 2016), the basic climate and carbon cycle feedback mechanisms will continue to operate and respond to natural as well as anthropogenic forcing.

A suite of model simulations provides projections for the Earth's warm future IPCC, 2013, under different CO_2 emission scenarios, estimating the extend of the warming in the atmosphere and ocean environment.

Most models that simulate the climate response to the anthropogenic perturbation grant insights in Earth system's response over the next decades and centuries. The computational costs of such simulations limits the feasibility of running them further into the future. This is unfortunate since the human-made perturbation of the global carbon cycle will certainly have effects on time-scales of thousands to tens of thousands of years (Archer, Kheshgi, et al., 1997; Plattner et al., 2008). Here, we use the global Earth System Models of Intermediate Complexity cGENIE (Ridgwell and Hargreaves, 2007; Ridgwell, Hargreaves, et al., 2007) to simulate the response of climate, ocean and carbon cycle to anthropogenic forcing over several ten thousand years. On

such time-scales, astronomically-forced variations in insolation become highly significant. Hence, the effects of natural Milankovitch insolation forcing are also considered in our simulations. This allows for a quantitative comparison of the effects of orbital and man-made forcing on multi-thousand-year time-scales.

Here, we assess the interaction between astronomical and anthropogenic forcing on 10^5 year time-scales. These interactions are at the mid-focus of several intriguing scientific questions: For example, Ganopolski, Winkelmann, et al., 2016 showed that the timing of the first anthropogenic greenhouse gas emissions was just right to break the glacial-interglacial climate variability and to prolong the duration of the current interglacial. However, what remains unclear to date, is whether the timing of human emissions will further modify their effect. In other words, would the long-term effect of the man-made perturbation on ocean and climate be different in case the anthropogenic forcing would take place under a different orbital configuration?

To assess this question, we design an experimental setup with the Earth System Model Intermediate Complexity cGENIE, in which the anthropogenic perturbation coincides with different astronomical configurations. The computational efficiency of cGENIE allows the allows each of these simulations to run for 500 thousand years (kyr). However, we will show that the effects of the anthropogenic perturbation are the same in all simulations. The astronomical forcing is thus completely overwhelmed by the anthropogenic forcing.

5.2 Methods

5.2.1 Earth System Model cGENIE

cGENIE is an Earth System Model that comprises a 3-D dynamical ocean circulation model, the 'Goldstein'-Ocean, a 2-D energy-moisture balance model of the atmosphere, and a thermodynamic sea ice model (Edwards and Marsh, 2005). Carbon cycling in the oceans is represented through the production, export and remineralization of both organic and inorganic forms of carbon (Ridgwell and Hargreaves, 2007; Ridgwell, Hargreaves, et al., 2007).

5.2.2 Experimental Setup

The experimental setup of this study is adapted from Archer, Eby, et al., 2009. The setup is a modern continent configuration at a resolution of 36x36 grid cells and 16 vertical depth layers.

The model is 'open' with respect to the inorganic carbon cycle, which is needed to allow for terrestrial rock weathering and burial of carbonate in deep sea sediments (Colbourn, Ridgwell, and Lenton, 2013; Ridgwell and Hargreaves, 2007; Ridgwell, Hargreaves, et al., 2007). This ensures that the carbonate system runs in equilibrium with internal variability before anthropogenic emission scenarios and returns to a self-detained stage after the perturbation.

Table 5.1: List of simulations performed in this study. We place the 'modern' experiment at today's orbital configuration and move the anthropogenic forcing for two experiments 10 kyr to the past (Obl+) and to the future (Obl-). Two additional experiments were performed so the anthropogenic forcing coincides with two more extreme orbital configurations (E+, E-). l.

Experiment	Position along time	Eccentricity	Obliquity	Precession angle
E^+	220.000 years ago	0.049	23.56°	239.547
E^-	373.000 years ago	0.0045	23.56°	212.142
Modern	1675.3 ppm	0.017	23.44°	282.918
Obl^-	10.000 years into future	0.01	22.61°	99.193
Obl^+	10.000 years into past	0.018	24.22°	115.265

We run the experiments in different stages. First, we carry out a spin-up stage that imposes a closed carbon cycle (i.e. no net weathering and sedimentation) and fixed atmospheric CO_2. This stage already includes the simulation of marine productivity. Second, we run an 'open system' spin-up that balances weathering and sedimentation using a temperature-dependent parameterization of carbonate and silicate weathering (Colbourn, Ridgwell, and M. Lenton, 2015; Kirtland Turner and Ridgwell, 2016). For both stages of spin-up, orbital parameters are fixed to modern values. References values for carbonate and silicate weathering and surface land temperature the second-stage for each experiment were obtained from the first spin-up (25.000 years) and helped to identify the equilibrium values for each experiment.

In a third stage, we carry out our experimental design. We dump CO_2 into the atmosphere according to emission scenario A1B Scenario (IPCC, 2013) under five different astronomical forcing regimes (Table 1). These experiments are then run for 100,000 years. Our control experiment ('modern') is characterized by an atmospheric CO_2 increase under present-day astronomical forcing. Experiments 'Obl+' and 'Obl-' represent the exact same model simulation, albeit under the astronomical forcing regime of 10 thousand years ago (ka) and 10 thousand years (kyr) in the future, respectively. In other words, these simulations take all boundary conditions from the modern experiment and solely apply a different astronomical forcing regime. The 'Obl-' simulation

thus does not represent the last glacial maximum, but only uses the astronomical regime of that time-slice. Experiments 'E+' and 'E-' are designed such that they represent extreme astronomical forcing regimes under maximum and minimum eccentricity configurations, respectively. These experiments correspond to the astronomical forcing regimes of 220 ka and 373 ka, but again do not take any other boundary condition of those times into account. Model input and configuration files can be accessed at: https://github.com/FionRo/ThesisAttachmentPublic/tree/master/Chap05.

5.2.3 Forcing Scenario A1B

The A1B- forcing scenario represents CO_2 emissions during the current and next centuries, considering rapid growth in economy and population, combined with a reduction in the use of fossil fuels for energy supply. For more details, see IPCC, 2013.
We start the 'modern' forcing in the year 2000, with 10-year step increasing CO_2 emissions until 2050. From 260 to 2100, the emissions continue but decrease stepwise in 10-year steps.
We test the effect of insolation at the time of the anthropogenic perturbation on the climate system internal response by simulating a specific emission scenario at different points in time, with different astronomical forcing regimes. We relate the results of these simulations to the modern scenario, which runs under a modern orbital configuration. We hypothesize that the magnitude of anthropogenic-like CO_2 emissions will overprint on natural climate variability forced by astronomical variability.

5.3 Results and Discussion

Anthropogenic-like ('modern') emissions accumulate to a maximum of 754 ppm atmospheric CO_2 about 50 years after the maximal emissions, which causes surface air temperature (SAT) increases about 3.94°C. Uptake of atm. CO_2 in the ocean induces causes ocean acidification (pH drops) and subsequently dissolution of carbonate sediments at the ocean floor (Fig. 5.2). Shortly after emissions cease, SAT and CO_2 values reduce quickly while atmospheric (atm.) CO_2 is gradually removed from the atmosphere, increasing the oceanic inorganic carbonate reservoir (dissolved inorganic carbon, DIC).

Although complete compensation of the surplus of atm. CO_2 in the aftermath of the perturba-

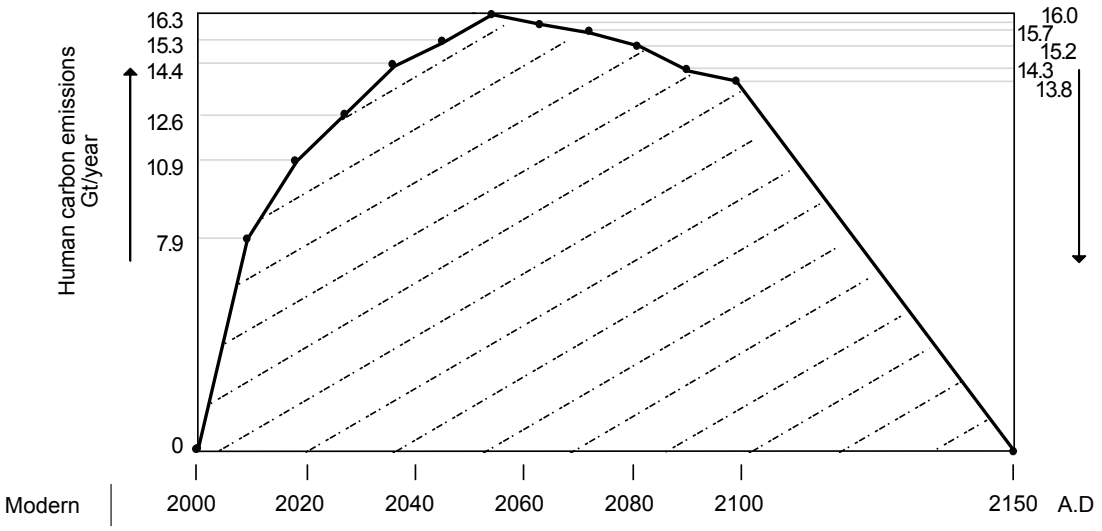

Figure 5.1: The A1B scenario perturbs all five experiments presented in this study, albeit under different astronomical forcing regimes.

tion will take much longer than the duration of this study's simulations (Colbourn, Ridgwell, and M. Lenton, 2015), we find the system returning to a SAT variability of about 0.5°C responding to summer insolation. Both SAT and CO_2 reach a new quasi-steady state, 13.000 years after the start of the emission, defined by a rate of change (ROC) in atm. CO_2 of 0.001 ppm/year equal to ROC to before the perturbation.

However, SAT and CO_2 values never return to the state prior to the greenhouse gas perturbation. The new quasi-steady state lies about 1°C and 40 ppm above the SAT and CO_2 that characterize our model simulations before the perturbation. While the size of the perturbation in the SAT record is a magnitude larger than the natural variability before and after the perturbation as simulated in cGENIE, simulated CO_2 variability through the perturbation is about 4x as large as the recorded variability of about 80 ppm of the last 500.000 years (see Fig. 5.3) (Petit et al., 1999).

5.3.1 Path and uptake of anthropogenic CO_2 by the ocean

A share of about 70% CO_2 of the total amount of the perturbation will be absorbed by the ocean via gas exchange with the atmosphere (Archer, Kheshgi, et al., 1998; Berner and Caldeira, 1997; Ridgwell and Zeebe, 2005).

The reaction of CO_2 with seawater forms carbonic acid (H_2CO_3), protons (H^+) and biocarbonate

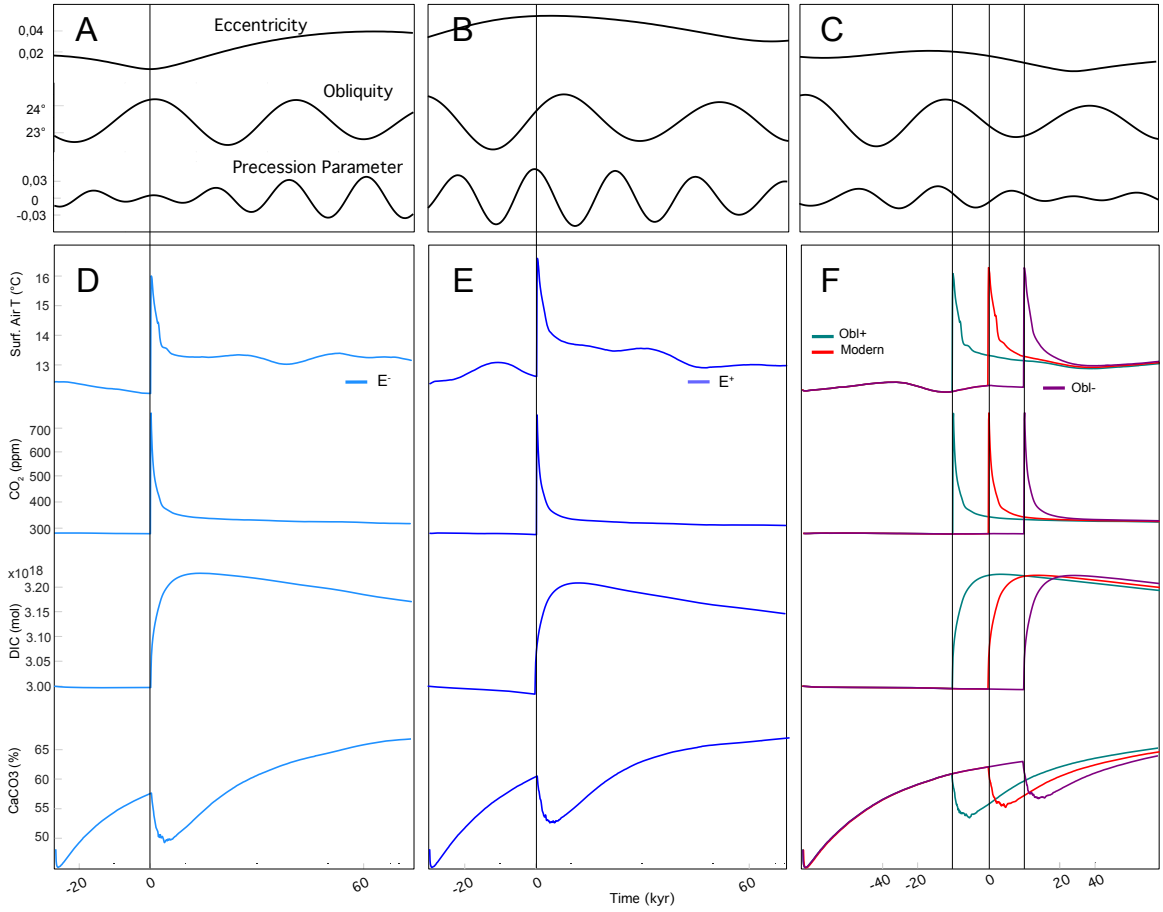

Figure 5.2: (A-C) Astronomical forcing during, and (D-F) model response to the anthropogenic-like perturbation of our five cGENIE simulations. The model's response to the A1B carbon cycle perturbation is similar between all experiments, despite different astronomical forcing regimes.

ions (HCO_3), the later will further partly disassociate into carbonate ions (CO_3^{2-}). The total sum of these carbonate species makes up the total concentration of dissolved inorganic carbon (DIC) of the ocean water and defines the pH values of the ocean water, the 'measure' of acidity. Lowering the pH value by inducing CO_2 to the ocean contributes to changes in the carbonate saturation state of ocean water (Ω). Ω describes the stability of calcium carbonate in solid form. By adding CO_2 to the water, the equilibrium reaction of Ω describes a dissolution of marine carbonates ($CaCO_3$) to 'fill' the missing Ca^{2+}, which will also cause a further release of CO_2 to the ocean and atmosphere (Zeebe and Wolf-Gladrow, 2001).

$$\Omega = \frac{[Ca^{2+}][CO_3^{2-}]}{K_{sp}} \tag{5.1}$$

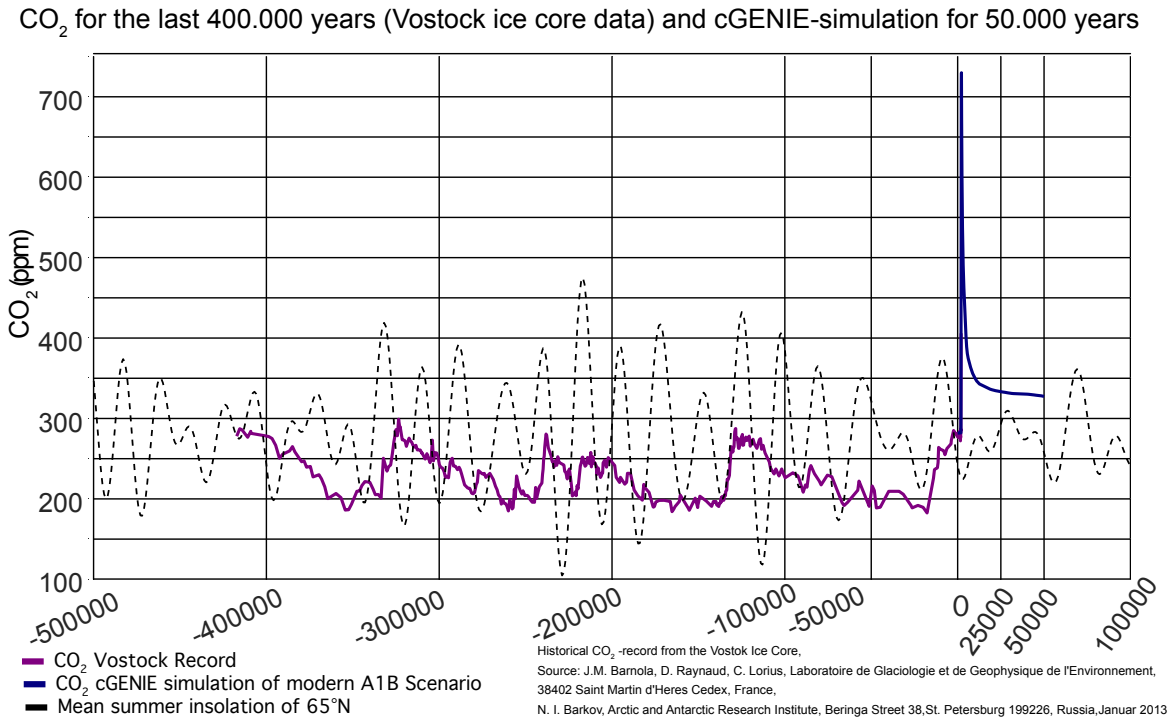

Figure 5.3: CO_2 record of the Vostok Ice Core of Antarctica along with the simulation of the modern A1B emission scenario results of cGENIE. We demonstrate, that the size of the anthropogenic emission is larger than any other natural variability within the last 400 ka of Earth's history.

Prior to the anthropogenic carbon perturbation, carbonate sediments are continuously formed, hardly affecting atm. CO_2 concentration and indicating a weak influence of the carbonate buildup on the global atm. CO_2 prior to the anthropogenic forcing.

When large amounts of CO_2 enter the atmosphere and subsequently the ocean, DIC increases and pH decreases. The surplus of carbonate ions is balanced by dissolution of carbonate sediments and organisms in the ocean. Modern ocean acidification has already contributed a change of 0.1 pH unit (Blackford et al., 2007; Caldeira and Wickett, 2003) and caused subsequent dissolution of marine organisms and sediments (Review in Riebesell, 2004; Riebesell et al., 2000). Our simulations respond to the anthropogenic-like forcing with a change of 0.3 pH unit, suggesting the current pH value change has not reached its maximum perturbation response (Fig. 5.4).

Changes in carbonate chemistry tell the uptake of CO_2 in the ocean allowing for a drop of atm. CO_2 to half its peak-value within only a few centuries. The excursion of Ω parallel to CO_2 and SAT indicates a short-lived strong dissolution event of marine carbonates. Yet, by the end of the simulation, DIC and pH have not recovered from the perturbation. DIC has reduced for about

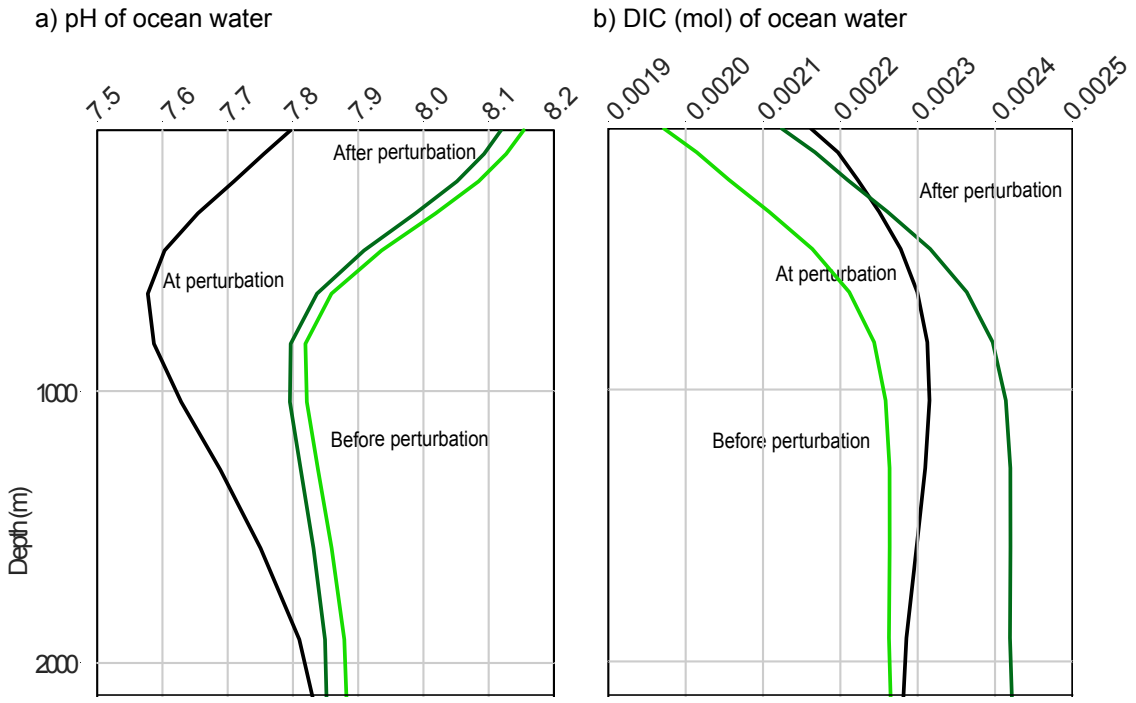

Figure 5.4: The depth profile for both pH and DIC in the ocean water shows significant changes at the time of the perturbation in the upper 2000 m of the water column. The pH decreases up to 0.3, indicating a large effect on the acidity of the ocean water. We correlate this drop to the dissolution event, mirrored in a decrease of $CaCO_3$ (%) of the sediment column.

1% from the maximum response to the forcing and pH is 0.03 pH units below preindustrial, which will certainly affect marine organisms on the long term (Riebesell et al., 2000). There is a consistent rate of change in DIC of about -0.0025 mol/100years from about 1000 years after the end of the perturbation until the end of the simulation. The surplus of DIC after the end of the perturbation correlates well to the constant increase of $CaCO_3$ formation in the sediment. This increase varies around 0.01 and 0.02 wt%/100 years from 1000 years after the onset of the perturbation until the end of the run. We calculate for the modern experiment, that 0.24% less $CaCO_3$ is accumulated, in comparison to a simulation without any anthropogenic forcing.

5.3.2 Effect of orbital variability on the response to astronomical forcing

Climate, ocean and carbon cycle of time-shifted simulations display a very similar response to the anthropogenic-like perturbation as described for the 'modern' experiment, independent of the astronomical forcing configuration (Fig. 5.5).

In terms of atmospheric CO_2, peak-CO_2 concentrations lie between 747 and 754 ppm. Correlation between peak-SAT and obliquity value is low, however, there is a clear trend of higher peak-SAT under high eccentricity (Figure 5.6). Experiment 'E^+' deviates from the 'modern' simulation with about 1.09 % in CO_2, about 0.3°C in SST. Slightly higher weathering rates of Ca (0.03 PgCa relative to the modern experiment at peak atm. CO_2 concentrations) might clarify the deviation in SAT and CO_2.

High seasonality under high eccentricity is associated with higher weathering rates of continental rocks, reducing atm. CO_2 concentrations (negative feedback). Indeed, atm. CO_2 is lower at the end of the 'E^+' simulation, relative to other simulations. During the emission forcing, as a 'short term effect', atm. CO_2 is removed from the atmosphere by dissolution of $CaCO_3$ (changes in Ω). On timescales of 5-10 kyr, CO_2 is consumed by the sequence of continental rock weathering and deposition of $CaCO_3$ on the ocean floor. With slightly increased (negative) weathering effect in 'E^+', more CO_2 will be extracted from the atmosphere relative to all other experiments. On these time scales, we conclude the dominance of the negative weathering effect after the end of the emission over the less effective CO_2 release of carbonate compensation.

5.4 Summary and Conclusion

The A1B scenario assumes anthropogenic CO_2 emissions to be shortened drastically between 2100 and 2150 (including forestation and decarbonization measures). Although emissions are cut, the climate system will not return to preindustrial conditions but reach a new steady state which still lies 1°C above the preindustrial state. Our results do not suggest any further cooling within the range of our long simulations.

This scenario is an example of a potential future and the choice for this perturbation defines the outcome and also 'long-tail' of our experiments. With a prolonged emission scenario (i.e. one of the B1-Family scenarios), not cutting the emission in the nearer future, reaching the new equilibrium would be postponed and increased (Archer and Brovkin, 2008; Colbourn, Ridgwell, and M. Lenton, 2015). Our simulations show that part of climate system is capable of returning to natural variability on insolation timescales but only 13.000 years after the perturbation. Natural variability forced by insolation changes will dominate the climate variation in the new equilibrium state reached after 13.000 years once the emissions have been cut in the year 2150. If perspective of a climate state 1°C above preindustrial state is not drastic enough to be pointed

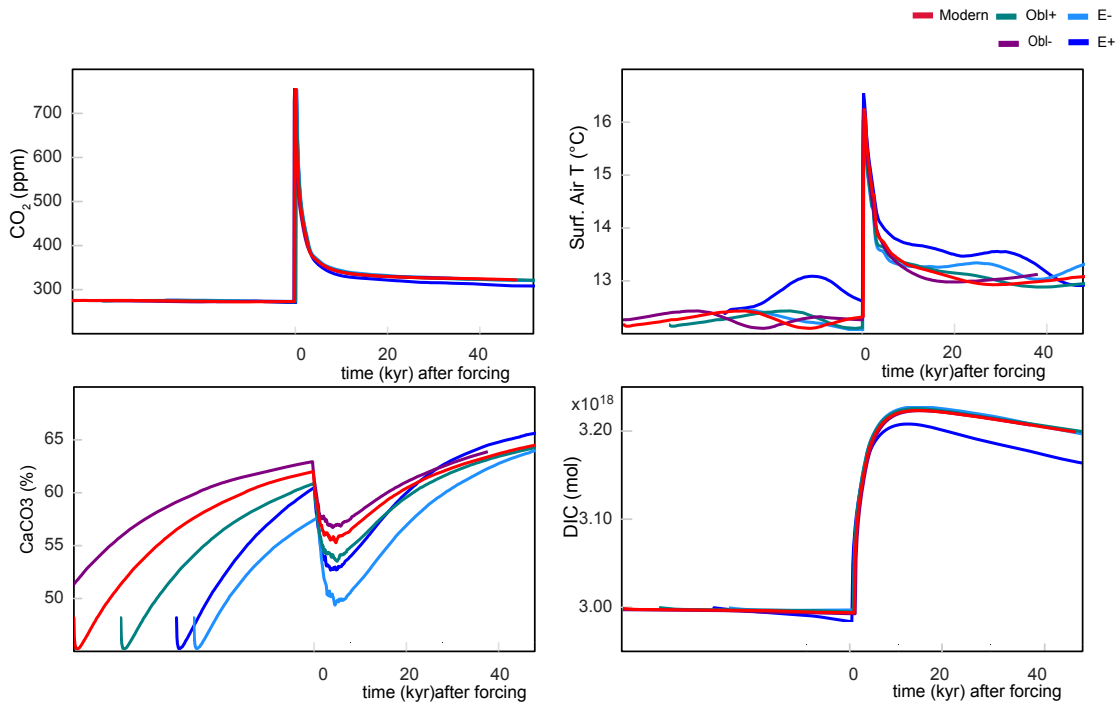

Figure 5.5: To demonstrate, that the size of the emission is the same for all five experiments, we adapt the time-scale of the emission so the position is moved on top of each other. While the differences among the simulation are small, 'E^{+}' deviates visibly from all other experiments.

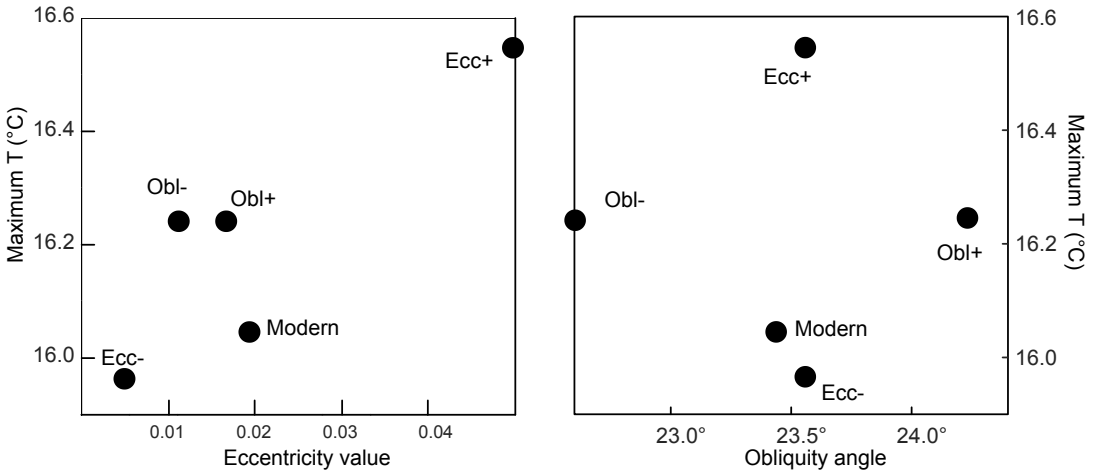

Figure 5.6: We relate eccentricity and obliquity values to maximum SAT during the forcing. Although differences are small, maximum eccentricity forces largest deviation from the modern experiment. Varying obliquity angle hardly affect maximum SAT.

out, the oceanic response to an atmospheric perturbation reveals a prolonged life-time of CO_2 as DIC in the ocean. Estimating the consequences for the marine carbonate system of the preceding warming event on short term has been part of several studies (e.g. Cao et al., 2007) and the long-lived consequences of elevated DIC in the ocean remains to be studied.

While astronomically driven insolation shapes the pattern of the climate outside the forcing and so the 'starting' value at the onset of the perturbation, the size of the perturbation is about a magnitude larger than the effect of the astronomical configuration on the response during the forcing. The eccentricity-related increase of weathering rates throughout the experiment is not strong enough to cause a notable deviation in the temperature during and after the perturbation. The temperature changed due to higher eccentricity is only 7.5% of the temperature change of 4°C caused by the anthropogenic-like forcing. Natural variability expected due to the astronomical configuration at the timing of the perturbation is overruled by the magnitude of the anthropogenic CO_2 forcing. Although the extend of the forcing, in relation to the length of the run may tempt the reader to assume a short effect of the forcing on the climate, but the total length of this best-case scenario is 500 human generations (one generation comprising roughly 30 years) being affected by an intense climate disturbance before our model suggest a steady-state scenario again.
The increase of CO_2 in the atmosphere expresses itself as an rise of DIC, atmospheric and ocean temperatures and a decrease in oceanic pH (acidification of the ocean) (Riebesell et al., 2000) is 'short' termed in relation to orbital variations. Though only on astronomical 'long' terms, temperature may recover after the cut of the emission, while conditions in the oceans remain critical until the end of the stimulations.
We find, that natural variability forced by orbital variation will dominate the variation in climate after the emission are cut, but the new, warmer equilibrium state will consist at least another 800.000 additional years.

Conclusions, Limitations and Outlook 6

6.1 Overall conclusions

The studies which make up this thesis show that carbon cycle feedbacks have the potential to dampen or amplify climatic variations induced by astronomical variability. Assessing long-term consequences of these climatic variations on carbon cycle feedbacks can improve the understanding of past climatic changes, as well as the future of the carbonate chemistry in a warming world. The generation of several 1-Ma-long simulations with Eocene background conditions (§**3** and §**4**) allows us to compare the response of the climate and carbon cycle to astronomical variability under various climate states. Both the climatic response to astronomical variations as well as the carbon cycle feedbacks indicate a variable response dependent on the prevalent climate state, which has two major implications for the interpretation of climate-carbon related feedbacks under cold and warm climate:

Firstly, the radiative forcing effect of atmospheric CO_2 increases relative to the insolation under warm climate conditions (§**3**). It is demonstrated that the relation of insolation and CO_2 as the main driving force on temperature changes under rising atmospheric CO_2. With simulated CO_2 mainly varying on 100-kr eccentricity cycles, this is subsequently represented by a shift from temperature varying mainly on 41-kyr cycles in cold climate state to predominantly 100-kyr cycle variability in warm climate conditions. This observation reveals the importance of the carbon cycle on the climatic response to astronomical variability in Earth's climate history and provides a potential explanation for the response to astronomical variability in times of absence of cryosphere.

Secondly, the main control of the carbonate saturation state will change as Earth's climate warms (§**4**). Under low CO_2 conditions, temperature variability has a stronger effect on the carbonate

saturation state in the ocean, than CO_2. Under high CO_2 conditions however, CO_2 variability, effectively the availability of carbonate ions and so the oceanic *p*H value, mainly control the carbonate saturation state. This has major consequences for any carbon perturbation and the path of the surplus of atmospheric CO_2. The prevalent climate state defines whether the negative silicate weathering effect will diminish the warming or the carbonate formation contributes to the warming effect of the perturbation. Considering the current global warming, the future path of anthropogenic emissions will determine the fate of the carbonate system in the future.
Applying cGENIE to simulate an anthropogenic-like A1B scenario under different orbital configurations (§**5**) demonstrates the spontaneous climate response to the perturbation as well as the long-term trend of the carbon budget in ocean and atmosphere after the perturbation. Some global climate parameters, such as global temperature and atm. CO_2 quickly respond to the perturbation but reduce with the end of the emissions to stabilize at a new, though higher, near-equilibrium state. However, high concentrations of dissolved inorganic carbon in the ocean indicate long-term residue of the perturbation in the ocean. In terms of future global climate change, this is an important finding. Not only will the extensive short-term response of the climate to the perturbation significantly affect the stability of the ecosystem in the ocean, lower *p*H value and high DIC concentrations indicate long-term unstable conditions for marine calcifying organisms. Past carbon perturbations are often amplified by 'warm' orbital constellations contributing or inducing a climatic change. The current anthropogenic CO_2 emissions induce a rapid climate change at shorter than astronomical time scales. The effect of astronomical changes on the climatic response to the anthropogenic carbon perturbation is small. The magnitude of the anthropogenic-like perturbation overprints on the climatic effect of the astronomical configuration, proving that the orbital constellation during the anthropogenic CO_2 perturbation has no effect on the size of the climatic response.

6.2 Limitations of model simulations

Enabling a temperature-dependent weathering feedback contains one inconsistency in all long high CO_2 simulations. Implementing carbon cycle and weathering feedbacks is a balance between the input (volcanic sources) and output (weathering) values, which based on the amount of carbonate preserved after the spin-up phase of each experiment. Under high CO_2, large amounts of carbonate (DIC) is stored in the ocean. Consequently, the capability of the ocean to form and

preserve calcium carbonate at the ocean floor is lowered which would incorrectly imply lower weathering rates in the high CO_2-simulations. This obscures the coherence of high weathering rates under warmer climate conditions. It is therefore likely that the effect of weathering on attenuating the climatic response initiated by astronomical variability is underestimated. In this thesis, it has not been possible to design and run a full 1-Ma simulation of model setup that would allow simulation of high CO_2 concentrations with high weathering rates. Such a setup would respond temperature-dependently to astronomical variability while high weathering rates should not cause a temperature and CO_2 drawdown during the course of the run. Despite this problem, model results show a clear shift in carbon cycle response to the climate state, independent from the weathering intensity. This confirms that the behavior of the marine carbonate system is strongly affected by the underlying climate state.

Even though anthropogenic perturbation results are reliable for tracking the climatic response on astronomical timescales, the low resolution of cGENIE and the lack of a dynamical vegetation model may falsify the results on short-term. CO_2 storage capacity of land biosphere might dampen the climate response at time of the forcing. We have picked orbital constellations of Earth's history that are partly correlated with completely different climatic conditions. While one orbital constellation happens to represent the Last Glacial Maximum (21 ka ago), the model is not set up with accurate climatic conditions from this period. To test the albedo effect of the large ice-sheets of this time and compare the outcome with proxy-data, an LGM-configuration would have been needed to test the effect of obliquity on amplifying or dampening the temperature once again. The same assumption is true for simulations representing astronomical constellations with high and low eccentricity values. These were similarly tested in a modern continental and climatic setup and certainly do not fully capture past climatic conditions from these times. Apart from using different climatic and continental setups, it would be desirable to test these simulations in a high-resolution Earth System Model that represent modern day conditions in more detail and additionally test other IPCC forcing scenarios, e.g. one of a less positive scenario. However, our simulations are reliable to study the long-term climatic response to the anthropogenic CO_2-forcing.

6.3 Outlook

To back up the state dependency response of the carbon cycle, it would be of great interest to design a final simulation for a high CO_2 world with realistically high weathering rates. This could potentially be achieved by increasing the sensitivity to radiative forcing whilst keeping the actual atmospheric CO_2 concentrations at pre-industrial values of 278 ppm. This should allow for simulation of a temperature-sensitive weathering feedback, whilst providing stable, though low atmospheric CO_2 values. Another approach could be a setup designed to keep up high weathering rates and high CO_2 values, balanced by high volcanic outgassing. The application of this simulation certainly needs further testing and most likely long run times for new Spin-Ups.
The next step in verifying the results of this study would ideally be a model-data comparison. The climate state dependency of the ocean's carbonate chemistry and the associated response of climate to the astronomical forcing does not rule out the importance of the cryosphere in amplifying the astronomical response at high latitudes. Our results rather provide an explanation for the shift in response times, where the cryosphere evolution plays a subordinate role in controlling the climate. It would be worthwhile to apply our observation to a more specific time in Earth history and test if the model simulations realistically represent proxy data observation.
Additionally, there remains a scientific question, that I have not been able to solve within the time frame of this thesis. The simulations were set up individually with different atm. CO_2 concentrations which created environmental conditions in equilibrium with the climate. If the system would experience a shift from cold to warm or from warm to cold climate during the run, would the same behavior in the carbon cycle state dependency be observed?
Given that much model development has been done in the last couple of years, using cGENIE's module of sediment diagenesis (Hülse, Arndt, Daines, et al., 2018), it would be worthwhile to be included in anthropogenic forcing simulations. The module coupled with cGENIE can represent the organic matter cycle and associated biogeochemical dynamics in detail and would give the opportunity to investigate the role of sediment formation to climate perturbations.

Appendix A

I support the principle of open access to research data. Model configuration and model data output is made accessible via open access. Publications resulting from this thesis will be made accessible by publishing open access. The following list links experiments and output to chapters of this thesis.

Experiment Name	Information, Original base-configuration
Sensitivity-setup	Chapter §2
Base Conf.	cgenie.eb_go_gs_ac_bg._rwlla.NONE, cgenie.eb_go_gs_ac_bg_sg_rg.p0055c.BASES
Adaptations	Abio_hE_lE_lO 278 ppm & 834 ppm
Adaptations	Weathering_hE_lE_lO 278 ppm & 834 ppm
Link to Config.	https://github.com/FionRo/ThesisAttachmentPublic/tree/master/Chapter02
Link to output	http://doi.org/10.5281/zenodo.3372356
Eocene-setup	Chapter §3, 4
Base Config.	Ridgwell and Schmidt, 2010, cgenie.eb_go_gs_ac_bg_sg_rg_gl.p0055c.BASES
Adaptations	1x, 3x, 6x, 12x CO_2
Link to Confi.	https://github.com/FionRo/ThesisAttachmentPublic/tree/master/Chap03:4
Link to output	http://doi.org/10.5281/zenodo.3372356
Modern-setup	Chapter §5
Base Conf.	Archer, Eby, et al., 2009, cgenie.eb_go_gs_ac_bg_sg_rg.worjh2.BASES
Adaptations	Modern, E-, E+, Obl-, Obl+
Link to Config.	https://github.com/FionRo/ThesisAttachmentPublic/tree/master/Chap05
Link to output	http://doi.org/10.5281/zenodo.3372356

Complete access to the working copy for cGENIE: https://github.com/FionRo/cgenie.muffin.FR_thesis
User manual, description of how to install and use cGENIE can be found on:
https://github.com/derpycode/muffindoc

References

Anagnostou, Eleni, Eleanor H. John, Kirsty M. Edgar, Gavin L. Foster, Andy Ridgwell, Gordon N. Inglis, Richard D. Pancost, Daniel J. Lunt, and Paul N. Pearson (2016).
"Changing atmospheric CO_2 concentration was the primary driver of early Cenozoic climate".
In: *Nature* 533, p. 380.

Archer, David E. (1996).
"An atlas of the distribution of calcium carbonate in sediments of the deep sea".
In: *Global Biogeochemical Cycles* 10.1, pp. 159–174.

Archer, David and Victor Brovkin (2008).
"The millennial atmospheric lifetime of anthropogenic CO_2".
In: *Climatic Change* 90.3, pp. 283–297.

Archer, David, Michael Eby, Victor Brovkin, Andy Ridgwell, Long Cao, Uwe Mikolajewicz, Ken Caldeira, Katsumi Matsumoto, Guy Munhoven, Alvaro Montenegro, and Kathy Tokos (2009).
"Atmospheric Lifetime of Fossil Fuel Carbon Dioxide".
In: *Annual Review of Earth and Planetary Sciences* 37.1, pp. 117–134.

Archer, David, Haroon Kheshgi, and Ernst Maier-Reimer (1997).
"Multiple timescales for neutralization of fossil fuel CO_2".
In: *Geophysical Research Letters* 24.4, pp. 405–408.

— (1998).
"Dynamics of fossil fuel CO_2 neutralization by marine CaCO3".
In: *Global Biogeochemical Cycles* 12.2, pp. 259–276.

Berger, A. (1976).
"Obliquity and precession for the last 5 000 000 years".
In: *Astronomy and Astrophysics* 51, pp. 127–135.

— (1978).

"Long-Term Variations of Daily Insolation and Quaternary Climatic Changes".

In: *Journal of the Atmospheric Sciences* 35.12, pp. 2362–2367.

Berger, A. (1988).

"Milankovitch Theory and climate".

In: *Reviews of Geophysics* 26.4, pp. 624–657.

ISSN: 1944-9208.

— (1989).

"Pleistocene climatic variability at astronomical frequencies".

In: *Quaternary International* 2, pp. 1–14.

ISSN: 1040-6182.

Berner, Robert A. (1991).

"A model for atmospheric CO2 over Phanerozoic time".

In: *American Journal of Science* 291, pp. 339–376.

— (1994).

"GEOCARB II: A revised model of atmospheric CO_2 over phanerozoic time".

In: *American Journal of Science;(United States)* 294.1.

— (1999).

"A new look at the long-term carbon cycle".

In: *GSA Today* 9, pp. 2–6.

Berner, Robert A. and Ken Caldeira (1997).

"The need for mass balance and feedback in the geochemical carbon cycle."

In: *Geology* 25, pp. 955–956.

Berner, Robert A., A. C. Lasaga, and R. M. Garrels (1983).

"The carbonate silicate geochemical cycle and its effect on atmospheric carbon dioxide over the past 100 million years".

In: *Am. J. Sci.* 283, pp. 641–683.

Blackford, J.C. and F.J. Gilbert (2007).

"pH variability and CO_2 induced acidification in the North Sea".

In: *Journal of Marine Systems* 64.1. Contributions from Advances in Marine Ecosystem Modelling Research, 27-29 June, 2005, Plymouth, UK, pp. 229–241.

ISSN: 0924-7963.

Bounceur, N., M. Crucifix, and R.D. Wilkinson (2015).

"Global sensitivity analysis of the climate?vegetation system to astronomical forcing: an emulator-based approach".

In: *Earth System Dynamics* 6.1. © Author(s) 2015. This work is distributed under the Creative Commons Attribution 3.0 License., pp. 205–224.

Brady, Patrick V. (1991).

"The effect of silicate weathering on global temperature and atmospheric CO_2".

In: *Journal of Geophysical Research: Solid Earth* 96.B11, pp. 18101–18106.

Broecker, Wallace S. and Tsung-Hung Peng (1987).

"The role of CaCO3 compensation in the glacial to interglacial atmospheric CO2 change".

In: *Global Biogeochemical Cycles* 1.1, pp. 15–29.

Broecker, William S. (2003).

"Does the trigger for abrupt climate change reside in the ocean or in the atmosphere?"

In: *Science* 300.5625, pp. 1519–1522.

Caldeira, Ken, Makoto Akai, Peter G Brewer, Baixin Chen, Peter Mosby Haugan, Toru Iwama, Paul Johnston, Haroon Kheshgi, Qingquan Li, Takashi Ohsumi, et al. (2005).

"Ocean storage".

In: *IPCC, 2005: IPCC Special Report on Carbon Dioxide Capture and Storage. Prepared by Working Group III*, p. 442.

Caldeira, Ken and Michael E. Wickett (2003).

"Anthropogenic carbon and ocean pH".

In: *Nature* 425.6956, pp. 365–365.

Cao, Long, Ken Caldeira, and Atul K. Jain (2007).

"Effects of carbon dioxide and climate change on ocean acidification and carbonate mineral saturation".

In: *Geophysical Research Letters* 34.5.

Chalk, Thomas B, Mathis P Hain, Gavin L. Foster, Eelco J. Rohling, Philip F. Sexton, Marcus PS Badger, Soraya G. Cherry, Adam P. Hasenfratz, Gerald H. Haug, Samuel L Jaccard, et al. (2017).

"Causes of ice age intensification across the Mid-Pleistocene Transition".

In: *Proceedings of the National Academy of Sciences* 114.50, pp. 13114–13119.

Ciais, Philippe, Christopher Sabine, Govindasamy Bala, Laurent Bopp, Victor Brovkin, Josep Canadell, Abha Chhabra, Ruth DeFries, James Galloway, Martin Heimann, et al. (2014).
"Carbon and other biogeochemical cycles".
In: *Climate change 2013: the physical science basis. Contribution of Working Group I to the Fifth Assessment Report of the Intergovernmental Panel on Climate Change*.
Cambridge University Press,
Pp. 465–570.

Claussen, Martin, L. Mysak, A. Weaver, Michel Crucifix, Thierry Fichefet, M.-F. Loutre, Shlomo Weber, Joseph Alcamo, Vladimir Alexeev, André Berger, et al. (2002).
"Earth system models of intermediate complexity: closing the gap in the spectrum of climate system models".
In: *Climate dynamics* 18.7, pp. 579–586.

Colbourn, G., A. Ridgwell, and T. M. Lenton (2015).
"The timescale of the silicate weathering negative feedback on atmospheric CO_2: Silicate Weathering Feedback Timescale".
In: *Global Biogeochemical Cycles* 29.

Colbourn, Greg, Andy Ridgwell, and Tim Lenton (2013).
"The Rock Geochemical Model (RokGeM) v0.9".
In: *Geoscientific Model Development* 6.5, pp. 1543–1573.

Cramer, Benjamin S., James D. Wright, Dennis V. Kent, and Marie-Pierre Aubry (2003).
"Orbital climate forcing of δ13C excursions in the late Paleocene-early Eocene (chrons C24n-C25n)".
In: *Paleoceanography* 18.4.

Crowley, Thomas J. and Gerald R. North (1991).
"Paleoclimatology".
In: *International Journal of Climatology,Oxford University Press (New York)* 14.1, pp. 114–115.

De Vleeschouwer, David, Maximilian Vahlenkamp, Michel Crucifix, and Heiko Pälike (2017).
"Alternating Southern and Northern Hemisphere climate response to astronomical forcing during the past 35 m.y."
In: *Geology* 45.4, p. 375.

Detlef, H., S. T. Belt, S. M. Sosdian, L. Smik, C. H. Lear, I. R. Hall, P. Cabedo-Sanz, K. Husum, and S. Kender (2018).

"Sea ice dynamics across the Mid-Pleistocene transition in the Bering Sea".

In: *Nature Communications* 9.1, p. 941.

Doney, Scott C., Victoria J. Fabry, Richard A. Feely, and Joan A. Kleypas (2009).

"Ocean acidification: the other CO_2 problem".

In: *Annual review of marine science* 1, pp. 169–192.

Eby, Michael, Andrew J. Weaver, K. Alexander, K. Zickfeld, A. Abe-Ouchi, A.A. Cimatoribus, E. Crespin, S.S. Drijfhout, N.R. Edwards, A.V. Eliseev, et al. (2013).

"Historical and idealized climate model experiments: an intercomparison of Earth system models of intermediate complexity".

In: *Climate of the Past* 9, pp. 1111–1140.

Edwards, Neil R. and Robert Marsh (2005).

"Uncertainties due to transport-parameter sensitivity in an efficient 3-D ocean-climate model".

In: *Climate Dynamics* 24.4, pp. 415–433.

ISSN: 1432-0894.

Feely, Richard A., Scott C. Doney, and Sarah R. Cooley (2009).

"Ocean acidification: Present conditions and future changes in a high-CO_2 world".

In: *Oceanography* 22.4, pp. 36–47.

Feely, Richard A., Christopher L. Sabine, Kitack Lee, Will Berelson, Joanie Kleypas, Victoria J. Fabry, and Frank J. Millero (2004).

"Impact of anthropogenic CO_2 on the CaCO3 system in the oceans".

In: *Science* 305.5682, pp. 362–366.

Flato, Gregory et al. (2013).

"Evaluation of climate models. Chapter 9 in climate change 2013: the physical science basis".

In: *Contribution of Working Group I to the Fifth Assessment Report of the Intergovernmental Panel on Climate Change*.

Frakes, Lawrence, J.E. Francis, and Jozef Syktus (1992).

Climate Modes of the Phanerozoic.

Frankignoulle, Michel, Christine Canon, and Jean-Pierre Gattuso (1994).

"Marine calcification as a source of carbon dioxide: Positive feedback of increasing atmospheric CO2".

In: *Limnology and Oceanography* 39.2, pp. 458–462.

Galeotti, Simone, Srinath Krishnan, Mark Pagani, Luca Lanci, Alberto Gaudio, James C Zachos, Simonetta Monechi, Guia Morelli, and Lucas Lourens (2010).

"Orbital chronology of Early Eocene hyperthermals from the Contessa Road section, central Italy".

In: *Earth and Planetary Science Letters* 290.1-2, pp. 192–200.

Ganopolski, Andrey and Didier Roche (2009).

"On the nature of lead-lag relationships during glacial-interglacial climate transitions".

In: *Quaternary Science Reviews* 28, pp. 3361–3378.

Ganopolski, Andrey, Ricarda Winkelmann, and Hans Joachim Schellnhuber (2016).

"Critical insolation - CO_2 relation for diagnosing past and future glacial inception".

In: *Nature* 529.7585, p. 200.

Genthon, C., J. Jouzel, J.-M. Barnola, D. Raynaud, and C. Lorius (1987).

"Vostok ice core - Climatic response to CO_2 and orbital forcing changes over the last climatic cycle".

In: *Nature* 329, pp. 414–418.

Gildor, Hezi and Eli Tziperman (2001).

"Physical mechanisms behind biogeochemical glacial-interglacial CO2 variations".

In: *Geophysical Research Letters* 28.12, pp. 2421–2424.

Goodwin P. Williams, R.G., Andy Ridgwell, and M.J. Follows (2009).

"Climate sensitivity to the carbon cycle modulated by past and future changes in ocean chemistry".

In: *Nature Geoscience* 2.2, p. 145.

Gutjahr, Marcus, Andy Ridgwell, Philip F. Sexton, Eleni Anagnostou, Paul N. Pearson, Heiko Pälike, Richard D. Norris, Ellen Thomas, and Gavin L. Foster (2017).

"Very large release of mostly volcanic carbon during the Palaeocene–Eocene Thermal Maximum".

In: *Nature* 548.7669, p. 573.

Haug, Gerald H. and Ralf Tiedemann (1998).

"Effect of the formation of the Isthmus of Panama on Atlantic Ocean thermohaline circulation". In: *Nature* 393.6686, pp. 673–676.

Hays, J.D., John Imbrie, and Nicholas J. Shackleton (1976).
"Variations in the earth's orbit: pacemaker of the ice ages".
In: *Science (Washington, D.C.); (United States)* 194:4270.

Hülse, D., S. Arndt, S. Daines, P. Regnier, and A. Ridgwell (2018).
"OMEN-SED 1.0: a novel, numerically efficient organic matter sediment diagenesis module for coupling to Earth system models".
In: *Geoscientific Model Development* 11.7, pp. 2649–2689.

Hülse, Dominik, Sandra Arndt, Jamie D. Wilson, Guy Munhoven, and Andy Ridgwell (2017).
"Understanding the causes and consequences of past marine carbon cycling variability through models".
In: *Earth-Science Reviews* 171.Supplement C, pp. 349–382.
ISSN: 0012-8252.

Imbrie, J., A. Berger, et al. (1993).
"On the structure and origin of major glaciation cycles 2. The 100,000-year cycle".
In: *Paleoceanography* 8.6, pp. 699–735.

Imbrie, J., E. A. Boyle, et al. (1992).
"On the Structure and Origin of Major Glaciation Cycles 1. Linear Responses to Milankovitch Forcing".
In: *Paleoceanography* 7.6, pp. 701–738.

Imbrie, John and John Z. Imbrie (1980).
"Modeling the Climatic Response to Orbital Variations".
In: *Science* 207.4434, pp. 943–953.
ISSN: 0036-8075.

IPCC (2013).
Climate Change 2013: The Physical Science Basis. Contribution of Working Group I to the Fifth Assessment Report of the Intergovernmental Panel on Climate Change.
Cambridge, United Kingdom and New York, NY, USA: Cambridge University Press,
P. 1535.
ISBN: ISBN 978-1-107-66182-0.

Joos, Fortunat and Renato Spahni (2008).

"Rates of change in natural and anthropogenic radiative forcing over the past 20,000 years".

In: *Proceedings of the National Academy of Sciences* 105.5, pp. 1425–1430.

ISSN: 0027-8424.

Keery, John S., Philip Holden, and Neil Edwards (2018).

"Sensitivity of the Eocene climate to CO_2 and orbital variability".

In: *Climate of the Past* 14.

Kirtland Turner, Sandra (2014).

"Pliocene switch in orbital-scale carbon cycle/climate dynamics".

In: *Paleoceanography* 29.12, pp. 1256–1266.

— (2018).

"Constraints on the onset duration of the Paleocene-Eocene Thermal Maximum".

In: 376.2130, p. 20170082.

Kirtland Turner, Sandra and Andy Ridgwell (2013).

"Recovering the true size of an Eocene hyperthermal from the marine sedimentary record".

In: *Paleoceanography* 28.4, pp. 700–712.

— (2016).

"Development of a novel empirical framework for interpreting geological carbon isotope excursions, with implications for the rate of carbon injection across the PETM".

In: *Earth and Planetary Science Letters* 435, pp. 1–13.

ISSN: 0012-821X.

Kleypas, Joan A., Robert .W Buddemeier, David Archer, Jean-Pierre Gattuso, Chris Langdon, and Bradley N Opdyke (1999).

"Geochemical consequences of increased atmospheric carbon dioxide on coral reefs".

In: *science* 284.5411, pp. 118–120.

Laskar, J., P. Robutel, F. Joutel, M. Gastineau, A.C.M. Correia, and B. Levrard (2004).

"A long-term numerical solution for the insolation quantities of the Earth".

In: *aap* 428, pp. 261–285.

Laskar, Jacques, Agnés Fienga, Mickael Gastineau, and Herve Manche (2011).

"La2010: a new orbital solution for the long-term motion of the Earth".

In: *Astronomy and Astrophysics - A&A* 532 (A89).

Lisiecki, Lorraine E. and Maureen E. Raymo (2005).

"A Pliocene-Pleistocene stack of 57 globally distributed benthic δ 18O records".

In: *Paleoceanography* 20.1. PA1003.

ISSN: 1944-9186.

Lourens, Lucas J., Appy Sluijs, Dick Kroon, James C. Zachos, Ellen Thomas, Ursula Röhl, Julie Bowles, and Isabella Raffi (2005).

"Astronomical pacing of late Palaeocene to early Eocene global warming events".

In: *Nature* 435, 1083 EP.

Lunt, Dale, Tom Dunkley Jones, Malte Heinemann, M. Huber, Allegra LeGrande, A. Winguth, C. Loptson, J. Marotzke, J. Tindall, Paul Valdes, and Cornelia Winguth (2012).

"A model-data comparison for a multi-model ensemble of early Eocene atmosphere-ocean simulations: EoMIP".

In: *Climate of the Past Discussions* 8, pp. 1229–1273.

Lunt, Dale, Paul Valdes, Tom Dunkley Jones, Andy Ridgwell, Alan M. Haywood, Daniela Schmidt, Robert Marsh, and Mark Maslin (2010).

"CO_2-driven ocean circulation changes as an amplifier of Paleocene-Eocene thermal maximum hydrate destabilization".

In: *Geology* 38, pp. 875–878.

Lunt, Daniel J., Andy Ridgwell, Appy Sluijs, James Zachos, Stephen Hunter, and Alan Haywood (2011).

"A model for orbital pacing of methane hydrate destabilization during the Palaeogene".

In: *Nature Geoscience* 4, p. 775.

Lüthi, Dieter, Martine Le Floch, Bernhard Bereiter, Thomas Blunier, Jean-Marc Barnola, Urs Siegenthaler, Dominique Raynaud, Jean Jouzel, Hubertus Fischer, Kenji Kawamura, et al. (2008).

"High-resolution carbon dioxide concentration record 650,000-800,000 years before present".

In: *Nature* 453.7193, p. 379.

Mackensen, Andreas and Gerhard Schmiedl (2019).

"Stable carbon isotopes in paleoceanography: atmosphere, oceans, and sediments".

In: *Earth-Science Reviews* 197, p. 102893.

ISSN: 0012-8252.

Mantsis, Damianos F., Amy C. Clement, Anthony J. Broccoli, and Michael P. Erb (2011).
"Climate Feedbacks in Response to Changes in Obliquity".
In: *Journal of Climate* 24.11, pp. 2830–2845.

Milankovitch, Milutin (1941).
Kanon der Erdebestrahlung und seine Anwendung auf das Eiszeitenproblem.
Königlich Serbische Akademie.

Millero, Frank J. (1995).
"Thermodynamics of the carbon dioxide system in the oceans".
In: *Geochimica et Cosmochimica Acta* 59.4, pp. 661–677.

Mucci, Alfonso (1983).
"The solubility of calcite and aragonite in seawater at various salinities, temperatures, and one atmosphere total pressure".
In: *American Journal of Science* 283.7, pp. 780–799.

NASA Goddard Institute for Space Studies (2019).
Panoply.
Version 4.5.1.

Naviaux, John D., Adam V. Subhas, Sijia Dong, Nick E. Rollins, Xuewu Liu, Robert H. Byrne, William M. Berelson, and Jess F. Adkins (2019).
"Calcite dissolution rates in seawater: Lab vs. in-situ measurements and inhibition by organic matter".
In: *Marine Chemistry*, p. 103684.

North, G. R., J. G. Mengel, and D. A. Short (1983).
"Simple energy balance model resolving the seasons and the continents: Application to the astronomical theory of the ice ages".
In: *Journal of Geophysical Research: Oceans* 88.C11, pp. 6576–6586.

Orr, J.C., J.M. Epitalon, and J.P. Gattuso (2015).
"Comparison of ten packages that compute ocean carbonate chemistry".
In: *Biogeosciences Discussions, European Geosciences Union* 12(5), pp. 1483–151.

Package 'seacarb' (2019).
URL: `http://vps.fmvz.usp.br/CRAN/web/packages/seacarb/seacarb.pdf`.

Paillard, Didier, LD Labeyrie, and Pascal Yiou (1996).

"AnalySeries 1.0: a Macintosh software for the analysis of geophysical time-series".
In: *Eos* 77, p. 379.

Pälike, Heiko, Richard D. Norris, Jens O. Herrle, Paul A. Wilson, Helen K. Coxall, Caroline H. Lear, Nicholas J. Shackleton, Aradhna K. Tripati, and Bridget S. Wade (2006).
"The Heartbeat of the Oligocene Climate System".
In: *Science* 314.5807, pp. 1894–1898.
ISSN: 0036-8075.

Panchuk, K., A. Ridgwell, and L.R. Kump (2008).
"Sedimentary response to Paleocene-Eocene Thermal Maximum carbon release: A model-data comparison".
In: *Geology* 36.4, pp. 315–318.
ISSN: 0091-7613.

Pearson, Paul N., Gavin L. Foster, and Bridget S. Wade (2009).
"Atmospheric carbon dioxide through the Eocene–Oligocene climate transition".
In: *Nature* 461, p. 1110.

Pearson, Paul N. and Martin R. Palmer (1999).
"Middle Eocene Seawater pH and Atmospheric Carbon Dioxide Concentrations".
In: *Science* 284.5421, pp. 1824–1826.
ISSN: 0036-8075.

— (2000).
"Atmospheric carbon dioxide concentrations over the past 60 million years".
In: *Nature* 406.6797, pp. 695–699.

Penman, Donald E, Bärbel Hönisch, Richard E. Zeebe, Ellen Thomas, and James C. Zachos (2014).
"Rapid and sustained surface ocean acidification during the Paleocene-Eocene Thermal Maximum".
In: *Paleoceanography* 29.5, pp. 357–369.

Petit, J. R. et al. (1999).
"Climate and atmospheric history of the past 420,000 years from the Vostok ice core, Antarctica".
In: *Nature* 399, p. 429.

Plattner, G.-K. et al. (2008).

"Long-Term Climate Commitments Projected with Climate‚ÄìCarbon Cycle Models".

In: *Journal of Climate* 21.12, pp. 2721–2751.

Python Software Foundation. (2019).

Python.

Version 2.7.1.

Ridgwell, Andy (2019).

cGENIE website.

URL: `http://www.seao2.info/mycgenie.html` (visited on 08/15/2019).

Ridgwell, Andy and J. C. Hargreaves (2007).

"Regulation of atmospheric CO_2 by deep-sea sediments in an Earth system model".

In: *Global Biogeochemical Cycles* 21.2. GB2008.

ISSN: 1944-9224.

Ridgwell, Andy, J. C. Hargreaves, N. R. Edwards, J. D. Annan, T. M. Lenton, R. Marsh, A. Yool, and A. Watson (2007).

"Marine geochemical data assimilation in an efficient Earth System Model of global biogeochemical cycling".

In: *Biogeosciences* 4.1, pp. 87–104.

Ridgwell, Andy and Daniela Schmidt (2010).

"Past constraints on the vulnerability of marine calcifiers to massive carbon dioxide release".

In: *Nature Geoscience* 3, pp. 196–200.

Ridgwell, Andy and Richard Zeebe (2005).

"The role of the global carbonate cycle in the regulation and evolution of the Earth system".

In: *Earth and Planetary Science Letters* 234.3, pp. 299–315.

ISSN: 0012-821X.

Riebesell, Ulf (2004).

"Effects of CO_2 Enrichment on Marine Phytoplankton".

In: *Journal of Oceanography* 60.4, pp. 719–729.

ISSN: 1573-868.

Riebesell, Ulf, Ingrid Zondervan, Björn Rost, Philippe D. Tortell, Richard E. Zeebe, and François M. M. Morel (2000).

"Reduced calcification of marine plankton in response to increased atmospheric CO_2".
In: *Nature* 407.6802, pp. 364–367.

Ruddiman, William F. (2003).
"Orbital insolation, ice volume, and greenhouse gases".
In: *Quaternary Science Reviews* 22, pp. 1597–1629.

Ruddiman, William F. and Andrew McIntyre (1981).
"Oceanic Mechanisms for Amplification of the 23,000-Year Ice-Volume Cycle".
In: *Science* 212.4495, pp. 617–627.
ISSN: 0036-8075.

Ruddiman, William F. and Maureen E. Raymo (2003).
"A methane-based time scale for Vostok ice".
In: *Quaternary Science Reviews* 22.2, pp. 141–155.
ISSN: 0277-3791.

Sabine, Christopher L., Richard A. Feely, Nicolas Gruber, Robert M. Key, Kitack Lee, John L. Bullister, Rik Wanninkhof, CSL Wong, Douglas WR Wallace, Bronte Tilbrook, et al. (2004).
"The oceanic sink for anthropogenic CO2".
In: *science* 305.5682, pp. 367–371.

Sarmiento, Jorge L. and Nicolas Gruber (2006).
Ocean biogeochemical dynamics.
Princeton University Press.

Shackleton, Nicholas J., M. A. Hall, I. Raffi, L. Tauxe, and J. Zachos (2000).
"Astronomical calibration age for the Oligocene-Miocene boundary".
In: *Geology* 28.5. n/a, pp. 447–450.

Short, David A., John G. Mengel, Thomas J. Crowley, William T. Hyde, and Gerald R. North (1991).
"Filtering of milankovitch cycles by earth's geography".
In: *Quaternary Research* 35.2, pp. 157–173.
ISSN: 0033-5894.

Sigman, Daniel M. and Edward A. Boyle (2000).
"Glacial/interglacial variations in atmospheric carbon dioxide".
In: *Nature* 407.6806, pp. 859–869.

Sundquist, Eric T. (1986).

"Geologic analogs: their value and limitations in carbon dioxide research".

In: *The changing carbon cycle*.

Springer,

Pp. 371–402.

— (1993).

"The global carbon dioxide budget".

In: *Science*, pp. 934–941.

Tuenter, E., S.L. Weber, F.J. Hilgen, and L.J. Lourens (2003).

"The response of the African summer monsoon to remote and local forcing due to precession and obliquity".

In: *Global and Planetary Change* 36.4, pp. 219–235.

ISSN: 0921-8181.

Turner, Sandra Kirtland and Andy Ridgwell (2016).

"Development of a novel empirical framework for interpreting geological carbon isotope excursions, with implications for the rate of carbon injection across the PETM".

In: *Earth and Planetary Science Letters* 435, pp. 1–13.

ISSN: 0012-821X.

Tziperman, Eli and Hezi Gildor (2003).

"On the mid-Pleistocene transition to 100-kyr glacial cycles and the asymmetry between glaciation and deglaciation times".

In: *Paleoceanography* 18.1, p. 1118.

Vahlenkamp, Maximilian, Igor Niezgodzki, David De Vleeschouwer, Torsten Bickert, Dustin Harper, Sandra Kirtland Turner, Gerrit Lohmann, Philip Sexton, James Zachos, and Heiko Pälike (2018).

"Astronomically paced changes in deep-water circulation in the western North Atlantic during the middle Eocene".

In: *Earth and Planetary Science Letters* 484, pp. 329–340.

ISSN: 0012-821X.

Volk, Tyler (1987).

"Feedbacks between weathering and atmospheric CO_2 over the last 100 million years."

In: *America Journal of Science*,

Pp. 763–779.

Walker, James C. G., P. B. Hays, and J. F. Kasting (1981).

"A negative feedback mechanism for the long-term stabilization of Earth's surface temperature".

In: *Journal of Geophysical Research: Oceans* 86.C10, pp. 9776–9782.

Walker, James C.G. and James F. Kasting (1992).

"Effects of fuel and forest conservation on future levels of atmospheric carbon dioxide".

In: *Palaeogeography, Palaeoclimatology, Palaeoecology* 97.3, pp. 151–189.

ISSN: 0031-0182.

Weaver, Andrew J. et al. (2001).

"The UVic earth system climate model: Model description, climatology, and applications to past, present and future climates".

In: *Atmosphere-Ocean* 39.4, pp. 361–428.

Winguth, A., C. Shellito, C. Shields, and C. Winguth (2010).

"Climate Response at the Paleocene - Eocene Thermal Maximum to Greenhouse Gas Forcing-A Model Study with CCSM3".

In: *Journal of Climate* 23.10, pp. 2562–2584.

Zachos, James C., Gerald R. Dickens, and Richard E. Zeebe (2008).

"An early Cenozoic perspective on greenhouse warming and carbon-cycle dynamics".

In: *Nature* 451.7176, p. 279.

Zachos, James C, Ursula Röhl, Stephen A. Schellenberg, Appy Sluijs, David A. Hodell, Daniel C. Kelly, Ellen Thomas, Micah Nicolo, Isabella Raffi, Lucas J. Lourens, et al. (2005).

"Rapid acidification of the ocean during the Paleocene-Eocene thermal maximum".

In: *Science* 308.5728, pp. 1611–1615.

Zachos, James, M. Pagani, L. Sloan, E. Thomas, and K. Billups (2001).

"Trends, Rhythms, and Aberrations in Global Climate 65 Ma to Present".

In: *Science* 292, pp. 686–693.

Zeebe, Richard E., Andy Ridgwell, and James C. Zachos (2016).

"Anthropogenic carbon release rate unprecedented during the past 66 million years".

In: *Nature Geoscience* 9, p. 325.

Zeebe, Richard E., Thomas Westerhold, Kate Littler, and James C. Zachos (2017).

"Orbital forcing of the Paleocene and Eocene carbon cycle".

In: *Paleoceanography* 32.5, pp. 440–465.

Zeebe, Richard E. and Dieter Wolf-Gladrow (2001).

CO_2 in seawater: equilibrium, kinetics, isotopes.